AN ABSTRACT OF THE DISSERTATION OF

Cheryl J. Buckholz for the degree of Doctor of Philosophy in Pharmacy presented on May 19, 2003

Title: Acute Bioactivation and Hepatotoxicity of Ketoconazole in Rat and the Determinant Presence of Flavin-containing Monooxygenase (FMO) Isoforms in Human Duodenum, Jejunum, Ileum, and Colon Microsomes and Caco-2 Cell Line.

Redacted for privacy

Abstract approved:_

Rosita J. Rodriguez

Two specific goals were addressed for this dissertation. First to investigate and identify the mechanistic profile of ketoconazole (KT)-induced hepatotoxicity by utilizing *in vivo* and *in vitro* approaches determining the mechanism of action for the hepatotoxicity incurred. To date, there has not been a mechanistic determination of the hepatotoxicity associated with KT *in vivo*. This dissertation evaluates the possible metabolic bioactivation of KT by cytochrome-P450 (CYP) or flavin-containing monooxygenases (FMO) resulting in covalent binding with hepatic macromolecules. The hypothesis of this study was to reveal whether covalent binding by the parent compound, KT, and/or reactive metabolites

produces hepatic damage associated with increased serum alanine aminotransaminase (ALT) release and decreased hepatic glutathione (GSH). The first objective was determination of *in vivo* covalent binding in a dose-time response comparison in Sprague-Dawley (SD) rat ALT and GSH levels. Increased ALT and reduced hepatic GSH levels occurred. The second objective was an *in vitro* comparison of covalent binding with GSH levels utilizing SD microsomal protein with incubations of KT. Covalent binding decreased with added GSH to microsomal incubations. Thirdly, correlate *in vivo* with *in vitro* findings. Covalent binding of KT *in vivo* and *in vitro* occurred with increased doses and time. The final objective was to determine the bioactivation pathway utilizing heat inactivation and no NADPH *in vitro*. Covalent binding of KT decreased in the absence of NADPH and deactivation of FMO.

The second goal was to determine and quantitate *in vitro* the presence of FMO isozymes in microsomes of the human intestinal duodenum, jejunum, ileum, and colon as well as the Caco-2 (HTB-37), epithelial intestinal (CCL-241) and colon (CRL1790) cell lines. The presence of FMO could result in a first-pass effect decreasing the bioavailability of soft nucleophiles or a toxicity effect due to inhibition or modulation of the enzyme from co-administration. To date, this is the first evaluation of FMO isoforms in human intestine and cell lines. Western blot techniques were utilized for detection of human FMO1, FMO3, and FMO5 using human FMO-expressed recombinant cDNA from a baculovirus system.

Quantifiable detection of FMO1 was verifiable for the jejunum, ileum, colon, and Caco-2 cells.

Acute Bioactivation and Hepatotoxicity of Ketoconazole in Rat and the Determinant Presence of Flavin-containing Monooxygenase (FMO) Isoforms in Human Duodenum, Jejunum, Ileum, and Colon Microsomes and Caco-2 Cell Line.

by
Cheryl J. Buckholz

A DISSERTATION

submitted to

Oregon State University

in partial fulfillment of
the requirements for the
degree of

Doctor of Philosophy

Presented May 19, 2003
Commencement June 2003

Doctor of Philosophy in Pharmacy dissertation of Cheryl J. Buckholz presented on May 19, 2003.

APPROVED:

Redacted for privacy

Major Professor, representing Pharmacy

Redacted for privacy

Dean of the College of Pharmacy

Redacted for privacy

Dean of the Graduate School

I understand that my dissertation will become part of the permanent collection of Oregon State University libraries. My signature below authorizes release of my dissertation to any reader upon request.

Redacted for privacy

Cheryl J. Buckholz, Author

ACKNOWLEDGEMENTS

The author expresses her profound appreciation to Professor Rodriguez for her diligent assistance in experimental investigation and the preparation of this manuscript. In addition, special thanks to my committee members Drs. Ayres, Christiansen, Hsu, and Williams for their input and encouragement as well as to Jan-Shiang Taur (Jesse) for his expertise in statistics and Professor Filtz for her molecular procedural knowledge and assistance.

The 1999-2000 Pharmaceutical Manufacturers of American Foundation Research Starter Grant, the University Club Foundation of Oregon, and the NIDDK- (DK-59266) supported the following research investigations.

TABLE OF CONTENTS

TABLE OF CONTENTS (Continued)

TABLE OF CONTENTS (Continued)

Page

TABLE OF CONTENTS (Continued)

Page

LIST OF FIGURES

LIST OF FIGURES (Continued)

LIST OF TABLES

APPENDIX: PROTOCOL INDEX

LIST OF APPENDIX FIGURES

DEDICATION

To my husband Dan whose devotion and encouragement aided in implementing my success, without him this endeavor would not have been possible.

Acute Bioactivation and Hepatotoxicity of Ketoconazole in Rat and the Determinant Presence of Flavin-containing Monooxygenase (FMO) Isoforms in Human Duodenum, Jejunum, Ileum, and Colon Microsomes and Caco-2 Cell Line.

CHAPTER 1: INTRODUCTION

1.1. BACKGROUND

Exogenous compounds, such as pharmacologically active drugs, are foreign to the body and upon entrance can be chemically altered by enzymatic metabolizing components present within the physiological system. Oral administration of therapeutic compounds has become increasingly popular versus the inconvenience and elevated cost of an intravenous (*i.v.*) dose requiring administration by a doctor or nurse. The absorption, bioavailability, distribution, and elimination of the compound determine the onset and duration of action.

Principle sites for drug metabolism occur in the small intestinal mucosa and the liver due to a high concentration of metabolic enzymes that conduct phase I and phase II biochemical reactions, such as oxidation, reduction, hydrolysis, and conjugation. Metabolism of an orally administered compound can result in reduced bioavailability or toxicity by either altering the metabolic profile or changing the rate of elimination. In humans, gender, genetics, other drug interactions by inhibition, induction, or modulation of enzymes, as well as environmental factors can alter the pharmacokinetics and/or pharmacodynamics of an orally administered drug. Other factors to consider for altered kinetics or

therapeutic effects are: drug instability in the gastrointestinal tract (GI), inadequate release from the dosage form, poor intestinal permeability, delayed or erratic rate of absorption, or a first-pass effect.

The GI tract, referred to as the alimentary tract or canal, is divided into 11 anatomical regions and is approximately 435 cm long. This canal is controlled by the enteric nervous and hormonal systems (Guyton 1991) and functions in absorption, digestion, and elimination of residual waste (Marieb 2001). The alimentary tract continually supplies the body with water, electrolytes, and nutrients by movement of food, secretion of digestive juices and digestion of food, absorption of digestive products, and the circulation of blood (Guyton 1991).

Several of the enzymes found in the liver are detected in the mucosal epithelium of the GI tract. These include cytochrome P450 (CYP) (Zhang, *et al.* 1999), glucuronosyl transferases, sulfotransferases, *N*-acetyl transferase, glutathione *S*-transferases, esterases, epoxide hydrolase, and alcohol dehydrogenase (Thummel, *et al.* 1997), amylases, peptidases, reductases, phosphatases, esterases (Renwick 1982), and Flavin-containing monooxygenases (FMO) (Larsen-Su and Williams 1996, Yeung, *et al.* 2000). Enzymes conducting metabolic reactions in the small intestine are as follows: CYP1A1, 2D6, 3A4 (Zhang, *et al.* 1999), monoamine oxidation, hydroxylation, dealkylation, desulfuration, reduction, hydrolysis, glucuronidation, sulfation, *N*-acetylation (Ilett and Davies 1982), O-methylation and glutathione (Caldwell and Marsh 1982). Table 1 indicates the detected enzymes found in the small intestine.

Table 1. Phase I enzymes and isozymes, and phase II reactions with cofactors/ enzymes detected in small intestine.

Phase I enzymes	**Isozymes**
CYP	1A1, 1A2, 2B, 2C (Oda and Kharasch 2001), 2D6, 3A4 (Zhang, *et al.* 1999)
FMO	FMO1 (Yeung, *et al.* 2000)
Alcohol dehydrogenase Prostaglandin H synthase	(Klaassen 1996)
Phase II reactions	**Cofactors and enzymes, respectively**
glucuronidation	uridine diphosphate (UDP)-glucuronic acid, UDP-glucuronosyltransferases (Ilett and Davies 1982)
sulfation	3'-phosphoadenosine-5'phosphosulfate (PAPS) sulfotransferases (Ilett and Davies 1982)
N-acetylation	acetyl-coenzyme A *N*-acetyl transferases (Ilett and Davies 1982)
O-methylation	*S*-adenosylmethionine (SAM) phenol-*O*-methyltranferase (POMT) catechol-*O*-methyltransferase (COMT) (Caldwell and Marsh 1982)
glutathione (GSH) conjugation	glutathione, glutathione synthetase (Caldwell and Marsh 1982)

The primary site of absorption for orally administered drugs is across the epithelial mucosa of the small intestine due to three factors: an extensive absorptive area of approximately 600 m^2 (Campbell 1993), lipophilic permeability, and high perfusion, total blood flow of 1.0 to 1.5 L/min (Rowland and Tozer 1995). Absorption in the gut wall has been stated to be highest in the duodenum and jejunum of the small intestine due to a folding of the mucosal epithelial lining, known as the plica, and the villi-microvilli appendages, increasing the surface area. The plica folds become obscured in the ileum and colon, resulting in a

decreased surface area in these regions. Until recently, intestinal absorption had been considered to occur without metabolic alteration; therefore, little attention was given to differentiating between possible metabolism occurring in the GI wall versus the liver (Ilett and Davies 1982).

During intestinal absorption and metabolism, a pre-systemic clearance resulting in a first-pass effect decreases the systemic availability of a compound (Ilett, *et al.* 1990). The enzymatic first-pass effect is responsible for altering or diminishing bioavailability and therapeutic effects of the fraction of a drug absorbed from the oral dose (*F*). Many of the metabolizing intestinal enzymes detected in the mucosal epithelium conduct biotransformation of orally administered drugs (Thummel, *et al.* 1997). For example, FMO has been detected in the small intestine (Yeung, *et al.* 2000), but little is known of the presence of or oxidative metabolism performed by individual FMO isoforms, specifically in the duodenum or jejunum. Therefore, the concept that metabolic alteration within the intestinal wall does not occur after drug absorption is misleading. Now, the first-pass effect consists of intestinal and liver metabolism.

1.2. ABSORPTION, BIOAVAILABILITY, AND KINETICS OF EXTRAVASCULAR (*e.v.*) DOSING

With extravascular (*e.v.*) dosing, the absorption phase is a prerequisite for bioavailability and therapeutic activity. Bioavailability refers to both the rate (ka) and extent of the dose-administered that reaches the systemic

system, and is defined by the area under the blood concentration-time curve (AUC). The fraction of the dose that is administered, *F*, that reaches the systemic circulation intact is determined by the ratio of the AUCs after extra- and intra-vascular drug administration. *F* is the measure of the extent of first-pass metabolism (Pond and Tozer 1984). At the peak of absorption, when drug absorption = drug elimination from the systemic system, the plasma concentration is at a maximum (C_{max}), and the time that it took to reach this peak is referred to as t_{max} (Rowland and Tozer 1995). Bioavailability comparisons are referred to as absolute and relative bioavailabilities. Absolute bioavailability is a comparison of the *e.v.*dose and an *i.v.* bolus dose, whereas relative bioavailabilities indicate the comparison of an *e.v.* dose with another *e.v.* dosage form, a different route, or different conditions (Winter 1994).

1.3. METABOLISM

1.3.1 First-pass effect

In recent findings, occurrence of first-pass metabolism and a reduction in concentration of a xenobiotic in the systemic system might be occurring in the small intestine (Fromm 1996, Holtbecker, *et al.* 1996, Paine, *et al.* 1996, Doherty and Charman 2002). Also, the first-pass effect may be greater through intestinal metabolism than the liver (Fromm 1996, Holtbecker, *et al.* 1996). The first-pass effect is characterized by the pre-systemic removal of a drug, resulting in reduced bioavailability after oral administration. First-pass metabolism

is affected by such factors as pH, unabsorbed nutrients and xenobiotics (chelation interactions), intestinal microflora (Renwick 1982), age, gender, disease states, enzyme induction and inhibition, and genetic polymorphism (Tam 1993). Drugs that undergo extensive first-pass metabolism often exhibit considerable variation in systemic bioavailability, due to interindividual therapeutic responses represented in the plasma concentration after an *e.v.* administration (Pond and Tozer 1984). Determining the enzyme presence and activity could aid in avoiding these problems.

Comparing both *e.v.* and *i.v.* administration, it is possible to determine the extent the drug is being removed before entrance into the systemic system, but differentiating the site of metabolism between the bacterial flora of the gut lumen, the gut wall, and the liver is difficult (Renwick and George 1989). Due to hepatic metabolism contributions to the first-pass effect, attempts to by-pass the liver by other routes, such as sublingual or rectal have been effective in increasing the bioavailability of drugs (Caldwell and Marsh 1982). The pre-systemic clearance becomes important when a significant amount of an *e.v.* dose is eliminated during the first passage of a drug. The availability of a drug is determined by the product of the fractions of the drug entering the tissue that are not lost in each successive tissue (Pond and Tozer 1984). F is expressed as: $F_{oral} = F_G * F_L * F_P$ where F_G, F_L, F_P are the fraction of the drug that has survived the GI tract, the liver, and the lung, respectively (Renwick and George 1989).

Another variable is metabolism conducted in the gut by the vast number of organisms, approximately 10^{10} per gram of gut contents. In humans most metabolic organisms are present in the lower bowel due to their anaerobic characteristic. Nearly all of the microbial metabolizing activity is found in the cecum (ileum connection to colon) and colon resulting in azo- and nitro-reduction, β-glucuronidase cyclamate hydrolysis, and sulfoxide reduction. Xenobiotics will reach the gut flora either by incomplete absorption from *e.v.* administration, biliary excretion, or secretion into the gut lumen from a systemic dose (Renwick and George 1989).

1.3.2. Detoxicaton/Bioactivation/Therapeutic window

Plasma concentrations of a drug must correlate with both the intensity and probability of therapeutic or toxic effects. Therapeutic failure can arise if the drug has a narrow therapeutic window and variability in the pharmacokinetics, erratic absorption, and non-compliance by the patient or if the patient is at risk due to genetic factors, disease, or multiple drug therapy (Rowland and Tozer 1995).

Metabolic toxicity from the parent compound and/or the metabolite(s) formation is dependent upon the C_{max} of the plasma concentrations achieved, the duration of the exposure to the toxicant above the threshold of the minimum toxicity level (MTL), or the accumulation of the toxicant within the systemic system. Metabolic activation of a xenobiotic to a bioactivated intermediate can alter the cellular function resulting in cellular necrosis and cell death by covalently

binding and altering cellular macromolecules leading to enzyme inactivation, altered functions of structural proteins or transcription, disruption of intracellular calcium homeostasis, loss of cellular membrane integrity due to lipid peroxidation or apoptosis (Pohl, *et al.* 1996). Utilizing pharmacokinetic parameters of absorption, metabolism and bioavailability, distribution, and elimination aid in predictable determinations of plasma concentrations within the systemic system (Cashman, *et al.* 1996). Determining the relationship of inter- and intra-individual metabolic alterations and how these relationships are changed by xenobiotic interaction is essential for future prediction of drug bioavailability (Hodgson, *et al.* 1995).

1.3.3. Phase I and Phase II Enzymes

There are two major group classifications for drug metabolizing enzymes, phase I and phase II. Phase I enzymes are classified as a non-synthetic reaction. They modify a drug by either introducing or exposing a polar functional group of the xenobiotic through oxidation, reduction, or hydrolysis, producing a metabolite rendering the compound active, inactive, or bioactive. The two major phase I metabolic enzyme systems that conduct oxidative metabolism are CYP and FMO. These enzymes are present in the membrane of the endoplasmic reticulum. The phase II enzymes conduct a conjugation of the parent compound and/or its phase I formed metabolite to a secondary metabolite resulting in increased polarity. Most therapeutic drugs are lipophilic, which undergo phase I and/or

phase II conjugation to increase the polarity of the metabolite in comparison with the parent compound escalating the excretability (Iyer and Sinz 1999).

Phase I metabolism creates metabolite(s) that may not reach the systemic system resulting in reduced bioavailability and efficacy. The CYP superfamily is a set of metabolizing phase I monooxygenase microsomal hemoproteins ubiquitous in nature (Cashman, *et al.* 1996). The major subfamilies of CYP enzymes metabolizing drugs are 1A2, 2C, 2D6, 2E1, and 3A (Doherty and Charman 2002). The following table, Table 2, presents the major CYP isoforms and the percentage of drugs each isoform will metabolize.

Table 2. An approximate proportion of all drugs metabolized by major CYP metabolizing enzymes.

CYP Isozymes	**% Proportion of CYP metabolism of drugs**
CYP1A2	2
CYP2C	16
CYP2D6	25
CYP2E1	2
CYP3A	55

The subfamily CYP3A is estimated to participate in 55% of the oxidative biotransformation of drugs. There are four members of the CYP3A subfamily found and characterized in humans. In the intestine and liver, the

CYP3A4 is the most abundant form, but CYP3A5 has been found to represent greater than 50% of the total CYP3A in some individuals (Thummel, *et al.* 1997). CYP requires the flavoprotein NADPH-cytochrome P450 reductase for metabolic activity (Klaassen 1996).

CYP REACTION:

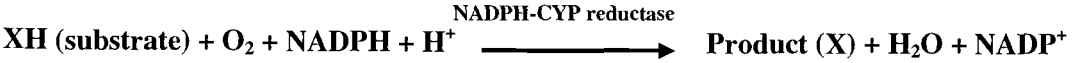

CYP has been found to conduct pre-systemic metabolism in both the liver and the mucosa of the small intestine resulting in a first-pass effect (Cashman, *et al.* 1996). The CYP isozymes 1A2, 2C9, 2C19 2D6, and 3A4 are implicated most often in first-pass elimination (Thummel, *et al.* 1997). Some of the CYP3A4 substrates undergoing metabolic extraction by the gut wall are cyclosporine, midazolam, nifedipine, verapamil (Thummel, *et al.* 1997), and methadone (Oda and Kharasch 2001). In the intestine, the total intestinal CYP3A4 enzyme protein concentration has been reported to be from 23 pmol/mg of intestinal microsomal protein (Thummel, *et al.* 1997) to as high as 70 nmol, predominantly in the jejunum (Hall, *et al.* 1999).

FMOs are also a phase I oxidative monooxygenase. FMO and CYP have often shown activity toward many of the same substrates, but generally FMO enzymes produce different metabolites with fewer bioactivations than CYP, which will be reviewed in the next section (Larsen-Su and Williams 1996).

1.4. HISTORY OF FLAVIN-CONTAINING MONOOXYGENASES (FMO)

1.4.1. Characteristics of FMO

Elucidation of the structure for the specificity of mammalian drug-metabolizing enzymes has made considerable progress in the past decade, due to x-ray crystal structures. In comparative analysis of the different FMOs amongst species, important leads have been determined for structure-function analysis (Halpert, *et al.* 1998). FMO, classified as EC1.14.13.8, a non-heme microsomal FAD-containing enzymatic system (Ziegler 1988), was initially purified from hog liver in the early 1970's. The FMO enzyme has been suggested to be anchored in the endoplasmic reticulum at the hydrophobic NH_2 and COOH termini (Dolphin, *et al.* 1991). FMO is NADPH and oxygen-dependent catalyzing soft nucleophilic compounds with an electron rich center (Ziegler 1988) in drugs, pesticides, and plant products (Halpert, *et al.* 1998, Park, *et al.* 2002) containing nitrogen, sulfur, (Ziegler 1980, Park, *et al.* 2002) phosphorus (Phillips, *et al.* 1995, Park, *et al.* 2002), or selenium (Phillips, *et al.* 1995, Halpert, *et al.* 1998).

The FMO biotransformation can either detoxify a lipophilic compound to a hydrophilic compound for excretion or undergo "bioactivation" resulting in a metabolite that can cause histological changes, carcinogenesis, mutagenesis, or teratogenesis. FMOs are known to produce a less reactive metabolite or completely detoxify a xenobiotic (Ziegler 1990), but can potentially be converted to a toxic intermediate by binding to DNA, RNA, and protein with

detrimental consequences (Atta-Asafo-Adjei, *et al.* 1993). For example, the oxidation of a thiocarbamide results in a sulfenic acid metabolite, which is a highly reactive electrophile (Poulson, *et al.* 1979, Krieter, *et al.* 1984, Decker and Doerge 1991) that can bind to macromolecules in the lung and the liver (Poulson, *et al.* 1979, Krieter, *et al.* 1984, Decker and Doerge 1991) or produce chemical species that inactive CYP (Poulson, *et al.* 1979, Krieter, *et al.* 1984, Decker and Doerge 1991)

1.4.2. Mechanism of FMO

FMOs are present in the cell in the oxygen-activated form and oxygenate soft-nucleophilic xenobiotics. The soft nucleophile can be oxidized when accessible by the enzyme-bound peroxy-flavin intermediate. Other oxidases and monooxygenases are not readily present in the oxygen-activated state, thus FMO is unique in its classification (Ziegler 1990). NADPH, the electron source, binds and reduces the flavin in the first step of the FMO catalytic cycle as shown in Figure 1. In steps two and three, dioxygen reacting with the reduced flavin creates a stable 4α-hydroperoxyflavin intermediate, in the absence of an oxygenatable substrate (Hines, *et al.* 1994). Transference of the oxygen from the hydroperoxyflavin to a substrate occurs in steps 4 and 5, without the formation of an intermediate during the oxygen transfer. The lack of an intermediate formation indicates activation of the substrate is not required. In steps six and seven, a release of the $NADP^+$ occurs. Because steps six and seven occur after substrate

oxygen addition and release of the oxygenated product, the mechanism predicts that at saturation all substrates are oxidized at the same velocity (Ziegler 1988). The energy required for catalysis is already present in the enzyme, therefore a structured enzyme and substrate fit is not required as with other enzymes (Atta-Asafo-Adjei, *et al.* 1993). The result is a catalyzation with efficiency. CYP can oxidize the same nucleophilic heteroatoms and create the same products as an FMO heteroatom oxidation, but CYP is less efficient (Cashman, *et al.* 1996).

FMO reaction: $YH + O_2 + NADPH + H^+ \longrightarrow YOH + H_2O + NADP^+$

(Where Y = substrate)

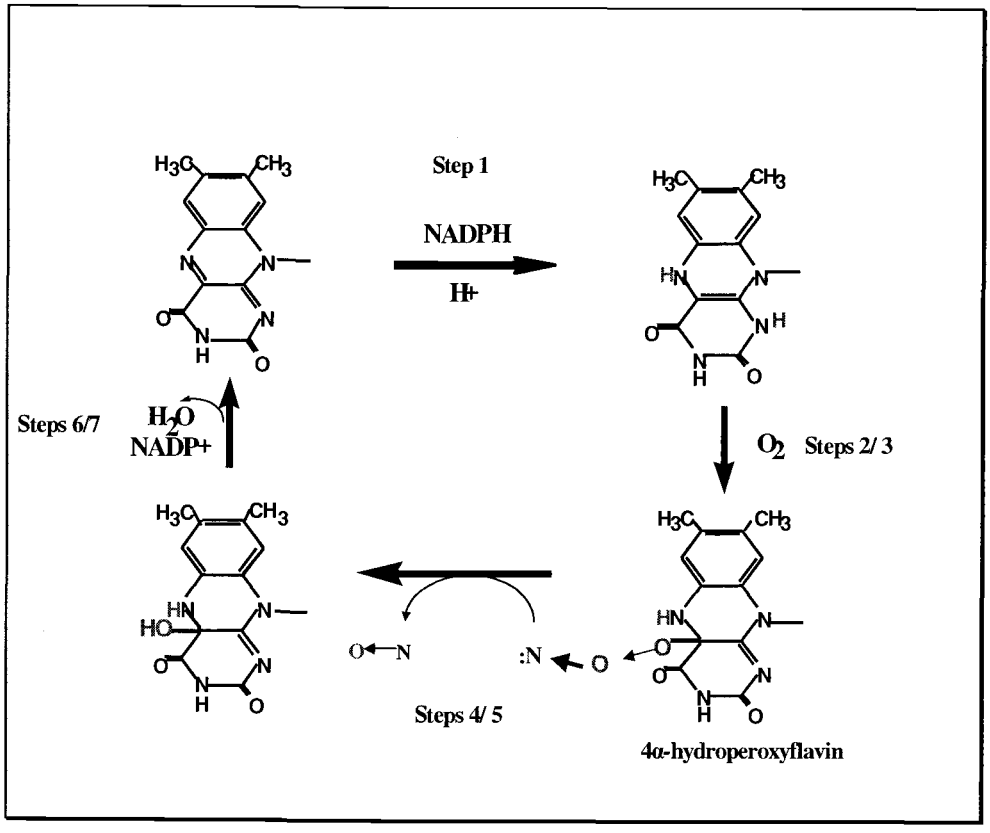

Figure 1: Schematic of the FMO metabolic cycle. Indicated is the substrate binding to the 4α-hydroperoxyflavin (active form) transferring the oxygen to the substrate (N) and reconfiguration to the active form by addition of NADPH and oxygen (Rettie and Fisher 1999).

1.4.3. FMO Isozymes

The FMO family contains five structurally related isoforms encoded by its own gene (Cashman 2002). The FMO gene encoding for all five of the isoforms is located on the chromosome 1q (14). FMO1 – FMO5 contain one non-coding exon and eight coding exons. The sequence and location of the binding domains of the FAD and NADPH motif are conserved in the mammalian isoforms FMO1, 2, 3 and 4 (Ziegler 1990). At the putative active site located between residues 9 –14, FAD is non-covalently bound. The NADPH putative binding site is located between residues 191-196 (Phillips, *et al.* 1995). Near the *N*-terminal region are 2 glycine-rich regions in FMO1 – FMO5, with inherent NADPH and FAD binding (Dolphin 1992). The highest conserved areas are found within four regions producing only 57% of the length of the polypeptide. They are from 1 - 230, 320 - 340, 350 - 370, and 455 to 500 (Phillips, *et al.* 1995). FMO1 – FMO5 contain a primary sequence that is 50-55% identical with each other (Ziegler 1990) and orthologs of various species of sequence identity is approximately 81-89% (Hines, *et al.* 1994). FMO1 – FMO5 are encoded for a functionally active protein, but FMO6 is not (Cashman 2002). Each of the first five mammalian FMOs exhibit distinct, but broad substrate specificity overlapping other FMO family members as well as with CYP isoforms (Hines, *et al.* 2002). Due to tissue specificity and amino acid sequencing, mammalian orthologs of FMO are assigned with amino acid identities greater than 80%. The following diagram, Figure 2, is a representation of pig FMO1 amino acid sequences. FMOs 1, 2, 3, 4 and 5 are 532

to 558 amino acids long (Dolphin, *et al.* 1991, Phillips, *et al.* 1995, Gasser 1996) on 9 exons (Krueger, Williams, *et al.* 2002), and 8 introns (Cashman 1995) and have a molecular mass of approximately 60 kDa to 63 kDa, with FMO 4 being the longest and heaviest. The guidelines for a systematic nomenclature for mammalian FMO followed the CYP identification procedure and were based upon divergent evolutionary relationships (Cashman 1995).

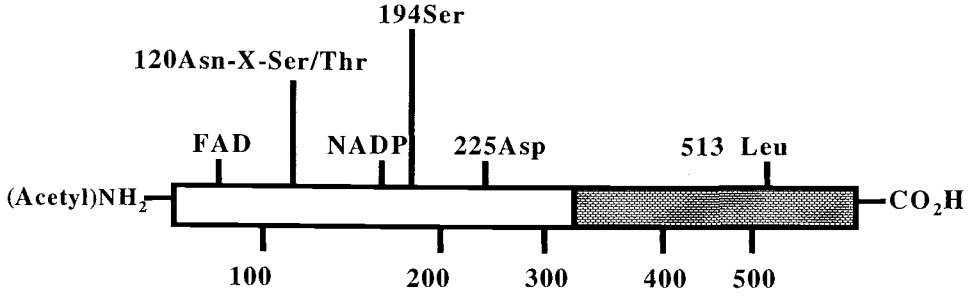

Figure 2: Schematic of the pig FMO1 amino acid sequence. The shaded bar region is the lipophilic C-terminus region of the protein (Cashman 1995).

FMO1 mRNA has been detected in the human fetal liver and is 86% identical to the porcine liver (Dolphin, *et al.* 1991, Gasser 1996), as well as the human adult kidney and skin, but not in the adult liver. Reportedly, FMO1 is expressed in the human adult kidney and in fetal liver tissue at concentrations of 47 ± 9 pmol/mg of microsomal protein and 8 ± 5 pmol/mg of microsomal protein,

respectively (Hines, *et al.* 2002). The lack of detection of FMO1 in the human adult liver, <1 pmol/mg of protein (Yeung, *et al.* 2000), is in contrast to other mammals. FMO1 is the major form of the FMO enzyme in an adult pig or rabbit liver (Phillips, *et al.* 1995). FMO3, the primary form found in abundance in the human adult liver (Lomri, *et al.* 1992, Yeung, *et al.* 2000), has been detected at protein levels of 60 ± 43 pmol/mg of microsomal protein (Hines, *et al.* 2002).

Due to the detection of FMO1 in the human fetal liver and minimal detection in the human adult liver, there appears to be a developmental change from FMO1 to FMO3. A temporal switch sometime after birth in hepatic FMO expression occurs, as found in CYP fetal expression (Yang, *et al.* 1994). During the first few days of birth, irrespective of gestational age, an increase in the CYP3A4 isoform from the CYP3A7 occurs during the early neonatal period suggesting a transition (Lacroix, *et al.* 1997). The FMO3 gene is also increased with developmental regulation, thus FMO1 and FMO3 are tissue-specific and regulatory. On the basis of tissue patterns and developmental expression, FMO isoforms such as FMO1 and FMO3 can be distinguished (Dolphin 1996). The FMO2, FMO4, and FMO5 are expressed in the human adult lung and liver (Dolphin, *et al.* 1991, Phillips, *et al.* 1995, Yeung, *et al.* 2000). FMO5 is also expressed in the kidney (Yeung, *et al.* 2000).

The sixth FMO-like gene was located and identified between the FMO2 and FMO3 genes. The motif of this isoform is 418 amino acids in length. An FMO full-length active protein of 539 amino acids contains both the FAD and

NADPH binding domains. FMO2 has displayed, in previous studies, a truncated version reduced by 64 amino acids that result in an inactive protein; therefore it is probable FMO6 would not exhibit oxidative monooxygenase activity. To date, FMO6 does not indicate the production of a protein and is being considered a pseudogene that is the product of an evolutionary event due to eukaryotic splicing events (Hines, *et al.* 2002). The following table, Table 3, depicts the isozyme and its location within the human body.

Table 3: Individual FMO isozymes present in human tissue.

FMO Isozymes	**Tissue identification and distribution**
FMO1	Adult kidney (Hines, *et al.* 2002), fetal liver (Dolphin, *et al.* 1991, Gasser 1996), intestine (Yeung, *et al.* 2000), esophagus and nasal mucosa (Cashman and Zhang 2002)
FMO2	Lung (Dolphin, *et al.* 1991, Phillips, *et al.* 1995)
FMO3	Liver (Lomri, *et al.* 1992, Yeung, *et al.* 2000, Hines and McCarver 2002), brain (Cashman and Zhang 2002)
FMO4	Lung, liver (Dolphin, *et al.* 1991, Phillips, *et al.* 1995, Yeung, *et al.* 2000), brain (Cashman and Zhang 2002)
FMO5	Lung (Dolphin 1998), kidney (Yeung, *et al.* 2000), brain (Cashman and Zhang 2002)
FMO6	Determined gene location (Hines, *et al.* 2002)

1.4.4. FMO Substrate specificity

Soft nucleophiles such as: secondary and tertiary alkylamines and arylamines, hydrazines, thiocarbamides, thioamides, sulfides, disulfides, and thiols are substrates for FMO oxidation (Ziegler 1990, Hines, *et al.* 1994). Nitrogen-

containing organic compounds such as tertiary amines are good substrates for FMO catalyzation producing an *N*-oxide. Secondary amines are metabolized to a hydroxylamine and/or a nitrone, primary amines to a hydroxylamine and/or oxime, and a hydrazine to a hydrozone (Ziegler 1984). Primary arylamines, when *N*-methylated by *S*-adenosylmethione (SAM), a phase II enzymatic cofactor required for methylation, are found to be good substrates for an FMO reaction. Arylamines such as *N*-methylarylamines undergo oxidation by FMOs to an intermediate hydroxylamine. Further metabolic alteration produce a nitrone and then a primary arylhydroxylamine (Ziegler 1990). FMOs are known for detoxification of organic sulfurs and alkaloids, but activation of mercaptopyrimidines and thiocarbamides result in chemical toxicity (Hines, *et al.* 1994).

Regeneration of a parent compound after reduction can result in a "futile cycle" (Decker and Doerge 1991). Conjugation by reduced glutathione (GSH), a phase II oxidative scavenger, can deactivate a bioactive metabolite. With a cyclic regeneration of the parent compound a depletion of GSH within the tissue can occur (Krieter, *et al.* 1984). For example, FMO-catalyzes oxidation of thioureas to a reactive metabolite, then the parent compound is regenerated upon reduction and established is a futile cycle by oxidation of cellular thiols by NADPH and oxygen that can deplete GSH within the tissues (Hines, *et al.* 1994).

GSH Reaction: $\mathrm{GSSG} \xrightarrow[\text{Glutathione reductase}]{\mathrm{NADPH} + \mathrm{H}^{+}} 2\ \mathrm{GSH}$

The following drugs are substrates for FMO oxidation: imipramine, a tricyclicantidepressant tertiary amine (Adali, *et al.* 1999) and an FMO1 substrate (Wyatt, *et al.* 1998); chlorpromazine, an antipsychotic tertiary amine drug and FMO1 substrate (Adali, *et al.* 1999); methimazole, antithyroid drug (Wyatt, *et al.* 1998) and FMO1/FMO3 substrate (Cashman 2000); and albendazole, a parasitic drug and FMO1 substrate (Villaverde, *et al.* 1995).

1.4.5. FMO Polymorphisms

Polymorphic expression of either phase I or phase II enzymes could have an effect on the efficacy or toxicity of therapeutic drugs. Expression of variable alleles resulting in enhanced or reduced metabolic capacities are associated with genetic predisposition. FMO2 and FMO3, the major adult isoforms in the lung and liver, respectively, have been found to carry polymorphisms. The mutations detected are homozygous amber mutations (premature termination), substitutions, deletions, and truncation mutations resulting in metabolic alterations. The expression of protein from pseudogene FMO6 isoform has not been demonstrated (Krueger, Martin, *et al.* 2002) and to date, a polymorphism in FMO1 has not been determined.

Polymorphism effects are variable between populations, which may indicate a specific mutant genotype (Forrest, *et al.* 2001). Interindividual variation of polymorphic effects in metabolism has been observed, which adds to the

complexity for determination of tissue-specific FMO expression. These variations with other drug metabolizing enzymes are influenced by both environmental and genetic factors, but environmental factors do not appear to have a profound affect on FMO expression (Whetstine, *et al.* 2000).

Genetic polymorphisms have been characterized in two of the six FMO gene families, FMO2 and FMO3 (Krueger, Williams, *et al.* 2002). Human FMO3 polymorphisms appear to be non-randomly distributed within a population. Trimethylaminuria (TMAU), an FMO3 polymorphic disorder, is a biochemical failure to oxidize trimethylamine (TMA) to the *N*-oxide (TMAO). TMAU is characterized by the excretion of an excessive amount of a tertiary aliphatic amine in the urine, sweat, breath and other bodily excretions (Mitchell and Smith 2001, Cashman 2002).

TMA has been shown to be rapidly absorbed from the human GI tract. TMA is metabolized in the gut to the major metabolite TMAO and is cleared by hepatic first-pass metabolism. The metabolism of TMA appears to be mediated by the FMO system (EC 1.14.13.8) and influenced by liver disease (Al-Waiz, *et al.* 1987, Lang, *et al.* 1998). TMAO stabilizes proteins and offsets the destabilizing effects of urea (Zou, *et al.* 2000). TMA arises from dietary choline, contained in egg yolks, organ meats, fish, legumes and whole soybeans (Treacy, *et al.* 1998), carnitine. TMAO may also be formed by intestinal bacterial degradation of choline and lecithin (Cashman, *et al.* 1997, Lang, *et al.* 1998). A diet of brassica vegetables, such as brussel sprouts, broccoli, cabbage, and cauliflower can alter the

urinary ratio of TMAO to TMA, resulting in a transient TMAU condition due to an inhibition effect of human FMO3 by acid condensation products from the presence of indole-3-carbinol (I-3-C) in these vegetables (Cashman, Xiong, Lin, *et al.* 1999). Patients with FMO3 mutations may exhibit an alteration in detoxification or possible bioactivation of drugs dependent upon hepatic FMO3 as a major route of metabolism (Krueger, Williams, *et al.* 2002), such as tricyclic antidepressants or nicotine (Mitchell and Smith 2001). The presence of TMA in human urine was reported for the first time in 1856 (Al-Waiz, *et al.* 1987), but historically anecdotal descriptions of individuals with fish malodor syndrome have been recorded from 1000 BC. Table 4 shows the research and clinical observations of TMA since the first clinical description in 1970 (Mitchell and Smith 2001).

.

Table 4: Observation dates and research regarding trimethylaminuria (TMAU) since the first clinical observation.

Period	Clinical observation since 1970
1970	**First description – "fish odor syndrome"** associated with excessive TMA excretion and Turner's syndrome
1970-1985	**Description of isolated and sporadic cases**
1980	**Recognition of "tainted egg" syndrome** - breed of chicken with dysfunctional *N*-oxidation
1980-1990	**Clinical and biochemical case studies from several countries** characterization of a human genetic polymorphism of TMA *N*- oxidation
1990s	**Molecular genetics of FMO and recognition of candidate mutations** for the fish malodor syndrome

1.5. METABOLIC ALTERATIONS

1.5.1 Concomitant administration of FMO substrates

Metabolic alterations may occur with concomitant administration of CYP/FMO substrates. In one study with human liver microsomes, chlorpromazine and imipramine were found to increase FMO3 metabolic activation of methimazole. The findings indicated the manner and extent of modulation are a function of not only the FMO isoform and effector molecule, but also the concentration of the substrate (Adali, *et al.* 1999).

Another study using FMO1 and FMO2 rabbit and pig, imipramine was found to inhibit and activate the same FMO isoform, which was dependent

upon the concentration of methimazole. In rabbit, imipramine modulated FMO1 and FMO2 and increased the metabolism of methimazole. With pig FMO1, imipramine inhibited the activity of methimazole and demonstrated competitive inhibition. Because rabbit and pig FMO1 orthologs are 87% identical in sequencing, the differences between the responses of pig and rabbit FMO1 could provide a starting point for investigation to determine the interaction of modulators with the FMO isoforms (Wyatt, *et al.* 1998).

In an *in vitro* study, methimazole inhibited rat intestinal microsomal FMO metabolism of albendazole (Villaverde, *et al.* 1995). When methimazole was added to the microsomal preparation containing albendazole, inhibition of the metabolism of albendazole was approximately 50-60%. The sulfoxidation inhibition by methimazole supports the theory that FMO may be involved in intestinal metabolism of albendazole (Villaverde, *et al.* 1995).

1.5.2. Modulation of FMO: inhibition/induction

Co-administration of food or drink can interfere or alter the metabolism, of a xenobiotic by altering the amount and/or activity of drug metabolizing enzymes. Phase I reactions appear to be more susceptible to the effects of food or drink than phase II reactions (Walter-Sack and Klotz 1996). An example is the concomitant administration of grapefruit juice and some medications, such as felodipine (Lown, *et al.* 1997), whereas a change in metabolism occurs (Fuhr, *et al.* 1993). Grapefruit juice has been shown to inhibit

the presystemic or first-pass elimination of certain drugs, such as felodipine, nifedipine, verapamil, and midazolam resulting in an increase in serum concentrations (Miniscalco, *et al.* 1992). CYP appears to be predominantly affected by grapefruit juice administration, particularly CYP3A4. Even though CYP3A4 is expressed in both the liver and the intestine, studies suggest grapefruit juice appears to be most effective at the intestinal level (Maskalyk 2002). For example, with co-administration of grapefruit juice and felodipine an increase in plasma concentrations of felodipine were detected in the systemic system. The grapefruit effect was isolated to CYP3A4 activity in the small intestine, whereas a reduction of CYP3A4 activity did not occur in the colonic mucosa or the liver. The bioavailability of felodipine is 20%, but with acute (one glass of grapefruit juice) and chronic (one glass of grapefruit juice 3 times a day for 5 days) administration of grapefruit juice, the plasma concentrations of felodipine doubled and tripled, respectively (Lown, *et al.* 1997) .

St. John's Wort, an herbal product for the treatment of depression, has been found to induce both intestinal and hepatic CYP3A4 activity. In two studies with concomitant use of St. John's wort and simvastatin (a drug used to lower plasma lipoprotein levels) a decrease in plasma concentrations of the simvastatin occurred (Sugimoto, *et al.* 2001). These findings indicated with the co-administration of herbals, such as St. John's Wort, an alteration in the therapeutics of drugs that are CYP3A4 substrates can occur.

Until recently, a major difference between FMO and CYP was the inability of exogenous xenobiotics to modulate FMO. There has been three *in vivo* dose-response studies conducted in male Fischer 344 rats utilizing indole-3-carbinol (I-3-C), as a modulator for FMO. The I-3-C plant alkaloid produced from the hydrolysis of indole glucosinolate (Katchamart, *et al.* 2000) is found in cruciferous vegetables (Larsen-Su and Williams 1996, Katchamart, *et al.* 2000). A reduction in FMO1 activity and protein levels both in the liver and the intestine and induction of CYP1A1 and CYP1A2 occurred. These studies demonstrated that there was an inhibition and induction from one monooxygenase to another (Larsen-Su and Williams 1996). Administration of I-3-C has the potential to alter metabolism of drugs that are substrates for both CYP and FMO, creating the potential for drug interactions (Katchamart, *et al.* 2000).

Lastly, it has been shown that hepatic Sprague Dawley rat FMO1 was induced by the administration of the polycyclic aromatic hydrocarbon 3-methylcholanthrene (3MC). These results indicated an increase of transcriptional FMO mRNA and enzymatic translational activity (Chung, *et al.* 1997).

1.5.3. Substrate metabolite formation by both CYP and FMO

Discovery of substrates being metabolized by either CYP or FMO is increasing. For example thioridazine, an antipsychotic, undergoes *N*-oxidization by FMO and/or converted to 2-sulfoxide, which is metabolized by CYP to a sulfone. The sulphone is the primary metabolite and has the greater antipsychotic

effect in humans (Hodgson, *et al.* 1995). The drug cimetidine, an H_2 receptor antagonist, which is utilized for the therapeutic treatment of peptic ulcers and gastric hypersecretory syndromes, undergoes metabolism to the *S*-oxide metabolite. Both CYP and FMO are responsible for the formation of an aliphatic sulfoxide of cimetidine in which the biotransformation was greater in the human jejunum than in both rabbit and rat (Lu, *et al.* 1998). *In vitro* microsomal inhibition studies using rabbit jejunum revealed with coincubation of imipramine (1 mM) the metabolite formation of cimetidine (0.4 mM) decreased by 45%. These inhibition studies also demonstrated that in the rabbit jejunum FMO contributed 70% to the sulfoxide metabolite formation of cimetidine and CYP in combination with nonenzymatic oxidation contributed about 30% to cimetidine sulfoxidation (Lu, *et al.* 1998).

In a human liver microsomal study, clozapine (CLZ), an antipsychotic drug, was metabolized by both FMO and CYP (Tugnait, *et al.* 1997). In humans, CLZ undergoes extensive hepatic metabolism of which CLZ *N*-oxide and *N*-desmethyl-CLZ are the major metabolites. Various FMO isozymes from several species were used in a study by Tugnait et al (1997), which used purified minipig FMO1, rabbit FMO2, and human FMO3. These purified FMO samples were incubated with CLZ to evaluate FMO metabolism. Purified FMO3 formed CLZ *N*-oxide, K_m 324 μM and V_{max} of 76.9 mol/mg protein/min. *N*-demethylation was not observed in this study. FMO being heat labile, with further studies of inhibition of FMO by heat inactivation verified FMO as the metabolic enzyme for

metabolite formation of the *N*-oxide, whereas CYP1A2 and CYP3A4 were found to produce the *N*-desmethyl-CLZ metabolite (Tugnait, *et al.* 1997). CLZ has been reported to undergo *N*-oxidization by both FMO and CYP in human liver, however in the rat liver and brain, FMO appears to be primarily responsible for catalyzing the reaction (Fang 2000).

Other examples of crossover metabolism of CYP and FMO enzymes are: (*S*)-nicotine and ranitidine. (*S*)-nicotine undergoes extensive metabolism in humans and 90% of a dose can be accounted for in the urinary metabolites (Cashman, *et al.* 1996). Ranitidine, an H_2-receptor antagonist, has an *e.v.* bioavailability ranging from 50 to 60% and is excreted in the urine (Williams, *et al.* 1992). In rat and human liver microsomes, ranitidine was metabolized to its major metabolite *N*-oxide by hepatic microsomal FMO. In human liver microsomes, ranitidine was converted to its *N*- and *S*-oxides by FMO greater than 93% and to the desmethyl metabolite by CYP1A2, 2C19, and 2D6 as indicated in the following table, Table 5. FMO3 produced a 4 to 1 ratio of *N*-versus *S*-oxide form (Chung, *et al.* 2000).

Table 5: *S*-nicotine and ranitidine substrates are converted to metabolites by individual CYP and FMO isozymes. Human liver microsomes were utilized.

Substrate	Metabolite	Isozyme	Reference
S-nicotine	*S*-cotinine *S*-nicotine *N*-1-oxide	CYP2A6 FMO3	(Cashman, *et al.* 1996)
Ranitidine	*N*- and *S*-oxide *N*-oxide *S*-oxide Desmethylranitidine	FMO1, FMO3 FMO2 FMO5 CYP2C19, 1A2, 2D6	(Chung, *et al.* 2000)

1.6. HUMAN TISSUE AND MODELS: SMALL INTESTINE

1.6.1. Intestinal structure

There are three major regions in the small intestine. They are: the duodenum, which is the shortest at about 20 to 30 cm long and 3 to 5 cm wide; the jejunum, the middle section is approximately 2 meters long; and the ileum is the distal end of the small intestine protruding into the colon, approximately 3 meters long. In comparison, the wall of the jejunum is thicker and wider than in the ileum. From the duodenum to the ileum there is a gradual narrowing of the lumen. The small intestine is comprised of a mucosa, submucosa, muscularis, basolateral membrane, crypt-villus axis, epithelial cells, goblet cells, paneth's cells, M cells, caveolated cells and various junctional complexes such as tight junctions (Thomson 1994) .

A major route for entry of exogenous compounds is the GI tract by serving as an interface with the dietary environment and is the first potential site for metabolism by the intestine (Renwick and George 1989). The GI tract consists of muscular coats lined with mucosal cells that conduct drug oxidation regulating the absorptive and secretory processes (Thomson 1994). The main functions of the mucosa are: secretion of mucus; digestive enzymes and hormones; absorption of the final products from digestion into the blood; and protection against infectious disease (Marieb 2001).

Three sub-layers comprise the digestive mucosa which are: the epithelial layer, a continuous sheet of epithelial cells lining the villi and the crypts; the lamina propria; and the muscularis mucosa which provides structure for the epithelial cells (Thomson 1994, Doherty and Charman 2002). When the sub-layers are combined, the sub-layers are called the crypt-villus unit (Thomson 1994). The epithelium lining contains the villi which contains absorptive cells (enterocytes) for absorption of nutrients and drug molecules. The concentration of the villi and microvilli is the highest in the duodenum and jejunum (Doherty and Charman 2002). Apical microvilli increase the apical surface area from 14 to 40 fold (Madara and Trier 1994). The highest metabolic response is found in the pylorus (opening from stomach to intestine) and small intestine, especially the duodenum and jejunum (Caldwell and Marsh 1982, Renwick and George 1989). Figure 3 indicates individual sites in the intestinal mucosal layer.

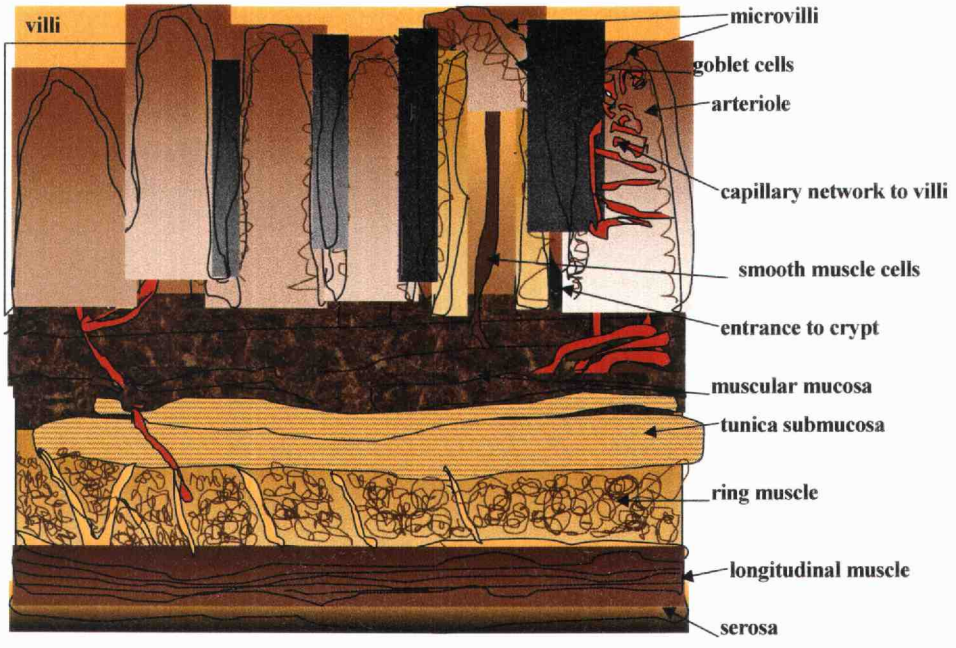

Figure 3: Schematic of small intestinal wall structure.

1.6.2. Intestinal function

Drug metabolism in the GI tract occurs with oral and rectal administration. With these types of administration, a xenobiotic can be metabolized within the lumen or while in the process of being absorbed as it is passing through the mucosa to make its way to the blood stream (Caldwell and Marsh 1982). The pH is 7.5 in the small intestine, with a slight increase in the cecum (junction of the ileum into the colon) to a pH of 8.0 (Renwick 1982). Absorption of water and nutrients is the primary function of the small intestine.

With activity, vasodilators such as vasoreactive intestinal peptides are released from the mucosa of the intestinal tract during digestion. Also, peptide hormones such as cholecystokinin, gastrin, and secretin are secreted from the intestinal mucosa. GI glands will also release kallidin and bradykinin into the gut wall, which are vasodilators. Oxygen concentration also decreases in the gut wall during GI activity resulting in vasodilation, probably due to the release of adenosine. All of the aforementioned contribute to increased blood flow. The GI absorptive capacity can be greatly diminished with a deficit of oxygen in the villus tips creating ischemia, resulting in a blunted villi or the disintegration of the whole villus (Guyton 1991, Madara and Trier 1994). Motor, secretory, and absorptive activity all increase after a meal. Thus, blood flow can increase between 100 to 150 percent and last approximately 3 to 6 hours (Guyton 1991). Of the total volume digested daily, 6 to 12 liters daily, only 10 to 20% passes into the colon (Weisbrodt 1987, Guyton 1991).

A secondary function of the small intestine is the ability to metabolize xenobiotics by phase I and phase II reactions by enzymes located in the epithelial cells (Caldwell and Marsh 1982, Renwick and George 1989, Ilett, *et al.* 1990, Krishna and Klotz 1994). There are two sources of enzymes in the human intestinal lumen: mammalian and bacterial. The bacterial enzymes tend to be more concentrated in the ileum and the colon than in the duodenum and jejunum. The duodenum and the jejunum have the highest activity for phase I

oxidation by CYP and phase II conjugations, such as glucuronidation (Renwick and George 1989).

There are two major pathways solutes will passively penetrate the epithelial mucosa. They are the transcellular and the paracellular pathways. The transcellular, which is across the cell into the cytosol, is accessible to lipophilic compounds and essentially impermeant to passive flow of intermediate to large hydrophilic compounds; therefore permeation by hydrophilic solutes penetrate through tight junctions that join the epithelial cells. The tight junctions regulate epithelial permeability through the paracellular flow of fluid (Madara and Trier 1994). Drug metabolizing enzymes are located in the enterocytes of the villi therefore metabolic biotransformation can occur when the drug enters the cytosol. Xenobiotics that are passively absorbed by way of the paracellular route are less likely to undergo significant biotransformation (Doherty and Charman 2002).

With phase II conjugation reactions, saturation can occur with the presence of excess substrate due to the low availability of cofactors. (Note: saturation can also occur with phase I reactions). With saturation, dose-dependent metabolism, and drug-drug interaction could occur with concomitant drug administration. Sulfation and glucuronidation conjugation reactions are more prevelant in the GI tract than phase I reactions (Caldwell and Marsh 1982). However, unknown variables still exist such as the presence of FMO within the intestinal mucosa, which could be a factor for determination.

1.7. LIVER: MODEL FOR DETECTION OF HEPATIC INJURY

1.7.1. Introduction

The first part of this dissertation investigates the acute hepatotoxicity of ketoconazole (KT) in Sprague-Dawley rats, thus a brief overview of the function/hepatic injury will be briefly discussed. The liver as a major organ of vertebrates conducts a complex role in excretion and detoxification. Xenobiotics are metabolized in the intestine and liver and both organs can be responsible for detoxication/bioactivation of orally administered drugs. The following diagram, Figure 4, represents the relationship of the liver, gall bladder, and small intestine within the human body, depicting the portal vein, hepatic artery, vena cava, and common bile duct locations.

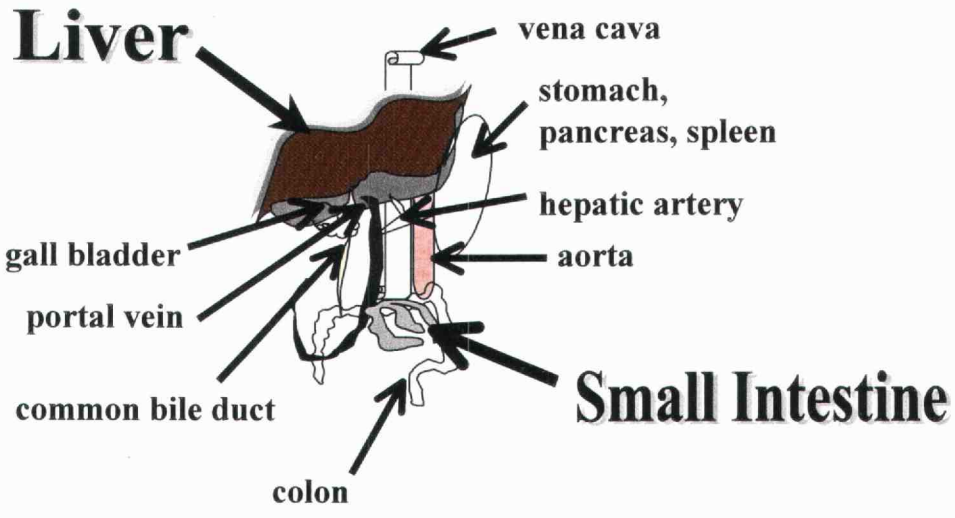

Figure 4: Schematic of the human liver in relationship to small intestine. Adapted from Klaassen (1996).

Within the liver, enzymes catalyzing xenobiotic biotransformation are located primarily in the endoplasmic reticulum (ER) or the soluble fraction of the cytoplasm, with lesser amounts in the mitochondria, nuclei, and lysosomes (Lewis 1998). A dual blood flow is supplied to the liver. Venous blood flows from the gut, spleen, and pancreas (60 –70 %) through the portal vein and on into the liver. From the liver, the blood passes through millions of fine liver sinusoids, and leaves the liver by the hepatic veins emptying into the vena cava (Guyton 1991). Oxygenated blood enters the liver through the hepatic artery (30 – 40% of blood flow to the liver) and passes through the sinusoids (channels between cords of cells

called hepatocytes) and is collected by hepatic veins that feed into the vena cava (Klaassen 1996). This dual blood supply aids in maintaining metabolic homeostasis. Cell types of the liver consist of: i) the parenchymal (hepatocytes) that are involved in active plasma membrane turnover (endocytosis); ii) the sinusoid cells, which are endothelial cells that exchange fluids and molecules such as proteins (i.e. albumin); iii) the Kupffer cells, the macrophages located within the lumen of the sinuosoids; and iv) the Ito cells, endothelial cells that store fat and vitamin A (Klaassen 1996).

Figure 5 represents the acinus, the functional unit of the liver. Terminal branches of the portal vein and hepatic artery extend out from the portal tracts of the acinus. Blood supplied by the portal vein and hepatic artery flows down the acinus past cords of hepatocytes. The acinus is divided into three regions: zone 1, zone 2, and zone 3. Zone 1 is the closest to the blood entrance and has the highest oxygen content, bile salt concentrations, and levels of glutathione (GSH). Zone 3 contains the highest levels of CYP (Klaassen 1996).

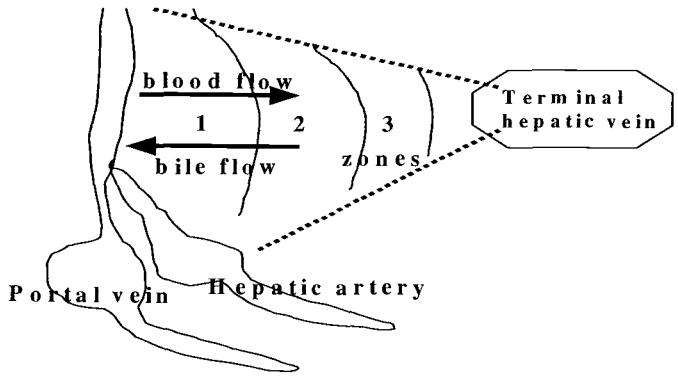

Figure 5: Diagram of the acinus, the functional unit of the liver. Featured is the blood and bile flow from the portal vein and hepatic artery passing through zones 1, 2, and 3 (where metabolism occurs) and out through the terminal hepatic vein.

1.7.2. Liver function

The formation of bile fluid is a specialized function of the liver. The bile, a dark yellow or brown-green alkaline secretion, contains cholesterol, bile salts (emulsification of dietary fats), bile pigments (bilirubin and biliverdin), lecithin, phospholipids, electrolytes, urea and various xenobiotics/metabolites (Gilman, *et al.* 1996). The bile will be moved from the bile duct into the duodenum by the pressure contractions of the gall bladder. The contents in the bile may either be excreted or recycled to the parent xenobiotic and/or metabolites. Recycling is referred to as enterohepatic circulation where a xenobiotic can undergo reabsorption. If the enterohepatic circulation process occurs several

times, a longer half-life for a xenobiotic will occur (Gilman, *et al.* 1996, Klaassen 1996).

With age the liver decreases in weight (20% in males and 11% in females) and appears brown due to an accumulation of pigmented waste products within the hepatocytes, 'brown atrophy'. Blood flow in the aging liver is reduced by 40%. Because phase I reactions are dependent upon oxygen, a reduction of phase I metabolism can occur in the elderly. Thus, drug dosage regimens should be altered for drugs that undergo phase I metabolism in aging patients (LeCouter and McLean 1998).

1.8. INTESTINAL CELL LINES

1.8.1. Cell culture

Intestinal cell cultures were used in the second part of this dissertation to detect the presence of FMO therefore a brief descriptive overview of a cell line will be presented. Cell line culture is derived from intact or dissociated tissues or an organ fragment known as a primary culture, as depicted in Figure 6. When a primary culture is propagated to another culture vessel, it is considered a subculture. The subculture is identified by a numbering system, known as a passage. Sub-cultured populations are considered cell strains based upon the expression of specific properties, functional characteristics, or markers. If a subculture is derived from a single cell it is considered a clonal culture.

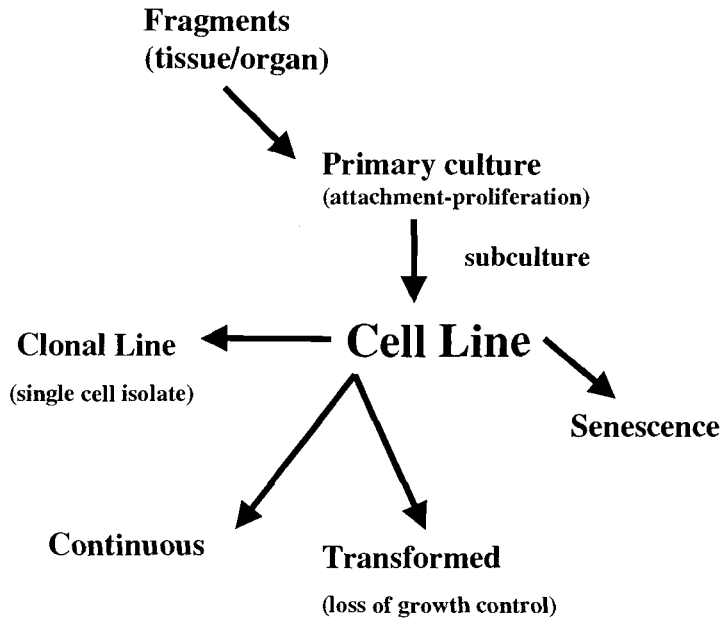

Figure 6: Schematic of a cell line lineage. Depicted are different types of cell lines created from a primary culture.

1.8.2. Cell line background

Mixed function oxidase activities are present not only in the liver, but also in other organs including the intestinal epithelium. Due to the anatomical relationships and functional properties, the intestinal epithelium contains the highest concentrations of ingested compounds resulting in an important role in intestinal metabolism (Bonkovsky, *et al.* 1985). The epithelium is highly dynamic and is continuously renewed by cell generation and migration from the proliferative stem cell population. In non-cancerous epithelial cell lines, such as

intestinal CCL241 and colon CRL1790, the size and shape properties of the cell and nuclei are nearly uniform. Confluent cells will not pile up and the confluent density is approximately 2 -16 x 10^4 cells/cm^2. With malignant cells, the size and shape of cells and nuclei vary with a confluent density as high as 2 – 12 x 10^5 cells/cm^2 (Owens, *et al.* 1976). Due to the unavailability and difficulty in production of normal human intestinal epithelial cell lines, most of the information concerning human intestinal cell regulation has been obtained from cell cultures generated from experimental animals and the human colon cancerous lines, such as Caco-2 cells (Perreault and Beaulieu 1998).

Even though Caco-2 cells are a colonic origin cell line, they spontaneously differentiate into columnar cells when cultured *in vitro*. They possess microvilli and have a polarized distribution of brush border enzymes, resulting in barrier-like characteristics resembling human primary small intestinal cells (Lampen, *et al.* 1998). The Caco-2 cells have been used for i) transport of drug studies (Karlsson, *et al.* 1993, Lampen, *et al.* 1998), ii) transport of bile acid investigation (Karlsson, *et al.* 1993, Lampen, *et al.* 1998), and, iii) expression of glutathione-*S*-transferases (Peters and Roelofs 1992). Enzymes detected in Caco-2 cells are: CYP1A1, CYP2E1, and CYP3A (Lampen, *et al.* 1998), but CYP3A4 has been found to be at low levels in Caco-2 cells. However, with continuous culture and induction with 1α, 25-dihydroxyvitamin D, a large increase in CYP3A4 activity occurs. A Caco-2 clone, TC7 cells, has been shown to express after confluency higher levels of the expression of CYP3A4 in both mRNA and

protein levels (Carriere, *et al.* 2001). CYP1A1, a bioactivator of procarcinogens (McNicholas, *et al.* 1990, Cross, *et al.* 1991), in Caco-2 cells has been found to be expressed at both the protein and mRNA levels. CYP1A1 also could be induced by β-naphtholflavone and 3-methylcholanthrene (3MC) (Lampen, *et al.* 1998). Also, alkaline phosphatase activity has been detected in Caco-2 cells and is considered a reliable marker for differentiated small intestinal enterocytes. Caco-2 cells have been a useful tool for evaluating metabolism of xenobiotics by the intestine (Lampen, *et al.* 1998).

1.9. KETOCONAZOLE (KT)

1.9.1. Pharmacokinetics (ADME)

Part of this dissertation investigates the possible metabolic bioactivation pathway associated with hepatotoxicity of KT, therefore a brief overview of KT will be presented. KT, following an oral administration of a 200 mg dose with a meal has a mean peak plasma level of approximately 3.5 μg/mL, which is reached within 1 to 2 hours. Metabolism of KT involves the conversion into several metabolites, such as the oxidation and degradation of the imidazole and piperazine rings, oxidative O-dealkylation and aromatic hydroxylation. Approximately 13% is excreted in the urine (2 – 4% unchanged), but the major route of excretion is through the bile into the intestinal tract. KT appears dose-dependent with a half-life from an oral 200 mg dose of 1.5 to 4 hours, but with repeated dosing the half-life has been found to increase (Gascoigne, *et al.* 1981,

Daneshmend, *et al.* 1983, Daneshmend and Warnock 1988). With administration of a higher dose (400 mg-KT/day), the half-life has been found to increase to 2.21 – 2.7 hours. In cancer patients, administration of a 400 to 800 mg-KT/day dose results in a mean half-life of 3 hours has been observed ranging from 1.3 to 11.6 hours (Daneshmend and Warnock 1988). Itraconazole, an azole family member, (Venkatakrishnan, *et al.* 2000) also exhibited dose dependant kinetics after multiple doses resulting in an increase in plasma levels. Absolute bioavailability in conditions of saturated first-pass metabolism was higher (Heykants, *et al.* 1989). Both KT and itraconazole have been found to reversibly interact through an azole nitrogen ligation with the heme group of CYP (Heykants, *et al.* 1989, Venkatakrishnan, *et al.* 2000). Thus, long-term administration would result in auto inhibition of metabolism and a potential problem for drug accumulation (Heel, *et al.* 1982). In human blood, only 1% of the compound KT is present as a free drug in plasma (Daneshmend and Warnock 1988), 83.7% is bound to plasma proteins and 15.3% is present within the blood cells (Daneshmend 1984). The therapeutic concentrations, dosages, and duration of treatment for KT vary depending upon the medical diagnosis. The mean peak serum concentrations of KT in humans range from 8 μM to 19 μM after a 200 mg/day dose (Heel, *et al.* 1982) and from 13 μM to 26 μM following a 400 mg/day dose (Baxter, *et al.* 1986). However, KT plasma concentrations have been reported to be as high as 94 μM (Baxter, *et al.* 1986, Sugar, *et al.* 1987). In humans, a disproportionate increase in the AUC has

been observed following oral doses of 100, 200, 400, 600, and 800 mg (Heel, *et al.* 1982). Figure 7 is a depiction of the molecular structure of KT.

KETOCONAZOLE (KT)

"Cis-1-acetyl-4-[4-[[2-(3,4-dichlorophenyl)-2-(1H-imidazol-1-yLmethyl)-1,3-dioxolan-4-yL]methoxy]phenyl]piperazine"

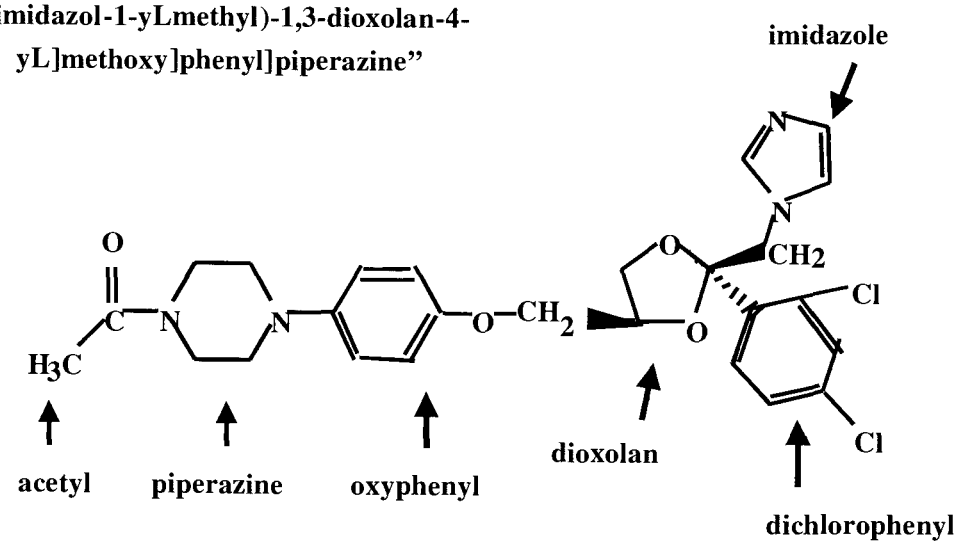

Figure 7: Structure of ketoconazole (KT). The compound is composed of (depicted by arrow indicators) an acetyl group, a piperazine ring, oxyphenyl group, dioxolan ring, dichlorophenyl ring, a methyl group, and an imidazole ring.

1.9.2. Application and clinical usage

KT is a broad-spectrum antifungal, which is therapeutically effective against systemic mycosis, especially in patients who are susceptible to opportunistic systemic fungal infections. KT is administered orally as a tablet or capsule (200 to 400 mg), or topically as a shampoo, cream, or ointment (2%) (PDR

1999). In fungi, KT blocks the conversion of lanosterol to ergosterol by inhibiting the CYP, lanosterol 14 α-demethylase, for the oxidative removal of C-14 methyl group from lanosterol. This incomplete removal results in a loss of membrane integrity.

In rats, plasma levels of 24 μM and 62 μM of KT resulted from 10 mg/kg and 20 mg/kg doses, respectively (Gascoigne, *et al.* 1981). After oral administration in rats, KT and/or its metabolites have shown a higher concentration in the liver than in the plasma (Gascoigne, *et al.* 1981, Whitehouse, *et al.* 1990). Specific tissue binding to hepatic microsomal fractions was reported to be 89% (Daneshmend and Warnock 1988), indicating possible inhibition of mixed function oxidative metabolism with the binding of KT to rat liver *in vivo* and *in vitro*.

Accumulation of KT is of concern due to the inhibition of the synthesis of testosterone when utilized for the therapeutic effects in the treatment of androgen-dependent afflictions such as prostate cancer. Prostate cancer is the second leading cause of cancer death in American men where the probability of one in five men will develop prostate cancer during their lifetime (IIT 1999). Inhibited are the precursors of testosterone. Inhibition of 17,20-lyase blocks the synthesis of dehydroepiandrosterone and androstenedione (Bok and Small 1999). High doses of KT 400 mg/8 hrs or 600-mg/12 hrs for six to nine months elicit significant deprivation of androgen, the major contributor to elevating prostate cancer (Decoster, *et al.* 1996, Bok and Small 1999).

1.9.3. Ketoconazole: adverse effects

There have been numerous documented cases of KT-induced hepatotoxicity. The hepatotoxic symptoms can be mild to severe and may develop within two days or up to one year after the initiation of therapy (Knight, *et al.* 1991). It has been speculated that the hepatotoxicity associated with KT may be a result of the parent compound and/or reactive metabolite(s) that covalently binds with hepatic macromolecules, thereby producing hepatic damage (Buckholz and Rodriguez 2000). The hepatotoxicity appears to be reversible with discontinued use of KT (Lewis, *et al.* 1984, Chien, *et al.* 1997). KT administration has been associated with fatalities (Duarte, *et al.* 1984, Janssen 1995) and numerous cases of hepatitis, resulting in an increase in serum liver enzymes from liver cytosolic enzymes indicating possible hepatic damage (MacNair, *et al.* 1981, Lewis, *et al.* 1984, Stricker, *et al.* 1986, Knight, *et al.* 1991, Chien, *et al.* 1997). Other symptomatic problems include malaise, dark urine, jaundice (Van Parys, *et al.* 1987), headache, dizziness, drowsiness, and papilloedema (Bok and Small 1999).

The first reported KT-induced hepatitis was in 1981 (MacNair, *et al.* 1981), and the first fatality occurred in 1982 due to hepatic coma (Duarte, *et al.* 1984). Sudden hepatitis has led to several deaths even though the patients undergo frequent laboratory and clinical evaluations (Lewis, *et al.* 1984, Duarte, *et al.* 1984, Bercoff, *et al.* 1985, Stricker, *et al.* 1986). Two other patients that suffered KT-induced hepatitis survived due to liver transplants (Knight, *et al.* 1991, Brusko and Marten 1991). The autopsy of a patient who died of KT treatment revealed

massive hepatocellular necrosis (Lewis, *et al.* 1984). Moreover, a European trial of high dose KT (1,200 mg/day) for prostate cancer resulted in 11 deaths out of 350 participants within two weeks of starting the high-dose therapy (Janssen 1995).

Mechanistic evaluation could aid in future structural analysis of an entire chemical family, such as the azoles. Clinical symptoms, such as increases in serum bilirubin and alanine transaminase (Van Parys, *et al.* 1987) indicate cellular damage, but the toxic mechanistic profile of KT is still unclear in humans (Bok and Small 1999) and animals. It is suspected that toxicity responses are not due to an immunoallergic mechanism (Bok and Small 1999), but a direct attack by either KT and/or its metabolites (Lewis, *et al.* 1984, Stricker, *et al.* 1986, Brusko and Marten 1991). Clinical results involving 270 patients demonstrated KT administration and the injury that was incurred was metabolic rather than a hypersensitive idiosyncracy (Chien, *et al.* 1997). An *in vitro* study using cultured rat hepatocytes demonstrated that the primary metabolite of KT, *N*-deacetyl ketoconazole (DAK), was more hepatotoxic than KT (Rodriguez and Acosta 1997). It has been established that the primary metabolite, DAK, undergoes FMO-mediated metabolism to the *N*-deacetyl-*N*-hydroxy ketoconazole (*N*-hydroxy-DAK) metabolite depicted in Figure 8 (Rodriguez and Acosta 1997, Rodriguez, *et al.* 1999). The *N*-hydroxy-DAK metabolite is a secondary hydroxylamine,

which is susceptible to further FMO-mediated oxidative reactions. Further FMO oxidation could produce toxic and reactive metabolites that might be responsible, in part, for the toxicity of KT.

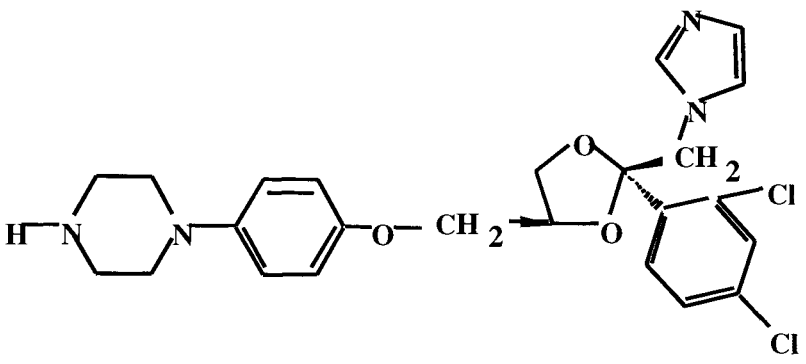

N-deacetyl ketoconazole (DAK)

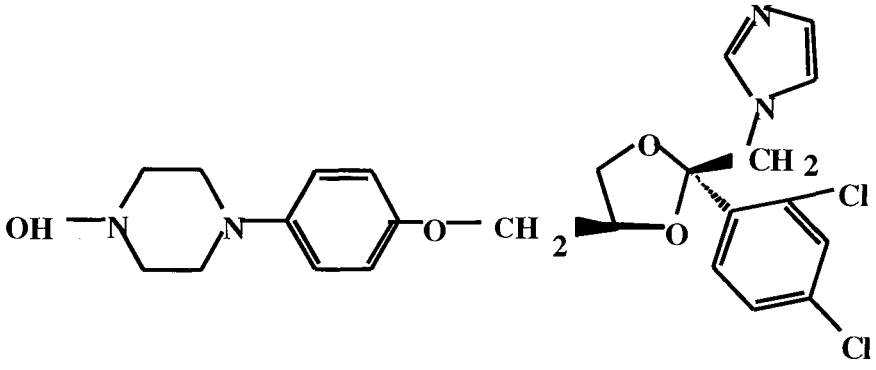

N-hydroxy-*N*-deacetyl ketoconazole (*N*-hydroxy-DAK)

Figure 8: *N*-deacetyl ketoconazole (DAK) and *N*-hydroxy-*N*-deacetyl ketoconazole (*N*-hydroxy-DAK).

To date, there has not been a mechanistic determination of the hepatotoxicity associated with KT *in vivo* as well as the investigation of the FMO isoforms within the human intestine and representative intestinal cell lines. The first part of this dissertation will evaluate the possible metabolic bioactivation pathways of KT by CYP or FMO, which could be responsible for producing toxic metabolites resulting in hepatic injury. The second part of this dissertation investigates the presence of individual FMO isoforms within the human intestinal tract components, as well as intestinal, human epithelial colon, and the colorectal Caco-2 cell line. Detection of FMO could aid in future predictions of drug metabolism and the outcome of an administered drug metabolized by FMO. The presence of FMO could result in reduced bioavailability due to a first-pass effect and/or toxicity effect with increased serum concentrations from modulation of FMO.

CHAPTER 2:HEPATOXICITY OF KETOCONAZOLE IN SPRAGUE DAWLEY RATS: GLUTATHIONE DEPLETION, FLAVIN-CONTAINING MONOOXYGENASES-MEDIATED BIOACTIVATION, AND HEPATIC COVALENT BINDING

C. J. Buckholz and R. J. Rodriguez
Submitted to Xenobiotica

2.1. ABSTRACT

This study evaluates ketoconazole (KT)-induced hepatotoxicity using *in vivo* and *in vitro* approaches. *In vivo* experiments were conducted using male Sprague-Dawley (SD) rats with ^{3}H-KT (1.5 μCi/mg) at 40 and 90 mg KT/kg doses. Blood and liver samples were collected 0 thru 24 hours for alanine aminotransaminase (ALT), glutathione (GSH), and covalent binding analyses. Covalent binding occurred as early as 0.5 hour, peaked at 2 hours (0.026 ± 0.01 nmol KT/mg protein) and 8 hours (0.088 ± 0.04 nmol KT/mg protein) for 40 and 90 mg KT/kg doses, respectively. Increases in ALT levels occurred at 0.5-hour for the 40 and 90 mg KT/kg doses (44.3 and 56.4 U/mL, respectively) in comparison to control, 22.7 U/mL. The 90 mg KT/kg dose at 24 hours reduced hepatic GSH levels from 9.92 ± 1.1 to 4.76 ± 0.3 nmol GSH/mg hepatic protein. Experiments to evaluate the role of the flavin-containing monooxygenases (FMO) utilized SD hepatic microsomes with 1, 10, and 100 μM [^{3}H] KT. Maximum covalent binding occurred at 100 μM KT. Heat inactivation of microsomal-FMO significantly decreased covalent binding by 75% while 1 mM GSH significantly reduced covalent binding by 65%. Co-treatment (heat inactivation and 1 mM GSH) resulted in 80% decreased covalent binding. Thus, KT-induced hepatotoxicity is dose- and time-dependent and appears to be FMO-mediated, in part, to metabolites that may react with protein and possibly, GSH.

2.2. INTRODUCTION

Analysis *in vivo* was conducted with Sprague Dawley (SD) rats to determine if a dose- and time-dependent response would result in tight or covalent binding effects, as well as to establish a correlation with a change in serum enzymes indicated by the release and reduction of alanine transaminase (ALT) and glutathione (GSH), respectively. Elucidation of these effects would indicate a relationship between metabolism, toxicity, and covalent binding. A reduction of GSH would be expected if bioactivation of an electrophilic metabolite occurred due to the conjugating nature of this cellular scavenger to preserve the integrity of the cell (Hogberg and Kristoferson 1977b). Comparative analysis *in vitro* with SD microsomes were conducted to determine if covalent binding effects would occur *in vitro* also and due to the nature of GSH as an electophilic scavenger by detoxification through conjugation (Hogberg and Kristoferson 1977a), covalent binding analysis was implement with the addition of 1 mM GSH (Cribb, *et al.* 1991, Pirmohamed, *et al.* 1995) to determine if the addition of GSH would alter binding effects in microsomal preparations. To determine the involvement of CYP and/or FMO bioactivation a comparative evaluation of covalent binding of KT, heat inactivation was implemented *in vitro* due to the heat lability of the FMO enzyme (Ziegler 1980). Also due to reported inhibition and induction of FMO and CYP by I-3-C in the liver and intestine of Fischer 344 rats (Larsen-Su and Williams 1996, Cashman, Xiong, Lin, *et al.* 1999, Katchamart, *et al.* 2000), respectively, *in vitro* analysis utilizing Fischer 344 rat microsomes (treated with I-

3-C) for covalent binding effects was implemented. The hepatotoxicity of KT is possibly due to a covalent binding effect with hepatic macromolecules by the parent compound and/or reactive metabolites; thereby producing hepatic damage. These experimental findings will aid in establishing a correlation between the *in vivo* and *in vitro* studies.

2.3. MATERIALS AND METHODS

2.3.1. Chemicals and Supplies

KT was a generous gift from Janssen Pharmaceuticals (Olen, Belgium), ^{3}H- KT (5 Ci/mmole, 98% purity) was purchased from American Radiolabeled Chemicals, Inc., (St. Louis, MO). Reduced glutathione (GSH), oxidized glutathione (GSSH) reductase, 5,5'-dithiobis(2-nitrobenzoic acid) (DTNB), NAPDH, trichloroacetic acid (TCA), sodium hydroxide, Trizma, ethylenediaminetetraacetic acid (EDTA), sucrose, glycerol, glucose-6-phosphate, glucose-6-phosphate dehydrogenase, and NADP+ were purchased from Sigma (St. Louis, MO). Alanine aminotransaminase (ALT) analysis was conducted with Sigma Diagnostics Transaminases kit (ALT/GPT), No. 505-P, (St. Louis, MO). HPLC grade methanol was purchased from Fisher Scientific (Fair Lawn, NJ) and CytoScint was purchased from ICN (Costa Mesa, CA). Sprague-Dawley (SD) rats were purchased from Simonsen Laboratories, Inc. (Gilroy, CA).

2.3.2. Statistical analysis – *in vivo* and *in vitro* SD rat covalent binding, GSH, ALT analyses, and SD microsomes:

SD rat statistical analysis of the analysis of variance (ANOVA) was performed by SAS statistical program, version 8.01, from SAS Institute, Inc., (Cary, NC) to determine *in vivo* covalent binding significance. Tukey's multiple comparison was performed for the *in vivo* ALT study and Dunnett's multiple comparison was performed for the *in vivo* GSH studies. ANOVA analyses were performed for the *in vitro* dose- and time-response studies of SD hepatic

microsomes, GSH, and heat inactivation analysis. Probability values of $P \leq 0.05$ were considered statistically significant.

2.3.3. Methods

2.3.3.1. Animal treatment and collection

Male SD rats (200 – 220 g) were treated intraperitoneally (ip) with ^{3}H-KT (1.5 μCi/mg) at doses of 40 and 90 mg KT/kg. Control rats were treated with 0.9% normal saline. Blood and liver samples were collected at 0, 0.5, 1, 2, 4, 8, 12 and 24 hours for ALT, GSH, and covalent binding analyses. The blood samples and approximately 1.1 gm of the liver were placed on ice for ALT, GSH, covalent binding, and protein determination. The remaining liver samples were snap-frozen and placed in a –80 ° C freezer for metabolite isolation, purification, and identification studies. All experiments were performed in triplicate.

2.3.3.2. *In vivo* - SD rat covalent binding, alanine aminotransaminase (ALT), and glutathione (GSH) analysis: (Protocols A, B, and C)

After the male SD rats were administered ^{3}H-KT (1.5 μCi/mg) at doses of 40 and 90 mg KT/kg, approximately 1 gram from each of the liver samples were homogenized with homogenization buffer. One mL of the homogenate was mixed with ice-cold trichloroacetic acid (TCA) and centrifuged for 10 minutes to precipitate the protein. The pellet was then washed thrice with ice-cold TCA and then washed six times with ice-cold methanol, until the

supernatant fraction of the wash achieved background levels of radioactivity. The final protein pellet was dissolved at 60 ° C for 1 hour and aliquoted into scintillation vials containing scintillation fluid with 1.5% (v/v) glacial acetic acid. Radioactivity was measured in disintegrations per minute (dpms) and normalized to nmol KT/mg protein. Protein concentrations were determined using the Coomassie Plus™ Protein Assay from Pierce (Rockford, IL). All studies were performed in triplicate.

ALT serum determinations were conducted utilizing blood samples collected at 0, 0.5, 1, 2, 4, 8, 12, and 24-hour time points and the blood samples were immediately placed on ice and allowed to coagulate prior to centrifugation at 4 ° C and 8,000 x g (Protocol B). The serum was collected and kept on ice. The ALT was assayed using a modified procedure for small sample volumes. Alanine alpha-ketoglutarate was placed into a test tube into a 37 ° C water bath with the addition of serum and normal saline. The sample mixture was gently mixed and placed back into the 37 ° C water bath and incubated. After incubation, the color reagent was added to the incubation-mixture, vortexed (low speed), and left at room temperature for 20 minutes, then 0.4 N NaOH was added to the mixture and vortexed. After 5 min, an allotted amount of the sample mixture was placed into a 96-well plate and the absorbance was measured spectrophotometrically in units/mL (U/mL). ALT catalyzes conversion of alpha-ketoglutarate and alanine to glutamate and pyruvate. Comparisons were made with control rats injected with normal saline. All experiments were performed in triplicate.

Collection of liver samples occurred between 8:30 AM and 11:30 AM to avoid diurnal pattern variations (Jaeger et al. 1973). The method of Roberts and Francetic in 1993 was used for GSH analysis. A 50 mg liver sample was immediately removed from the rat, blotted dry, weighed, and placed in sulfosalicylic acid (SSA, w/v in water) (Protocol C). The liver samples were homogenized and centrifuged for 10 minutes. The resulting supernatant was diluted 10-fold with sample buffer and placed on ice. A 300 μL aliquot of the sample was combined in a vial with sample buffer, and vortexed. A100 μL sample was placed into a 96-well plate in duplicate. After a 1 minute incubation in the 96-well plate, 100 μL NADPH was added to the sample mixture, mixed, and absorbance was monitored on a spectrophotometer at 412 nm at time zero and every 30 seconds for 1.5 minutes. The change in absorbance per minute was determined and converted to μmol GSH using a calibration curve with known standards. The results were expressed in µmol GSH/g protein.

2.3.3.3. SD rat *in vitro* microsomal preparation for covalent binding analysis: (Protocol D)

The liver tissues were removed from male SD rats and immediately placed on ice. The tissues were homogenized in homogenization buffer. Microsomes were prepared by standard differential centrifugation and stored in resuspension buffer, pH 7.5. The microsomes were frozen in liquid nitrogen and stored at –80 ° C. Protein concentrations were determined using the Coomassie

Plus™ Protein Assay from Pierce (Rockford, IL). Fischer rat microsomes were courtesy of Dr. D. E. Williams, Oregon State University, Corvallis, Oregon.

2.3.3.4. SD rat *in vitro* covalent binding, GSH, and metabolic pathway analyses in hepatic microsomes : (Protocol E)

Covalent binding of KT and/or its metabolites to hepatic microsomal protein and a protein variation analyses were performed to determine linearity. The microsomal-incubation mixture consisted of three different microsomal protein concentrations, incubation buffer, increasing concentrations of KT with ^{3}H-KT (1 μCi/mL), and the NADPH-generating system and was incubated at 37 ° C in a total volume of 0.5 mL. A negative control without the NADPH-generating system was performed with each experiment. The microsomal-incubations were terminated at respective time points and the protein was precipitated, washed, and radioactivity was determined. All experiments were performed in triplicate.

To evaluate the affect of GSH on the 'covalent' binding of KT and/or its metabolites, co-incubations of 100 μM ^{3}H-KT (1 μCi/mL) and 1 mM GSH using the 1 mg/mL microsomal-incubations in were performed in triplicate and terminated at the 0, 1, 4, and 8 hour time points.

To evaluate the effect of FMO on the covalent binding of KT and/or its metabolites, microsomal-FMO activity, not CYP activity, was inhibited by heat-inactivation (Ziegler 1980). The microsomes were heated at 50 ° C for 90 sec before adding them to the incubation mixture containing 100 μM ^{3}H-KT (1 μCi/mL), 1 mg/mL microsomal protein, and incubation buffer for a total volume of

0.5 mL. The microsomal incubation was terminated at 0, 1, 4, and 8 hours with 0.5 mL 0.9 M trichloroacetic acid (TCA). Lastly, heat-inactivation and 1 mM GSH incubation was performed with 100 μM ^{3}H-KT (1 μCi/mL), 1 mg/mL microsomal protein, and incubation buffer for a total of 0.5 mL was performed at 0, 1, 4, and 8 hours (Protocol E). Comparisons of GSH incubations and heat-inactivated experiments were compared with the normal experimental conditions.

2.3.3.5. *In vitro* microsomal analyses of pretreated Fischer rats with indole-3-carbinol (I-3-C)

Due to a predicted inhibition of the FMO enzyme by I-3-C in the liver and intestine of Fischer 344 rats (Larsen-Su and Williams 1996, Cashman, Xiong, Lin, *et al.* 1999) and reported induction of CYP (Katchamart, *et al.* 2000), comparative experiments were conducted to observe whether covalent binding would occur where possible inhibition of FMO would occur. Three experiments utilizing microsomes from pretreated Fischer 344 rats with I-3-C were conducted with a concentration of 1 mM microsomal protein, 10 μM of KT with 3H-KT (1 μCi/mL), and the NADPH-generating system, incubated at 37 ° C in a total

volume of 0.5 mL (Protocol E) and terminated at the 0, 0.5, 1, 2, and 4-hour time points. The protein was precipitated, washed, and radioactivity was determined. The negative controls were the microsomes from rats untreated with I-3-C. The protein concentration for each sample was as follows in mg/mL: Control, 1A = 47.27, 1B = 46.66; 2500 ppm, 1A = 45.05, 1 B = 43.29; and dimer 2500 ppm, 1 A = 48.87, 1 B = 48.46. All experiments were performed in triplicate.

2.4. RESULTS – COVALENT BINDING ANALYSES

2.4.1. *In vivo* SD rat covalent binding analyses

Figure 9 shows the covalent binding of KT-derived [^{3}H] to hepatic proteins from SD rats treated i.p. with KT (40 mg/kg or 90 mg/kg; 1.5 μCi/mg). The radioactivity was normalized to nmol KT/mg hepatic protein. The 40 mg/kg dose represents a low dose that will be expected to produce KT plasma concentrations in the 10 – 60 μM range while the 90 mg/kg represents high-dose treatment for prostate cancer that will produce KT concentrations in the 75 – 100 μM range. There was a significant difference between KT-derived [^{3}H]-binding to hepatic protein over the 24-hour period using ANOVA ($P = 0.014$, n = 3). Covalent binding occurred as early as 0.5 hour after treatment for both doses. The 40 mg KT/kg dose peaked at 2 hours (0.03 ± 0.01 nmol KT/mg protein) with a steady decline. The 90 mg KT/kg dose peaked at 8 hours (0.09 ± 0.04 nmol KT/mg protein), and then there was a steady decline to the 24-hour time point (0.04 ± 0.02 nmol KT/mg protein). All results are reported as the mean ± the standard deviation.

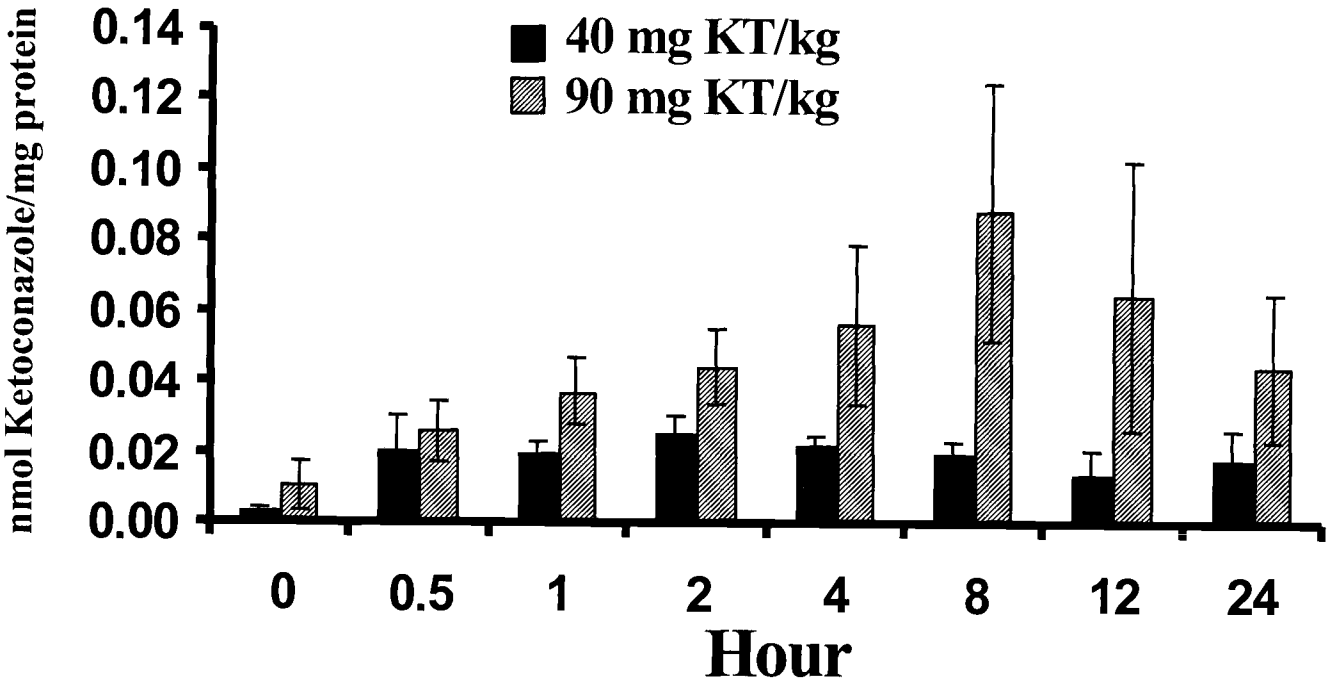

Figure 9: 'Covalent' binding of ketoconazole (KT) to hepatic proteins in Sprague Dawley rats. Treatment was ip with ^{3}H-KT (40 mg/kg or 90 mg/kg; 1.5 μCi/mg). The radioactivity was normalized to nmol ketoconazole-derived [^{3}H]/mg hepatic protein. There was a significant difference between the 40 and 90 mg/kg treatments over time using ANOVA ($P = 0.014$, n = 3).

Figure 10 shows the effect of ip administration of KT, 40 mg/kg or 90 mg/kg, on serum ALT activity in SD rats. Due to diurnal variation concerns regarding GSH levels, all doses were initiated to coordinate extractions between 7 and 11 am when GSH levels would be at the highest level. Interestingly, there was an immediate increase in ALT levels as early as 0.5 hours after treatment for both doses (44.2 U/mL and 56.4 U/mL for the 40 mg/kg and 90 mg/kg doses, respectively). The control rats treated with normal saline had an ALT value of 22.7 ± 9.7 U/mL.

There was an apparent and steady increase in ALT levels from 8 hours to 24 hours for the 90 mg KT/kg dose and a significant difference between 90 mg KT/kg dose and control using Tukey's multiple comparison ($P < 0.05$). Also, there was a significant difference between the 40 mg/kg and 90 mg/kg doses at the12-hour and 24-hour time points after KT administration using Tukey's multiple comparison ($P < 0.05$).

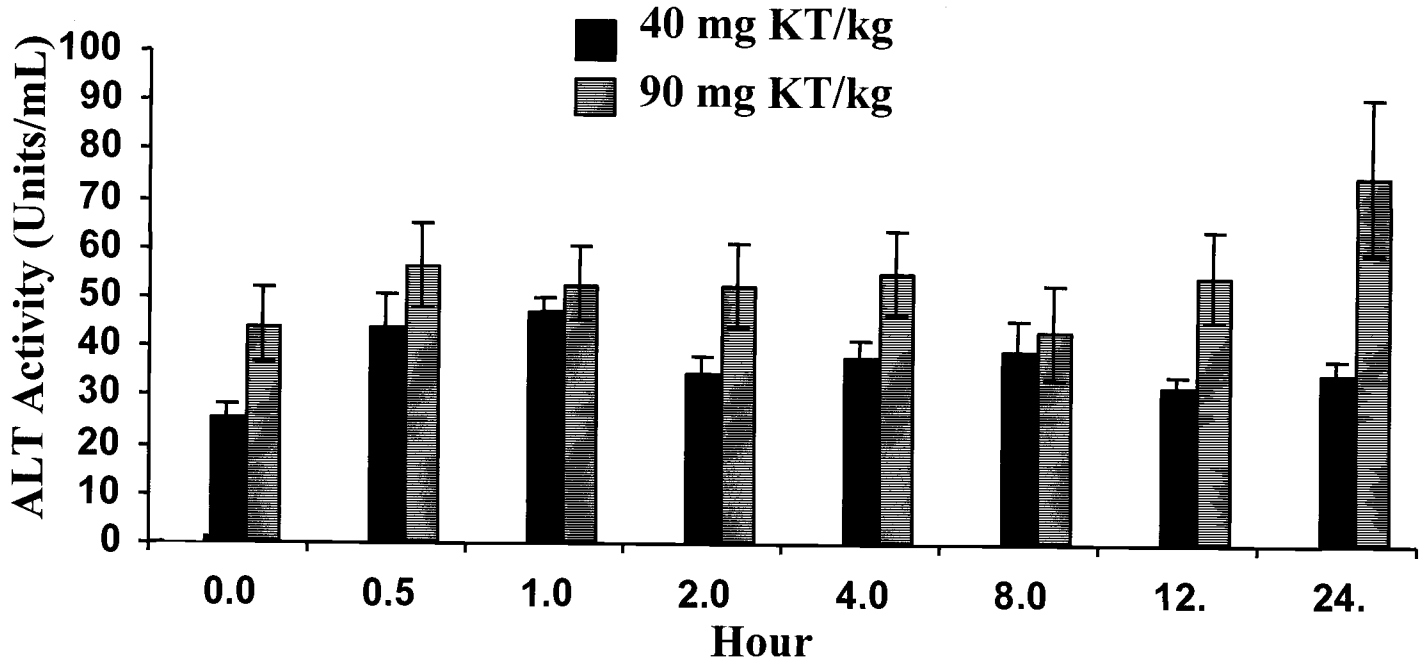

Figure 10: Graph of serum alanine aminotransaminase (ALT) activity after administration of ketoconazole (KT) in Sprague Dawley (SD) rats. Treatment concentration was 40 mg/kg or 90 mg/kg. The dashed line represents the ALT control value of saline-treated rats, 22.7 ± 9.7 U/mL. Tukey's multiple comparison indicates significant differences between 90 mg KT/kg dose and control and between 40 mg KT/kg and 90 mg KT/kg doses ($P < 0.05$).

Figure 11 demonstrated the effect of KT on hepatic GSH levels in SD rats. Due to diurnal variation concerns regarding GSH levels, all doses were conducted to coordinate extractions between 8:30 and 11:30 am, when GSH levels would be at the highest level. The hepatic GSH levels implicated for the control rats were 9.66 ± 1.51 nmol GSH/mg protein. There was a significant difference between the 40 mg KT/mg and the control rats at 0.5 hours and 8 hours where the GSH levels were 6.89 ± 1.1 nmol GSH/mg protein and 5.87 ± 1.1 nmol GSH/mg protein, respectively ($P < 0.05$). Afterwards, the GSH levels increased back to control values. The 90 mg KT/kg was significantly different from the control rats at 4, 8, 12, and 24 hours where the GSH levels were 6.1 ± 0.91, 4.7 ± 0.19, 4.17 ± 0.9, and 4.76 ± 0.34 nmol GSH/mg protein, respectively using the Dunnett's multiple comparison ($P < 0.05$). At 24 hours, there was a significant difference between the 40 mg/kg and 90 mg/kg doses, 8.55 ± 1.64 nmol GSH/mg protein and 4.76 ± 0.34 nmol GSH/mg protein, respectively ($P < 0.05$).

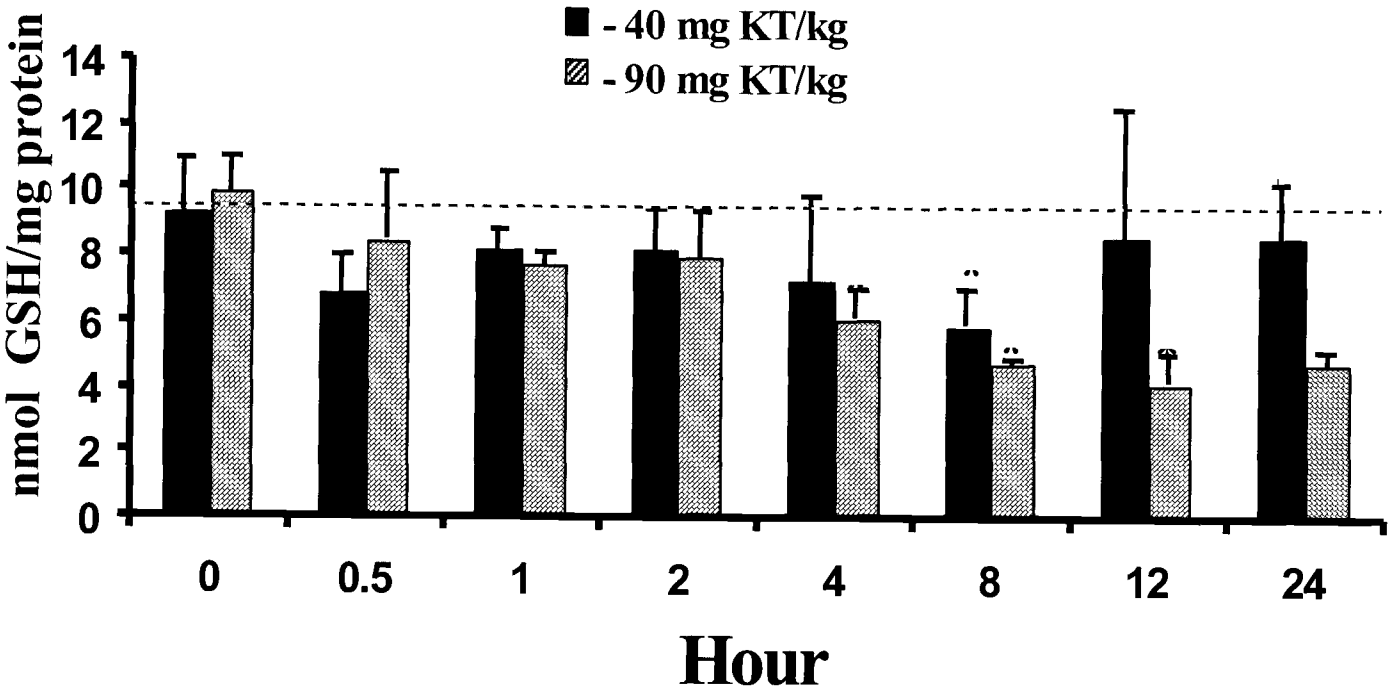

Figure 11: Graph of hepatic glutathione (GSH) levels after ip administration of ketoconazole (KT) in Sprague Dawley rats. Treatment concentration was 40 mg/kg or 90 mg/kg. The dashed line represents the GSH control value of saline-treated rats, 9.66 ± 1.51 nmol GSH/mg protein. Dunnett's multiple comparison indicated a significant difference between 40 mg KT/mg dose or 90 mg KT/kg dose and control ($P < 0.05$).

2.4.2. SD rat *in vitro* covalent binding with hepatic microsomes

The covalent binding of ^{3}H-KT (1 μM, 10 μM, and 100 μM; 1 μCi/mL) to hepatic microsomes from SD rats in an *in vitro* NADPH-generating system containing 1 mg/mL hepatic microsomal protein is shown in Figure 12. Controls without NADPH were used for comparison for each concentration studied. The radioactivity was normalized to nmol KT/mg microsomal protein. All three KT incubation concentrations, 1 μM, 10 μM, and 100 μM, resulted in significant differences with control incubation conditions using an ANOVA ($P \leq 0.01$). As the concentration of KT increased, so did the covalent binding to hepatic protein. In addition, there appeared to be an increase in covalent binding with increasing incubation periods for the 10 μM and 100 μM KT. The 100 μM KT incubation had the highest covalent binding at 8 hours (0.51 ± 0.06 nmol KT/mg of protein). The control levels at 8 hours were approximately 10-fold lower (0.06 ± 0.01 nmol KT/mg of protein); thus, indicating an NADPH dependent mechanism of covalent binding of KT-derived activity. The profile for the 1 μM KT-incubation at a protein concentration of 1 mg/mL was consistent throughout ranging from 0.0027 ± 0.004 nmol KT/ mg of protein to the highest at the 2-hour time point of 0.018 ± 0.00002 nmol KT/ mg of protein. The 10 μM KT-incubation appears to reach a plateau at 2 hours, with the highest point of binding at 0.157 ± 0.02 nmol KT/ mg of protein. Thus, there is a dose proportionality between 1 and 10 μM KT and saturation at 100 μM KT which is NADPH-dependent. The protein concentration experiments of 0.250, 0.50, and 1 mg/ml produced the same metabolic profile

when comparing the ^{3}H-KT 1, 10, and 100 μM doses within each experiment. There was a linear increase over time (0 through 8 hours) in the covalent binding of KT to the hepatic protein with 0.25 mg/mL microsomal proteins having a plateau at 3 hours (data not shown).

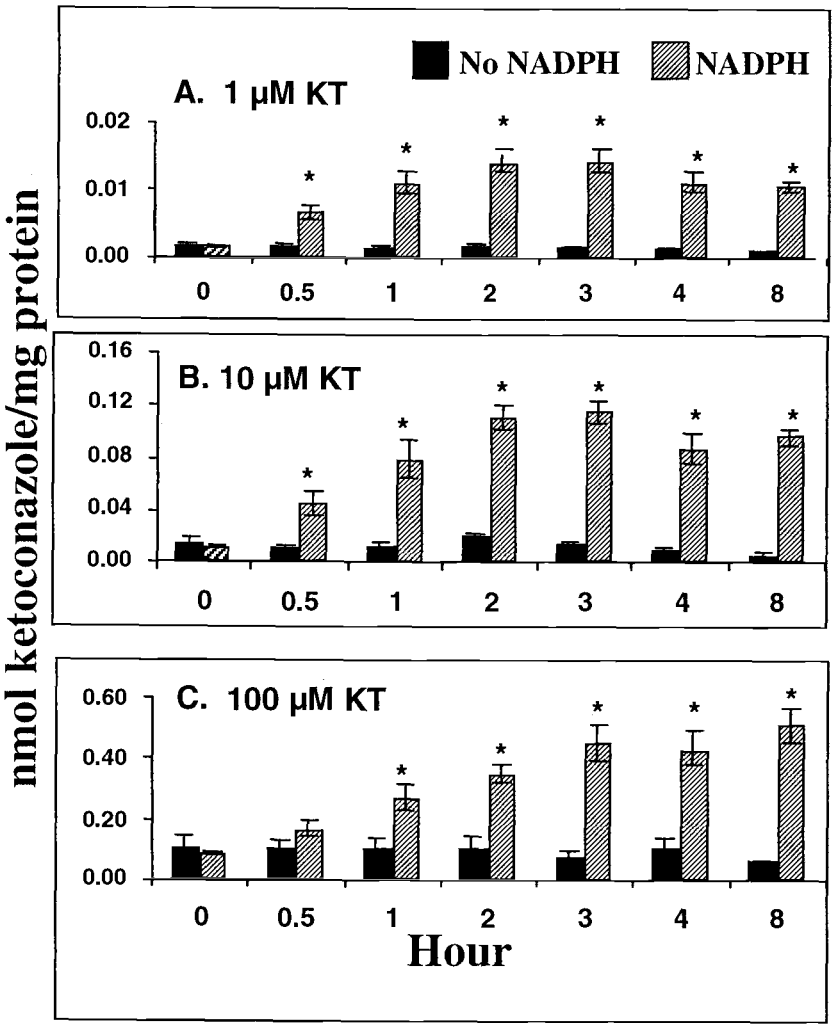

Figure 12: The covalent binding analysis conducted *in vitro* from the addition of ^{3}H-ketoconazole (KT) in hepatic microsomes from Sprague-Dawley (SD) rats. ^{3}H-KT (1 μCi/mL) was in an NADPH-generating system. Controls without NADPH were used for comparison for each concentration. The radioactivity was normalized to nmol KT/mg microsomal protein. In Figure 14a, (*) indicates a significant difference between the 1μM KT and control using ANOVA ($P < 0.05$, n = 6). In Figure 14b, (*) indicates a significant difference between the 10 μM KT and control using ANOVA ($P \leq 0.05$, n = 6). Figure 14c, (*) indicates a significant difference between 100 μM KT and control using ANOVA ($P \leq 0.05$, n = 6).

The *in vitro* covalent binding of 100 μM ^{3}H-KT (1 μCi/mL) to hepatic microsomes (1 mg/mL) from SD rats in an NADPH-generating system with 1 mM GSH is shown in Figure 13. Control incubations without GSH were used for comparison for each of the time points evaluated. The radioactivity was normalized to nmol KT/mg microsomal protein. There was a significant reduction of covalent binding to hepatic protein at the 4-hour and 8-hour using ANOVA ($P \leq 0.01$); even as early as 1 hour after treatment, metabolic activation appears to occur; thus suggesting that KT might also bind to hepatic GSH.

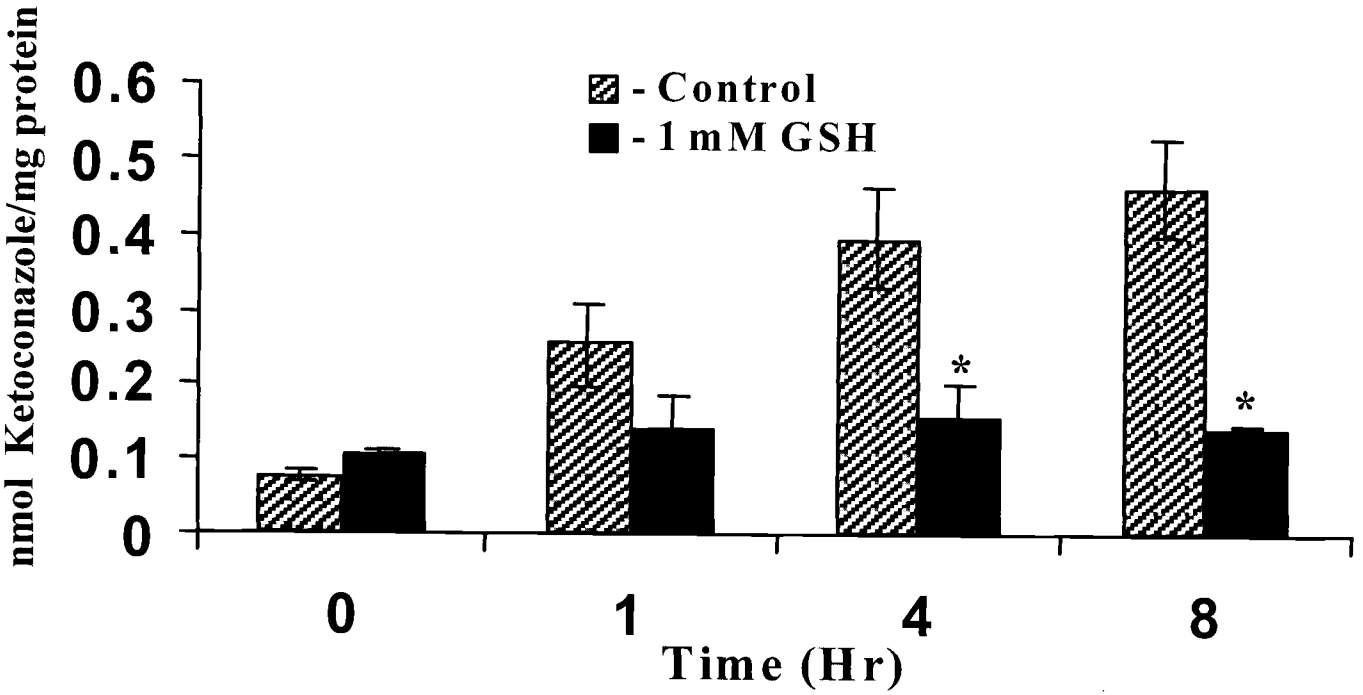

Figure 13: *In vitro* graph indicates reduction of ^{3}H-ketoconazole (KT-100 μM) covalent binding effect to SD rat hepatic microsomes after the addition of 100μM glutathione (GSH). Treatment of microsomes consisted of ^{3}H-KT (1 μCi/mL) and ketoconazole (1, 10, and 100 μM)in an NADPH-generating system. Controls without GSH were used for comparison. The radioactivity was normalized to nmol KT/mg microsomal protein. The (*) indicated a significant difference using ANOVA ($P \leq 0.05$, n = 6).

Figure 14 shows the effect of heat inactivation (HI) on *in vitro* covalent binding of 100μM ^{3}H-KT (1 μCi/mL) to SD rat hepatic microsomes in an NADPH-generating system containing 1 mg/mL microsomal protein. Control incubations without HI treatment were used for comparison at each time point evaluated. The radioactivity was normalized to nmol KT/mg microsomal protein. Interestingly, HI significantly reduced the covalent binding of KT-derived radioactivity to the hepatic protein at the 1, 4, and 8-hour time points using ANOVA ($P < 0.05$). The 8-hour incubation had a greater than 4-fold decrease from 0.46 ± 0.06 nmol KT/mg protein to 0.11 ± 0.01 nmol KT/mg protein.

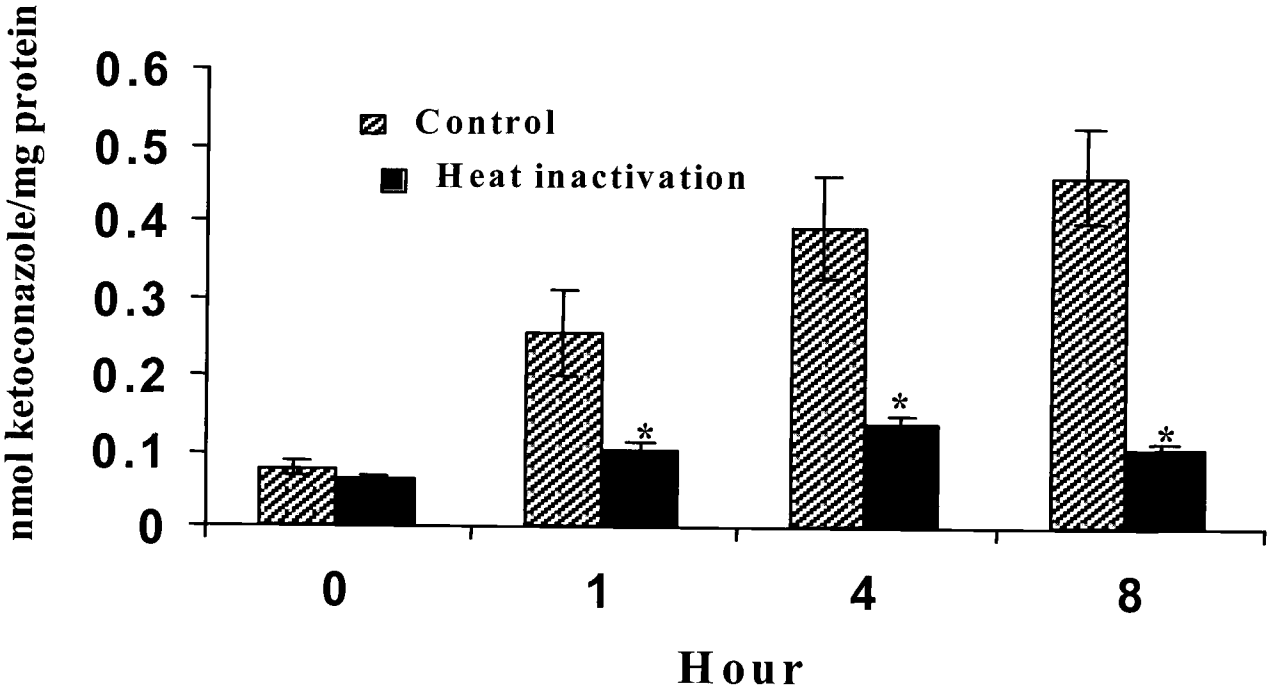

Figure 14: *In vitro* graph indicates reduction of ^{3}H-ketoconazole (KT) 'covalent' binding effect from heat inactivation (HI), 50 °C for 90 sec in Sprague Dawley (SD) rat hepatic microsomes. Treatment of microsomes consisted of ^{3}H-KT (1 μCi/mL) and ketoconazole (100 μM) in an NADPH-generating system. Controls without HI were used for comparison. The radioactivity was normalized to nmol KT/mg microsomal protein. An asterisk (*) indicates a significant difference using ANOVA ($P \leq 0.05$, n = 6).

The largest reduction of covalent binding occurred when both were applied with a final result at the 8-hour time point of 0.0900 ± 0.0075 nmol KT/mg protein. Figure 15 a and b depicts a comparison of GSH-KT, HI-KT with KT only and Figure 16 is a comparative analysis of the GSH-KT and HI-KT with co-incubation of GSH-HI-KT.

a)

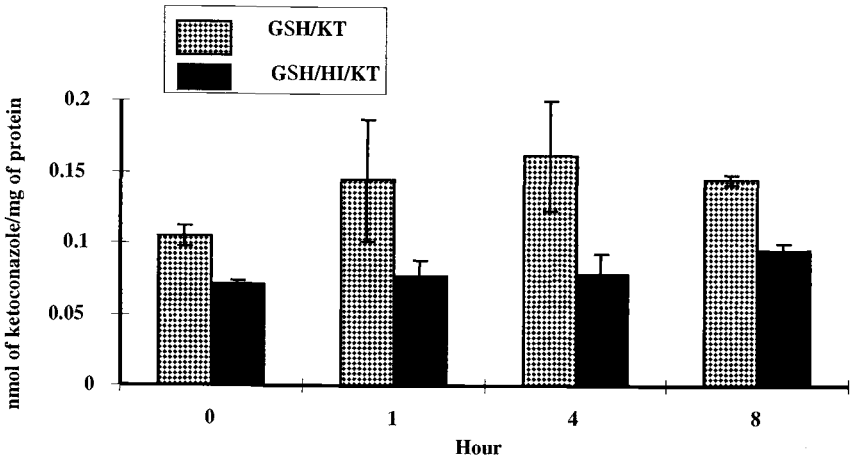

b)

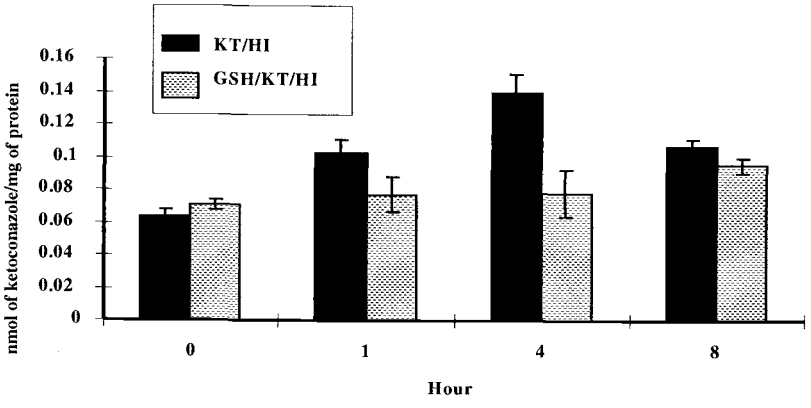

Figure 15: Graphs a and b depict the *in vitro* comparisons of ^{3}H-ketoconazole (KT) (1 uCi/mL) covalent binding effect in Sprague Dawley (SD) rat hepatic microsomal incubations (1mg/mL) with/without the addition of glutathione (GSH, 1mM) and heat inactivation (HI). **a:** SD hepatic microsomal (1 mg/mL) incubation *in vitro* comparison of l mM GSH , KT (100 μM), ^{3}H-KT (1μCi/mL) with GSH (1 mM)-HI-KT (100 μM). **b:** SD hepatic microsomal (1 mg/mL) incubation *in vitro* comparison of HI and KT (100 μM) with GSH (1 mM)-HI-KT (100 μM).

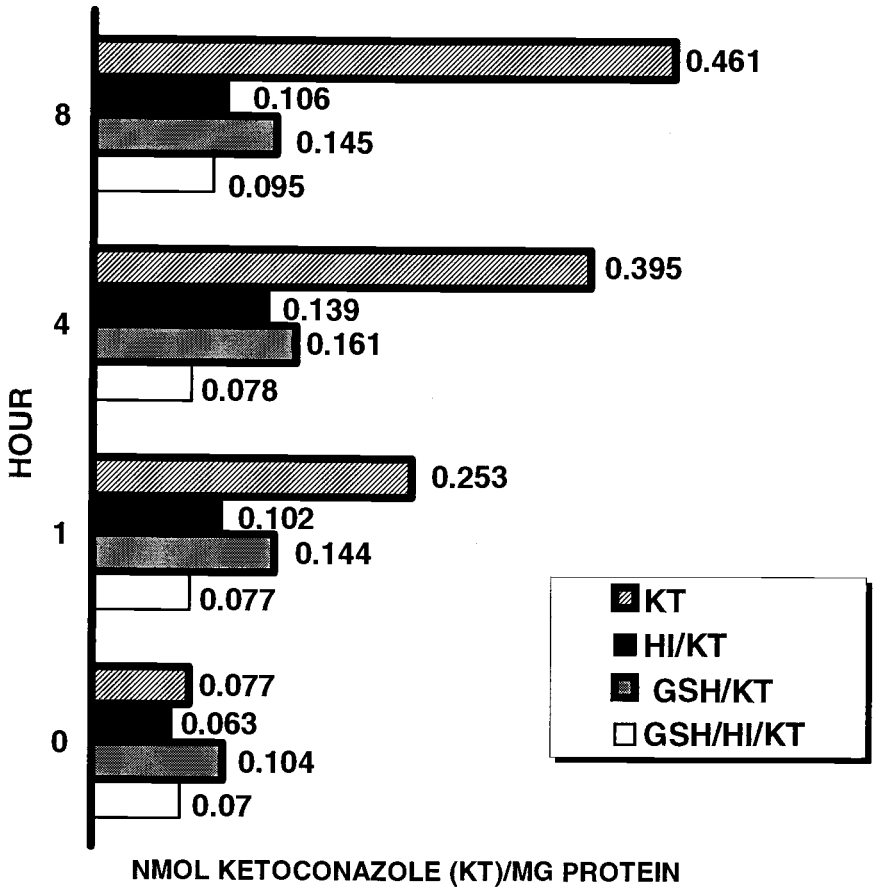

Figure 16: A comparative analysis of *in vitro* studies. Implemented were the combined procedures of GSH (1 mM)-heat inactivation (HI)- KT (100 μM). Comparison with individual experimental analysis of GSH (1 mM), heat inactivation (HI), and KT (100 μM) covalent binding studies resulted in the lowest covalent binding of (KT)/metabolite(s) in Sprague Dawley rat microsomes (1 mg/mL). The radioactivity was normalized to nmol of KT/mg of protein.

2.4.3. Fischer 344 rat *in vitro* covalent binding in hepatic microsomes with and without I-3-C

Figure 17a is a comparison of microsomal preparations of Fischer 344 rats with and without I-3-C. Three experiments were conducted using microsomes from Fischer rats pretreated with I-3-C utilizing a KT concentration of 10 μM at 0, 0.5, 1, 2, and 4-hour time points. Controls were Fischer rat microsomes without I-3-C pretreatment. Results indicated covalent binding effects at all time points when compared with the controls with an early peak at 0.5 hour of 0.086 ± 0.002 nmol of KT/mg of protein for the 2500 PPM and a later peak at 2 hours of 0.07 ± 0.002 nmol of KT/mg of protein for the dimer. The highest indication of binding for the controls was at two hours with a peak of 0.027 ± 0.01 nmol of ketoconazole/mg of protein. Figure 17b is a comparison of covalent binding in SD microsomal preparations (Figure 12) with Fischer 344 hepatic microsomes utilizing 10 μM for comparative results. The 2500 ppm indicated a decline by the 2-hour time point (0.068 ± 0.006), and the dimer increased to the 2-hour time point (0.071 ± 0.001) and declined to 0.06 ± 0.002 at the 4-hour time-point, whereas the SD microsomal preparations utilizing 10 uM peaked higher at 0.111 ± 0.011 at 2 hours with a slight decline at the 4-hour (0.09 ± 0.021) time point.

a)

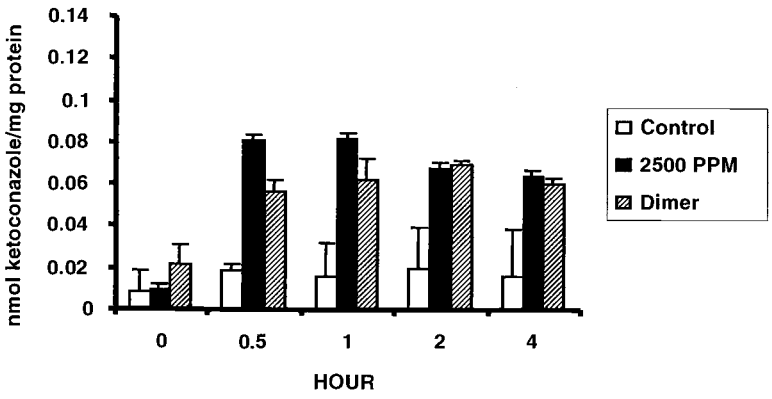

b)

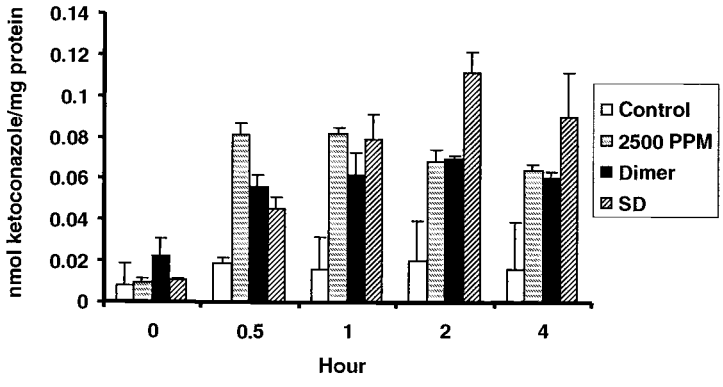

Figure 17: Graphs a and b depict an *in vitro* comparison of 10 μM of ketoconazole (KT) in microsomal incubations (1 mg/mL) from Fischer rats with and without (control) I-3-C pretreatment and SD rat microsomes. Concentration of radioactivity of ^{3}H-ketoconazole (KT) was 1μCi/mL. **a)** Samples with I-3-C are: 2500 PPM and 2500 PPM-dimer. **b)** Comparative hepatic microsomal analysis of Fischer and SD rats.

2.5. DISCUSSION

This study is the first to investigate the hepatotoxicity associated with KT *in vivo*. All of the *in vivo* parameters evaluated, ALT levels, hepatic GSH levels, and hepatic covalent binding, suggest that KT produce hepatic injury as indicated with increases in ALT levels after KT administration (Figure 10). This hepatic injury occurred as early as 0.5 hr with both the 40 mg/kg and 90 mg/kg doses. The 90 mg KT/kg dose is representative of high dose KT treatment that is seen in patients treated for prostate cancer. The high-dose KT therapy for prostate cancer ranges from 400 mg KT/8 hours or 600 mg KT/12 hours for a total daily dose of 1,200 mg for six to nine months (Decoster, *et al.* 1996, Bok and Small 1999). Shown in Figure 10, there is an initial and significant increase in ALT levels for the 40 and 90 mg KT/kg dose. The 90 mg KT/kg declines after 4 hours and then increases at 12 hours and 24 hours. In the past hepatic injury was suspect as being a reaction assault by KT or its metabolite(s) and not due to an immunoallergic response (Lewis, *et al.* 1984, Stricker, *et al.* 1986, Bok and Small 1999). Thus, the early release of ALT may be due to the parent compound, KT, while the later increase of ALT at 12 and 24 hours may be due to reactive metabolite(s).

The present study also investigated the possibility that KT may covalently bind to hepatic macromolecules and/or hepatic GSH in a dose- and time-dependent response. Figure 9 demonstrated *in vivo* that there was a definite dose-response in KT covalent binding to hepatic SD rat protein. The 90 mg KT/kg dose produced higher

levels of nmol of KT-Derived [^{3}H]/mg of protein in comparison to the 40 mg KT/kg dose over the 24-hour time period. Figure 11 indicated hepatic GSH levels were significantly decreased after a 90 mg KT/kg dose in a dose-dependent manner. The 90 mg KT/kg dose resulted in lower hepatic GSH levels than the 40 mg KT/kg dose at 4, 8, 12, and 24-hour time points with the greatest difference between the doses at 24 hours. In the 40 mg KT/kg dose, the GSH levels appear to decrease from 0 thru 8 hours, then increase back to control GSH levels at 12 and 24 hours. It is likely the liver was able to recover from low dose treatment and return to normal hepatic GSH levels. On the other hand, the 90 mg KT/kg treatment continued to deplete the hepatic GSH at the 12-hour and 24-hour time points. When comparing the *in vivo* hepatic GSH levels to the 'covalent' binding studies of KT to hepatic protein and the ALT studies, no significant correlations were made between the *in vivo* alterations in ALT and GSH levels (Figures 10 and 11, respectively) to the covalent binding (Figure 9) that occurred.

It is possible that as KT undergoes oxidative metabolism such that the metabolite(s) of KT may be reacting to GSH because the decrease in GSH occurs hours after exposure to KT rather than earlier. Thus, the parent compound, KT, may be directly binding to hepatic protein while the metabolite(s) are binding to hepatic protein and hepatic GSH. Earlier studies indicate the primary metabolite of KT is *N*-deacetyl ketoconazole (DAK) in mice (Whitehouse, *et al.* 1990) and rat (Rodriguez and Acosta 1997, Rodriguez, *et al.* 1999) and DAK was more hepatotoxic in an *in vitro* rat hepatocyte culture system (Rodriguez and Acosta

1997). Furthermore, DAK is further metabolized by FMO to the *N*-deacetyl-*N*-hydroxy ketoconazole, a secondary hydroxylamine (*N*-hydroxy-DAK), metabolite (Rodriguez and Acosta 1997, Rodriguez, *et al.* 1999). *N*-hydroxy-DAK is susceptible to further FMO-mediated oxidative assaults, where it has been speculated toxic and reactive metabolites could be creating a primary hydroxylamine, a nitrone, and an oxime whereas KT could be responsible, in part, for the toxicity of KT (Rodriguez, *et al.* 1999). Soft nucleophilic sulphur, selenium, nitrogen, or phosphorus pharmaceuticals can undergo oxidative metabolism catalyzed by FMOs (Ziegler 1988). Hydroxylamines may directly interact with biomacromolecules to impair cellular function (Cashman, Xiong, Xu, *et al.* 1999). Therefore, a reduction of GSH would be expected if bioactivation of an electrophilic metabolite such as DAK and *N*-hydroxy-DAK occurred due to the conjugating nature of this cellular scavenger to preserve the integrity of the cell (Hogberg and Kristoferson 1977b). Another possibility is DAK will undergo phase II metabolism by sulfation and/or glucuronide conjugation, which would provide good leaving groups resulting in a nitrenium cation that could possibly bind to protein and DNA leading to adduct formation.

The *in vitro* covalent binding studies of KT and/or its metabolite(s) to SD rat hepatic microsomal protein was found to be NADPH-dependent and was inhibited by co-incubation with GSH (Figures 12 and 13). Figure 13 demonstrates the addition of GSH in the microsomal-incubation significantly reduced the covalent binding of KT and/or its metabolites to hepatic protein implicating GSH

as an important detoxification pathway through conjugation. The 1 mM GSH *in vitro* incubation with KT would prevent the formation of protein- and/or DNA-KT adducts; thereby, possibly forming GSH-KT adducts. To dissect CYP- or FMO-mediated bioactivation to potential reactive metabolite(s), heat inactivation of microsomal-FMO fractions inactivated FMO activity but CYP activity remained unimpaired (Ziegler 1980). Earlier studies of DAK employed SKF-525A, a compound that does not affect FMO activity and inhibits CYP and octylamine, a known positive effector for FMO and also an inhibitor of CYP (Rodriguez and Acosta 1997) resulted in unaltered metabolism. Furthermore, *in vitro* activity comparisons of DAK by implementing a pH of 7.4 (optimum for CYP) vs. 8.8 (optimum for FMO) a significant reduction occurred with the lower pH in microsomal incubations (Rodriguez, *et al.* 1999). Figure 14 demonstrates with NADPH present profound and significant reduction in KT and/or its metabolite(s) covalent binding to hepatic protein by FMO heat-inactivation of the rat liver microsomes. Because FMO-mediated metabolism was inhibited, it is speculated that the metabolite(s) of KT is/are primarily responsible for the covalent binding to hepatic proteins.

Continued efforts are being made to identify whether KT and/or its metabolite(s) are binding to the hepatic protein and to identify the nature of the protein adduct. Further studies are also being conducted to determine or verify the binding of KT or its metabolites to GSH mediated by liver microsomal FMOs or

individual FMO isoforms. If a GSH adduct is formed, attempts will be made to characterize its structure by mass spectrometry and NMR methods.

The microsomes from the pretreated Fischer rats with I-3-C, a compound that has been found to inhibit the FMO enzyme, produced lower peaks for covalent binding than the SD rat microsomes. The 10 μM KT-incubation of SD rat microsomes reached a plateau at 2 hours, with a peak and a profile that was consistently higher than the Fischer rat microsomes. Implicated was a possible inhibition imposed on the FMO enzyme by the pretreatment of I-3-C in the Fischer rat. Possibly, if implementation of the higher concentration of 100 μM had been utilized for comparison, an increased difference would have been observed.

To evaluate the role of microsomal-FMO bioactivation of KT to reactive metabolite(s) that may bind to hepatic protein, heat inactivation of microsomal-FMO was performed. Microsomal-FMO activity was inhibited by heat-inactivation of the microsomes at 50 ° C for 90 seconds, which is an established method to dissect FMO- and CYP-microsomal activity (Ziegler 1980). Reportedly, heat inactivation pretreatment does not affect CYP (Kedderis and Rickert 1985). Figure 14 indicated the effect of heat inactivation on *in vitro* covalent binding of 100 μM ^{3}H-KT (1 μCi/mL) by a >4-fold reduction by the 8-hour time point.

Due to a decrease in *in vivo* hepatic GSH levels, *in vitro* comparative analyses utilizing 1 mM GSH (Cribb, *et al.* 1991, Pirmohamed, *et al.* 1995) in microsomal incubations were conducted to determine whether a reduction of

covalent binding to hepatic proteins would occur. GSH has been found to be an important protective factor by decreasing protein binding in hepatic microsomal fractions therefore reducing associated toxicity (Gao, *et al.* 1996). Because a reduction in covalent binding occurred *in vitro* with heat inactivation or the addition of GSH experimental analyses were implemented utilizing both procedures for comparative analysis represented in Figures 15 a and b, and 16. The final analysis indicated the highest reduction in covalent binding with implementation of both procedures.

In summary, these studies support that KT-induced hepatotoxicity is dose- and time-dependent and appears to be dependent, in part, upon its bioactivation by FMO to metabolite(s), due to the reduction of covalent binding observed with heat inactivation, that may react with protein and possibly, GSH. Thus, our combined *in vitro* studies and *in vivo* studies point to potential mechanisms of KT-induced hepatotoxicity that merit further investigation. Mechanistic information regarding the hepatic microsomal monooxygenase mediated covalent binding of KT to proteins was implicated in this study. Mechanistic profiling is a necessary component in drug administration "Adverse drug reactions are common and a significant cause of morbidity and mortality " (Park and Pirmohamed 2001); therefore determining metabolic pathways that can be utilized for efficacy and minimize toxicological effects is vital. Drug induced toxicities cause toxicity by covalently altering cellular macromolecules leading to enzyme inactivation, altered functions of structural proteins or transcription,

disruption of intracellular calcium homoeostasis, loss of cellular membrane integrity due to lipid peroxidation or apoptosis (Pohl, *et al.* 1996). Patients taking drugs that induce the mixed-function oxidase system are at risk for co-administration including over-the-counter drugs such as acetaminophen due to potential hepatotoxicity (Simon 1992). Therefore, qualitative predictions are dependent upon knowledge of the enzyme specificity for a substrate based upon chemical structure that can be readily utilized for future application.

CHAPTER 3: FMO DETECTION IN THE HUMAN INTESTINAL TRACT AND CACO-2 CELL LINE

3.1. ABSTRACT

This study investigated the presence of the flavin-containing monooxygenase (FMO) isoforms FMO1, FMO3, and FMO5 within the human intestinal tract, which may be responsible for first-pass metabolism, decreased bioavailability, or bioactivation of xenobiotics. Comparative western blot analyses utilizing polyclonal primary antibodies and goat-anti-rabbit secondary antibodies coupled with chemiluminescence were conducted with microsomes from human jejunal mucosa, duodenal tissue, ileum, colon, and Caco-2 cells. Densitometry of the bands followed by quantitative analysis were performed to evaluate FMO protein expression. FMO1 protein, 58 kDa, was detected in all samples. There appeared to be inter-individual variability of FMO1 within the human samples, 54.2 ± 20.7 pmol FMO1/mg protein and 14.98 ± 9.94 pmol FMO1/mg protein in human jejunum and Caco-2 cell line, respectively. FMO3 and FMO5 were not detected in any of the human samples. The level of FMO1 protein from the human jejunum samples inversely correlated with age ($p < 0.05$). In the FMO1 westerns, there were non-specific immunoreactive bands observed with the FMO1 primary antibody at the 40 kDa and 65 kDa. *N*-glycosylation studies were performed to determine if the 65 kDa band was glycosylated FMO1. A band shift to the 58 kDa species following endoglycosidase H treatment of microsomes suggested that the 65 kDa band is glycosylated FMO1 protein. However, results were variable in the

duodenal tissue and jejunal mucosa microsomal preparations. These findings indicate that FMO1 is present in human duodenum, jejunum, ileum, and colon as well as the Caco-2 cell line, which may be responsible for the low bioavailability of drugs that are substrates for FMO1. Studies to determine the activity of FMO still remain to be conducted.

3.2. INTRODUCTION

The major oxidative monooxygenase phase I enzymes are cytochrome P450 (CYP) and flavin-containing monooxygenases (FMO), which have been detected in the liver (Bonkovsky, *et al.* 1985) and enterocytes of the small intestine (Hall, *et al.* 1999, Yeung, *et al.* 2000). The most common biotransformation reaction is oxidative phase I, which can result in significant first-pass (Thummel, *et al.* 1997). This contributes to the pre-systemic removal of a drug resulting in reduced bioavailability after oral administration. Hepatic drug metabolism was considered to be the major contributor to systemic drug elimination, however, recent studies have shown that intestinal drug metabolism also contributes to the first-pass effect (Hall, *et al.* 1999). CYP is an example of oxidative metabolism in both the liver and the mucosa of the small intestine which can result in significant first-pass effects (Cashman 1996, Thummel, *et al.* 1997). FMO often shows activity toward CYP substrates (Larsen-Su and Williams 1996). A total of five FMO isoforms have been reported (Hines, *et al.* 2002). FMO1, FMO2, FMO3, and FMO5 display selective substrate specificity metabolism of soft nucleophiles, such as sulfur (S), phosphorus (P), selenium (Se), and nitrogen (N) (Koukouritaki, *et al.* 2002). The cDNAs encoding FMO4 have extended coding regions. The derived sequences of human FMO4 contain 558 residues, whereas other FMO isoforms are 535 – 539 residues in length, thus FMO4 does not express the same activity characteristics as other FMO isoforms unless truncated (Itagaki, *et al.* 1996). Also FMO1, FMO3, and FMO4 display a distinct

pattern of developmental and tissue-specific expression (Dolphin 1996), possibly contributing to organ-susceptibility to xenobiotics (Koukouritaki, *et al.* 2002).

Variability in therapeutic responses to orally administered drugs are often due to first-pass effects. Variations in plasma concentrations can also be due to inter-individual therapeutic responses (Pond and Tozer 1984), which adds to the complexity of tissue-specific FMO expression (Whetstine, *et al.* 2000). FMO activity may contribute to the variability of individual drug response and drug clearance (Stormer, *et al.* 2000). Variation in therapeutic responses can occur due to drug-drug/drug-food interactions (Tam 1993) or polymorphism (Forrest, *et al.* 2001). FMO genetic polymorphisms have been characterized in FMO2 and FMO3 (Cashman 2002). Patients with mutations may exhibit an alteration in detoxification or possible bioactivation of drugs (Krueger, Williams, *et al.* 2002).

Absorption in the gut wall has been reported to be highest in the duodenum and jejunum due to the increased surface area from both the plica folds and villi-microvilli appendages. Absorption begins to decrease down the GI tract into the ileum and colon where there are less plica folds and villi (Ilett and Davies 1982). The highest metabolizing activity is found in the pylorus and in the upper small intestine (Caldwell and Marsh 1982, Renwick and George 1989).

Understanding the alterations in drug-metabolizing enzyme expression and the ability to predict therapeutic dosing in order to avoid reduced bioavailability and toxicity is difficult (Hines and McCarver 2002). It is important to determine the intestinal enzymes and their tissue distribution in order to assess

the relative contribution of each enzyme to intestinal metabolism (Lin, *et al.* 1999). A better understanding of these systems will foster optimal drug development and therapeutic predictions (Carriere, *et al.* 2001).

CYP3A is responsible for the metabolism of approximately 50% of the marketable drugs currently on the market (Thummel, *et al.* 1997). Moreover, CYP has been detected and quantitated in the jejunum, ileum, and duodenum (Hall, *et al.* 1999). While CYP has been studied in great detail over the past decade, limited information is available regarding the human intestinal FMO.

Commonly used in pharmaceutical drug discovery, Caco-2 cells have been characterized to be similar to the human GI epithelium including the expression of many of the brush border hydrolases, ion transport properties and carrier systems (Bailey, *et al.* 1996). Caco-2 cells have been utilized for determinations of intestinal metabolism (Carriere, *et al.* 2001) and transport studies (Lampen, *et al.* 1998). CYP1A1, CYP2E1, and CYP3A (Lampen, *et al.* 1998), but CYP3A4 has been found to be at low levels in Caco-2 cells. However, with continuous culture and induction with 1α, 25-dihydroxyvitamin D, a large increase in CYP3A4 activity does occur. A Caco-2 clone, TC7 cells, has been shown to express after confluency higher levels of the expression of CYP3A4 in both mRNA and protein levels (Carriere, *et al.* 2001). CYP1A1 has been found to be highly expressed in dividing Caco-2 cells (Lampen, *et al.* 1998, Carriere, *et al.* 2001). Elucidation of FMO expression and activity in the Caco-2 cells could aid in metabolism predictions performed at pharmaceutical industries. Functional

FMO in the intestine could be responsible for reduced bioavailability and altered metabolism leading to toxicity from soft nucleophiles such as N, S, P, or Se as seen with albendazole (F = 0.14) and chlorpromazine (F = 0.32). Therefore, investigation of the presence of FMO isoforms and the functional activity is warranted.

3.3. MATERIALS AND METHODS

3.3.1. Chemicals and supplies

Dulbecco's modified eagle medium (DMEM), Dulbecco's modified eagle medium (DMEM)/ F12 (Ham), fibronectin (human α-Chymotryptic 120K fragment), epidermal growth factor (EGF), trypsin-EDTA, Dulbecco's phosphate buffered saline (PBS), and MEM100X non-essential amino acids were purchased from Gibco (Rockville, MD). Fetal bovine serum (FBS) was purchased from Summit (Fort Collins, CO). Vitrogen (purified collagen) was purchased from Cohesion Tech (Palo Alto, CA). Sodium hydroxide was purchased from Mallinckrodt (Paris, KY). Sodium azide, 30% acrylamide/0.8% bisacrylamide and TEMED were purchased from Bio-Rad Laboratories (Hercules, CA). Glycerol, dithiothreitol (DTT), aprotinin, tris base, potassium phosphate, sodium dodecyl sulfate (SDS), bromo phenol blue, methanol, sodium chloride (NaCl), Tween-20, ammonium persulfate (APS) and urea were purchased from Fisher Scientific (Fairlawn, NJ). Sodium pyruvate, antibiotic/antimycotic solution (10 mg/mL streptomycin, 10,000 Units/mL penicillin G, 25 μg/mL amphotericin B), oxaloacetic acid, insulin, bovine serum albumin, apo-transferrin, phosphorylethanolamine, triiodothyronine, ethanolamine, hepes, sodium selenite, hydrocortisone, L-glutamic acid, dimethyl sulfoxide (DMSO), sucrose, phenylmethylsulfonyl fluoride (PMSF), protease inhibitor cocktail, trypsin inhibitor, 4-amidinophenylmethanesulfonyl fluoride (APMSF), pepstatin A, trizma, sodium ethylenediaminetetraacetic acid (EDTA), potassium chloride,

tetrasodium pyrophosphate, tris hydrochloride, glycine, trypan blue, endoglycosidase (Endo H), and Kodak™ film were purchased from Sigma Chemical Co. (St. Louis, MO). Ethanol (ETOH) was purchased from Oregon State University Chemical Distribution (Corvallis, OR) and Safeway Natural Non-fat Dry Milk was purchased from local grocery store. All solutions were brought to volume with double distilled water (dds).

3.3.2. Human donor and cell line material

Human duodenal tissue, jejunal mucosa, and human jejunum, ileum, and colon microsomes were purchased from the Human Cell Culture Center, Inc (HCCC) (Laurel, MD). Of the fourteen donors, 9 were female and 5 were male. Twelve of the donors were Caucasian and 2 were African American ranging from 3 to 59 yrs in age. Seven donors were smokers, and 12 consumed alcohol or took prescription medications or both. The cause of death of donors were intracranial bleed, head trauma/stroke, anoxia, intracranial hemmorage, or myocardial infarction.

Caco-2 cells (HTB-37) passages used in these studies were numbers 27, 29, and 31, was obtained from American Type Culture Collection (ATCC) (Rockville, MD). Protein concentrations from microsomal preparations were determined with the Coomassie® Plus Protein Assay (Pierce, Rockford, IL).

3.3.3. Statistical analysis

Statistical analysis used ANOVA performed by the SAS-system 8.01.01 TS Level O1MO (1999-2000), with the Windows version 4.90.3 (SAS Institute, Cary, NC, USA). Determined was the significance of FMO1 expression as a function of age, gender, drug and alcohol consumption, ethnicity, or smoking versus non-smoking habits of donors. Probability values of $P \leq 0.05$ were considered statistically significant.

3.3.4. Culturing of Caco-2 cells

Cell seeding and maintenance (Protocol I): Seeding: Caco-2 cells were thawed quickly at 37 ° C, seeded and maintained in 25, 75, or 162 cm^2 polystyrene flasks (Fisher Scientific, Fairlawn, NJ). **Maintenance:** the cells were maintained at 37 ° C in an atmosphere of 5% CO_2 (Industrial Welding, Albany, OR) and 95% relative humidity in CO_2 water-jacketed incubators (Nuaire model 2700/2700E Austin, TX). **Caco-2 (HTB-37) cells** (Protocol H): Upon receipt from ATCC, cells were immediately seeded into a 75 cm^2 polycarbonate flask. Cells were fed a complete media (DMEM: F-12 (Ham) with L-glutamate, 10 % FBS, 0.1 mM non-essential amino acids, 1:100 sodium pyruvate, and 1:100 antibiotic/antimycotic solution) every two days until harvest. For microsomal preparations, the cells were allowed to grow one day beyond 100% confluency to increase protein content.

3.3.5. Microsomal Preparation

3.3.5.1. Human donor mucosa/tissue: (Protocol K)

Human donor jejunum mucosa (JM1, JM2, JM3, JM4, JM5, JM6, JM7, and JM8) and duodenal tissue (DT1) were converted into microsomal preparations according to the method of Lu et al. (1998) with the modification of the addition of protease inhibitors such as aprotinin (Gobinet-Georges et al., 2000, Kelly and Struthers, 2001), APMSF, PMSF, and the Sigma® protease inhibitor cocktail. Briefly, the upper villus layer of the mucosa was removed with a glass slide edge and suspended in cold potassium phosphate homogenization buffer (PPB) (100 mM potassium phosphate, pH 7.4, 1 mM EDTA, 150 mM, 0.1 mM DTT, 250 mM sucrose, 0.228 mM pepstatin A, 10 mg/20 mL trypsin inhibitor, 0.25 mM APMSF, 0.25 mM PMSF, 0.25 mL/20 mL protease inhibitor cocktail, 4000 KIU/total volume aprotinin). Mucosal cells were pelleted at 5000 rpm (3,440 *g*) for 6 minutes at 4 ° C (Beckman J2-HS, rotor JA17, Fullerton, CA) and then washed with PPB. By weight, the pellet was homogenized in a 4-fold volume of PPB and sonicated (Fisher Scientific sonicator dismembrator, Model 100, Fairlawn, NJ) for 10 seconds. The homogenate was pelleted at 12000 *g* for 30 minutes at 4 ° C and washed in minimal buffer (100 mM tetrasodium pyrophosphate, pH 7.4, 1 mM EDTA). After washing, the buffer was centrifuged at 30,000 rpm (100,000 *g)* for 15 minutes in an ultracentrifuge (Beckman L8-70M, Fullerton, CA). Microsomes were resuspended in 0.1M PPB (pH 7.4) with 250 mM sucrose and 1 mM EDTA. The microsomes were then aliquoted (1

mL/vial) into cryogenic vials, snap-frozen in liquid nitrogen and stored at –80 ° C. A sample of each aliquot was set aside for protein determination.

3.3.5.2. Cell culture: (Protocol J)

At harvest, flasks were removed from the incubator and cells were washed 3 times with warmed (37 ° C) PBS. The cells were then bathed in 2 mL of a cold protease (0.25 mM PMSF, 0.25 mL/20mL protease inhibitor cocktail, 10 mg/20mL trypsin inhibitor, 0.25 mM APMSF, 0.228 mM pepstatin A) and homogenization buffer (100 mM trizma, 1 mM EDTA, 250 mM sucrose) and placed immediately on ice. After 5 minutes, the cells were scraped to dislodge cells from the bottom of the flask and then transferred to another flask in a stepwise transference procedure until the cells from all the flasks were combined.

After harvesting, the cells were made into microsomes. Briefly, the cells were sheared and the cell suspension was microscopically observed (trypan blue exclusion test). The cell suspension was centrifuged at 2200 g at 4 ° C for 5 minutes. The supernatant was removed from the resultant spin and centrifuged again at 9000 g for 10 minutes. The final supernatant was ultracentrifuged (100,000 *g*, 90 minutes, 4 ° C, Beckman L8-70M). The supernatant was discarded and the resulting pellet was resuspended in buffer (10 mM trizma, 1 mM EDTA, 20% glycerol, pH 7.5), transferred into cryogenic vials (0.5 mL), flash-frozen in liquid nitrogen and stored at –80 ° C. A sample of each aliquot was set aside for protein determination.

3.3.6. Western blot analyses: (Protocol L)

3.3.6.1. Detection FMO1, FMO3, FMO5

Vertical minigel western blot analyses (Thummel, *et al.* 1988) were conducted utilizing SDS-PAGE (10% resolving gel). Briefly, the aforementioned microsomal samples were thawed on ice. FMO1, FMO3, and FMO5 Supersomes® (Gentest Corp., Woburn, MA), purified FMO human cDNA proteins, from an insect baculovirus system, were utilized as controls in the experiments. Half of a microgram of each FMO protein was loaded onto the gels. Kaleidoscope pre-stained molecular weight standards () (BioRad, Hercules, CA), and pre-stained SDS-PAGE low range molecular weight standards (5 µL) (BioRad, Hercules, CA) with molecular weights from 206 kDa to 7 kDa and from 110 kDa to 21.4 kDa, respectively were utilized. In all experiments, 4X loading buffer (6 g urea, 1 g SDS, 1.2 g DTT, 100 mM tris base (pH 8.0), 1 mg/10 mL bromophenol blue) volume was kept constant (15 µL) to avoid possible gel migration. Loading buffer was added to the microsomal samples. The amount of protein loaded varied among experiments. The total loading volume was 60 µL. Due to the low protein concentrations of the cell culture microsomes, the total loading volume was increased to 75 µL. Samples were boiled at 100 ° C for 2 – 3 minutes, placed immediately on ice, vortexed, and loaded for SDS-PAGE resolve. FMO1, FMO3, and FMO5 1° Ab of 1:500 and 1:1000 dilutions (Gentest Corp., Woburn, MA) were used with nitrocellulose (BioRad, Hercules, CA) or polyvinyl difluoride (PVDF) (Immobilon™-P, VWR, Seattle, WA) membranes, pore size of

0.45 cm for transference. The gel was transferred (CBC Scientific Company, Inc., Del Mar, CA) with transblot buffer (25 mM tris base, 192 mM glycine, 20% MeOH), for 1 hour (100 volts). Various immunblot buffer [IB] (20 mM tris base, 500 mM NaCl, pH 7.2) blocking techniques were implemented using either 3% BSA or 1, 2, 3, 4, or 5% powdered milk and 2° Ab adjustments of 1:2000 to 1:10,000 dilutions were used to reduce the non-specific binding. After the 1° and 2° antibody incubations, the membranes were washed with IB-0/05% Tween 20, 1° and 2° antibody incubations, and washings were conducted on a rotating shaker (Labline Rotator, model 1314, Melrose Park, IL). Bands were detected by autoradiography with ECL (Amersham Pharmacia, Sunnyvale, CA) or Immunostar chemiluminescence (BioRad Laboratories, Hercules, CA).

3.3.6.2. FMO1 detection:Human donor microsomes

Microsomal samples of the human duodenum (donor DT1), jejunum (donors J1, J2, J3, J4, J5, J6, J7, J8, J9, J10, J11, JM1, JM2, JM3), ileum (donor I11), and colon (donor C11) were utilized in several western blot analyses. FMO1 and FMO5 (0.5 μg) as the positive and negative controls, respectively, molecular markers, and microsomal samples of the jejunum, ileum, duodenum, or colon (75, 100, or 50 μg) were evaluated on each gel.

Nitrocellulose or PVDF membranes were used for comparison due to high background noise with the nitrocellulose membrane. The nitrocellulose membrane was blocked for 30 minutes with BSA in IB and exposed to the FMO1

1° Ab (1% BSA- IB, 1:500) overnight at room temperature. The following day, the membrane was washed 3 times (20 minutes each) and exposed to IgG-alkaline phosphatase 2° (1:2000) (Biorad Laboratories, Hercules, CA) for one hour at room temperature. After five washings of the membrane, 1 mL of the chemiluminescence (Immunostar) reagent was applied to the membrane and exposures were conducted. Timed exposures were from 30 sec to 45 minutes, dependent upon signal clarification. The PVDF membrane was blocked for 30 minutes with 1%, 2%, 3%, 4%, or 5% powdered milk in IB, exposed to 1° Ab-IB concentrations of 1:500 to 1:1000 dilutions, with 0.5% powdered milk for 2, 3, or 4 hours. PVDF membrane washings after 1° and 2° Ab were as with the nitrocellulose membrane, however after the 2° Ab the washings were reduced to three instead of four. Secondary Ab (1:2000 to 1:10,000) was anti-rabbit horseradish peroxidase (Gentest Corp., Woburn, MA) in IB with 0.5% powdered milk. A membrane comparison was conducted to determine if the IB conditions with either BSA or powdered milk would reduce the non-specific binding so an adequate assessment of the FMO protein signal could be determined.

3.3.6.3. Caco-2 cell microsomes

Western blot analyses of microsomal Caco-2 cells were conducted with FMO1 and FMO5 as the positive and negative controls, respectively as well as a colon (donor C11) sample as a second positive control. Microsomal samples of 75, 100, 150, or 300 μg protein were evaluated. Blotting was performed with either nitrocellulose or PVDF membranes. The procedure was identical to that described in 3.3.6.2. and a 2° Ab concentration of 1:2000 was used. Microsomes were prepared Caco-2 cell passages 27, 29, and 31.

3.3.6.4. Immunoprecipitation: (Protocol M)

Immunoprecipitation was conducted to form an antigen-antibody complex with FMO1 and the FMO1 primary antibody in an attempt to collect only the FMO1 protein and remove unwanted contaminants. This procedure could aid in reducing background noise. Immunoprecipitation experiments were conducted using the human jejunal microsomal samples J1, J3, and J9 loading 300 μg per lane. Increased protein concentrations were used to increase the probability of the antibody complexing with the antigen. Briefly, samples (300 μg) were diluted with 0.5 mL of 2.5% triton dilution/homogenization buffer with 2.5% Triton X-100, 0.2% protease inhibitor cocktail to homogenization buffer (100 mM trizma, 250 mM sucrose, 1 mM EDTA, pH 7.4). Samples were tumbled on a rotary platform for 1 hour, centrifuged, and the resultant supernatant was tumbled with FMO1 1° Ab (1:500) overnight at 4 ° C. The following day, 50 μL from a PAS

(50%) slurry (75 mg PAS/0.6 mL homogenization buffer), for complex formation was added to each sample and incubated for 1 hour at 4 ° C. Samples were centrifuged (14,000 rpm) for 4 minutes to obtain a pellet. Supernatant was removed and each sample pellet was washed (vortexed) 4 times with an equal volume (~1 mL) of 2.5% triton dilution/homogenization buffer and the pellet was resuspended and briefly centrifuged for 5 min at 14,000 rpm. Then, the pellets were washed with homogenization buffer without detergent twice, centrifuged, and the resulting supernatant was discarded. Samples were boiled for 2 to 3 minutes, pelleted at 14,000 rpm, and the supernatant was utilized for resolve. FMO1 and FMO5 were utilized as the positive and negative controls, respectively. Individual samples of FMO1 were run with and without PAS, and FMO5 contained PAS.

3.3.6.5. *N*-glycosylation

When conducting the de-glycosylation experiments, there was a slight modification in the western blot sample preparation. Briefly, the microsomes from human jejunal mucosa, JM1, JM2, JM3, and human duodenal, DT1, were prepared as previously described in the western blot instructions. After the samples have been boiled with 4X buffer and resuspension buffer, the samples were allowed to cool and then transferred to disposable glass vials. Endo H (1 milliunit/μL) and 50 mM potassium phosphate buffer (pH 5.5) were added to each sample (60 μL) for a total volume of 120 μL. The vials were capped with paraffin film to avoid evaporation and incubated for 20 hours at 37 ° C in a water bath or

cell culture incubator. After 20 hours the sample was centrifuged (14,000 rpm) for 5 minutes. The pellet and supernatant were separated into individual eppendorf vials. The supernatant was loaded for resolve without any additional preparation. The pellet was combined with a prepared 4X buffer and resuspension buffer solution as per western blot instructions (Protocol L) and resolved.

3.3.6.6. FMO3/FMO5 detection: human donor microsomes/cell lines

Western blot analyses were conducted for detection of FMO3 and FMO5 in human jejunal microsomes and microsomal Caco-2 cells. Jejunum (J1, J2, J3, J4, J5, and J6), colon (C11), and Caco-2 cell (pass 27, and 29) microsomes were utilized. The positive and negative controls of FMO1, FMO3 and FMO5, were resolved on separate blots with indicated samples. Total microsomal protein loading was 150 μg/lane for the human jejunum and colon microsomes, and 300 μg/lane for Caco-2 cell microsomes. Nitrocellulose membrane and exposure to alkaline-phosphatase 1° Ab and chemiluminescence was performed with an Immunostar kit as previously described in section 3.3.6.2.

3.4. RESULTS – WESTERN BLOT ANALYSIS

3.4.1. FMO1 in human donor microsomes

Figures 18, 19, and 20 indicated the presence of FMO1 with chemiluminescence on a nitrocellulose membrane utilizing microsomal samples from the human donor jejunum (J1, J2, J3, J4, J5, J6, J7, J8, J9, J10, and J11), ileum (I11), and colon (C11). FMO1, 58 kDa, levels in jejunum ranged from 29.8 to 88.6 pmol FMO1/mg protein. The average FMO1 protein concentration in human jejunal microsomes (16 samples, performed in duplicate) was 54.2 ± 20.7 pmol FMO1/mg microsomal protein. The highest and lowest protein concentrations were 88.6 pmol of FMO1/mg protein from a 27 yr African American male (donor J9-Figure 19) and 29.9 pmol of FMO1/mg protein from a 40 yr Caucasian female (donor J11-Figure 19), respectively. FMO1 protein levels detected for the youngest and the oldest donor ages were 44.8 pmol FMO1/mg protein from a 3 yr African American male (donor J5-Figure 18) and 35.8 pmol FMO1/mg protein from a 59 yr Caucasian male (donor JM2-Figure 20), respectively.

Shown in Figures 18, 19, and 20 is non-specific binding of FMO1 1° antibody at 40 kDa and 65 kDa. Figures 18 and 19 represent J1, J2, J3, J4, J5, J6, J7, J8, J9, J10, and J11 (150 µg) and Figure 20 represents JM1, JM2, and JM3 (100 µg).

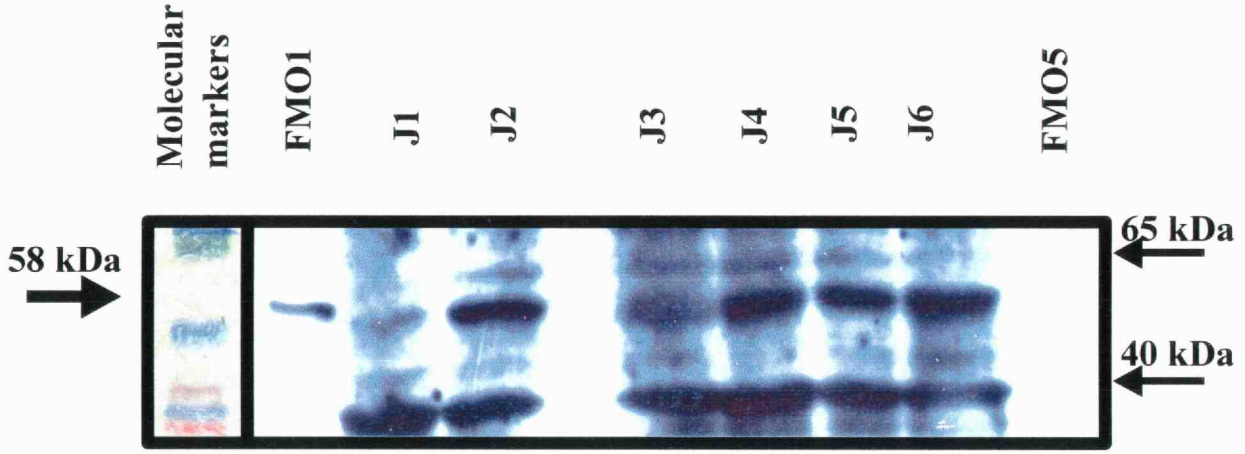

Figure 18: FMO1 western blot nitrocellulose detection in human donor jejunum microsomes. Depicted are FMO1, 0.5 μg and FMO5, 0.5 μg as the positive and negative controls, respectively. Microsomal protein loading was 150 μg/lane. The 58 kDa arrow represents the apparent molecular weight for FMO1.

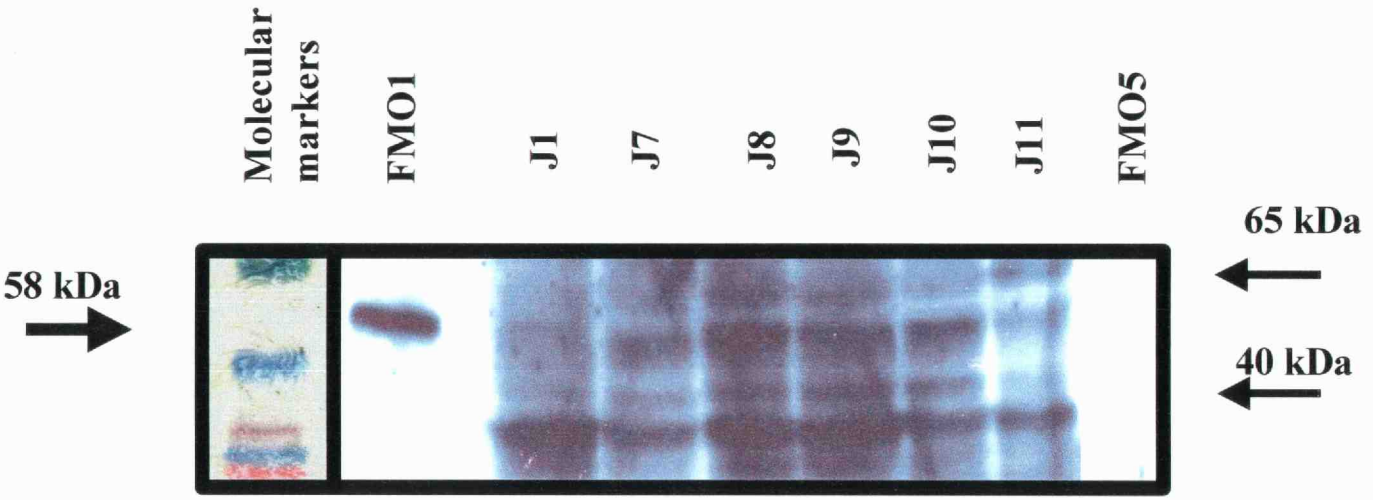

Figure 19: FMO1 western blot nitrocellulose detection in human donor jejunum microsomes. Depicted are FMO1, 0.5 µg and FMO5, 0.5 µg as the positive and negative controls, respectively. Microsomal protein loading was 150 µg/lane. The 58 kDa arrow represents the apparent molecular weight for FMO1.

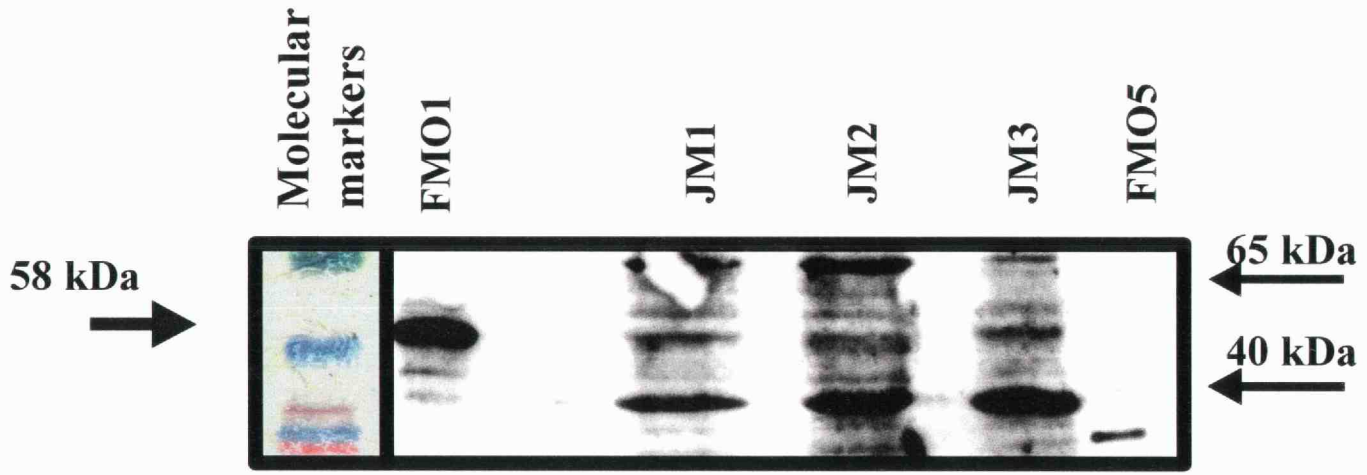

Figure 20: FMO1 western blot nitrocellulose detection in human donor jejunum microsomes. Depicted are FMO1, 0.5 µg and FMO5, 0.5 µg as the positive and negative controls, respectively. Microsomal protein loading was 100 µg/lane. .The 58 kDa arrow represents the apparent molecular weight for FMO1.

Figure 21a displays the variation of pmol of FMO1 according to age of donors and Figure 21b represents the averages of the donors according to < 36 yr and > 36 yr. A significant difference was seen with increasing age where there was a decrease in the amount of detectable FMO1 (ANOVA, $p < 0.05$, $n = 12$). Averages according to age revealed < 36 yr 68.6 ± 21.5 pmol FMO1/mg protein and >36 yr 37.9 ± 6.1 pmol FMO1/mg protein. The 3 yr and 12 yr donors were not utilized for statistical analysis due to developmental factors. Table 6 depicts information regarding each individual donor and their cause of death.

a)

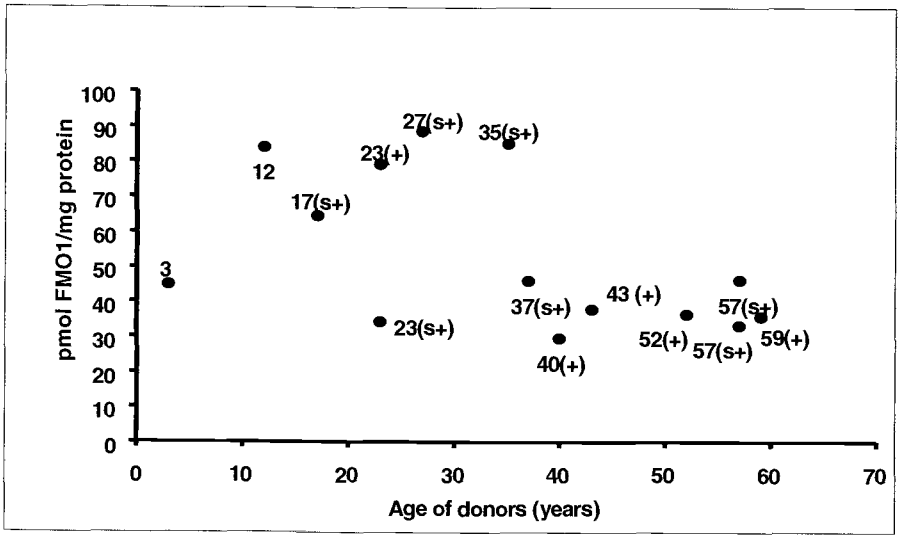

b)

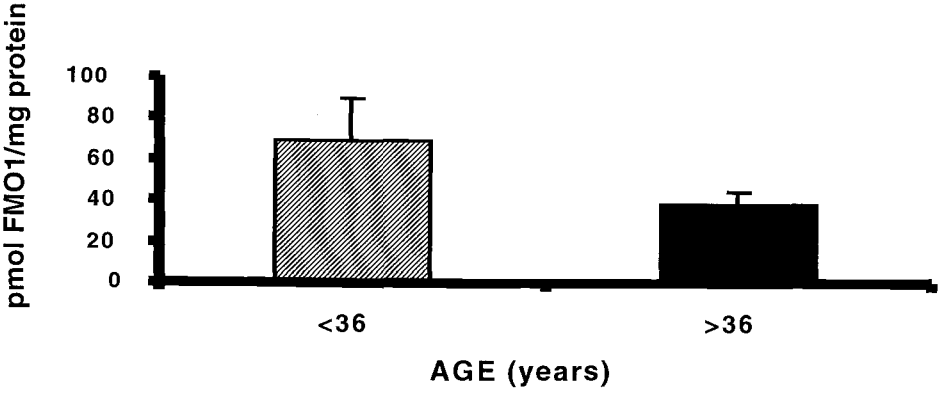

Figure 21: Comparison of pmol of FMO1/ mg of protein in human donor jejunal microsomes. ($p < 0.05$, $n = 12$) **a)** Numerical values of individual locations are representative of age in years. Also represented are whether the donor was a smoker by the letter "s" or alcohol/prescribed medication consumption by a "+" sign listed next to the respective age of the donor. **b)** The average and standard deviations of donors <36 yrs of age and donors >36 yrs of age.

Table 6: Donor Information. Abbreviations are as follows: ICB-intracranial bleed; CHI-head trauma/stroke; ICH-intracranial hemorrhage; HT-head trauma; MI-myocardial infarction; NIIDM-non insulin dependent.

Donor Age Caucasian (C) African American (A) Male (m) Female (f) (donor identification)	**Smoker versus non-smoker**	**Ingestion of alcohol/ medication**	**Pre-existing illness**	**Cause of death**
57 – C – f – (J1)	+	+	emphysema, ulcer	ICB
12 – C – f – (J2)	-	-	-	CHI
35 – C – f – (J3)	+	+	-	Anoxia
43 – C – m – (J4)	-	+	-	ICH
3 – B – m – (J5)	-	-	-	Anoxia
23 – C – f – (J6)	-	+	-	HT
37 – C – m – (J7)	+	+	hypertension	ICH
17 – C – f – (J8)	+	+	anorexia	CHI
27 – B – m – (J9)	+	+	-	CHI
57 – C – f – (J10)	+	+	border diabetes	ICB
40 – C – f – (J11)	-	+	asthma	CHI
23 – C – f – (JM1)	+	+	asthma	Anoxia
59 – C – m – (JM2)	-	+	NIIDM (16 years) hypertension	MI
52 – C – f – (JM3)	-	+	asthma, arthritis	Anoxia

Figure 22 indicates the presence of FMO1 in the human jejunum, ileum, and colon (donor 11) on a nitrocellulose membrane. The analysis of band intensity indicated 60.9 pmol FMO1/mg protein in the human jejunum, with the ileum and colon comparable at 53.1 and 54.3 pmol FMO1/mg protein, respectively. Donor J11 was also analyzed previously, shown in Figure 19, resulting in the lowest protein concentration detection of 29.9 pmol of FMO1/mg protein. Therefore, intra-variability was indicated.

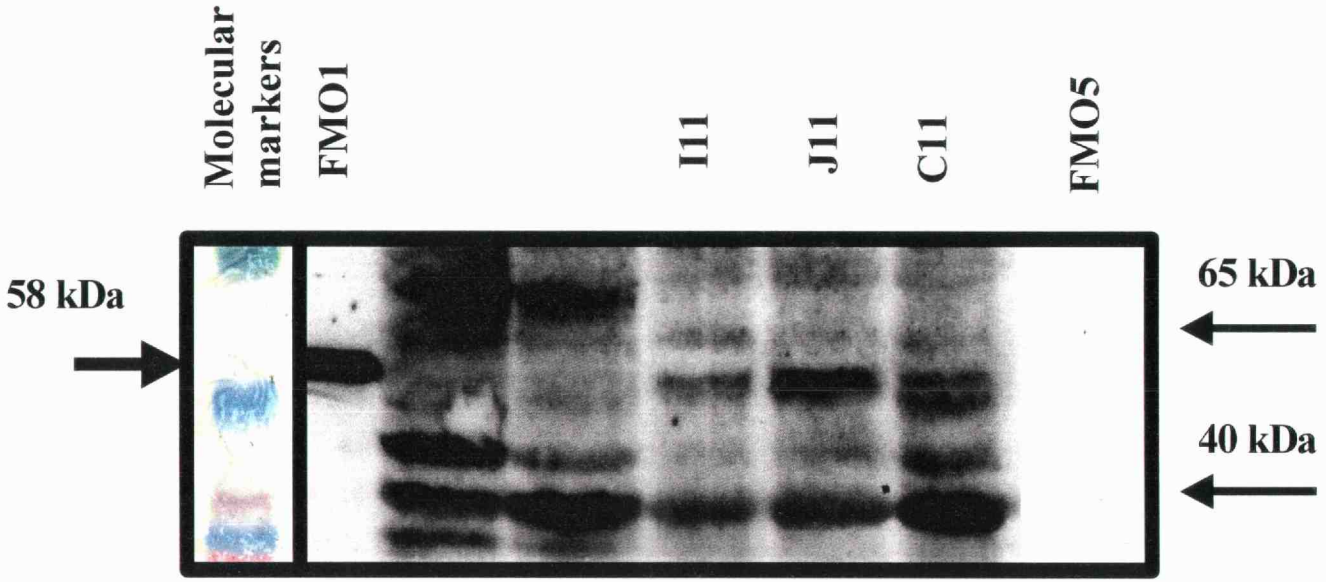

Figure 22: FMO1 western blot nitrocellulose analysis from human ileum, jejunum and colon microsomes. FMO1 (0.5 μg) and FMO5 (0.5 μg) as the positive and negative controls, respectively. Microsomal protein loading was 150 μg/lane. The 58 kDa arrow represents the apparent molecular weight of FMO1.

3.4.2. Immunoprecipitation and *N*-glycosylation

Immunoprecipitation was utilized to form an antibody-antigen complex to avoid non-specific binding results. In these experiments, the pellets were difficult to visualize during the washing process and appeared fragile, therefore it is probable part of the pellet was being lost. Experiments produced variable results from a faint band at approximately 58 kDa to a definite band with a stepladder visual throughout the individual sample lane for the human jejunum samples. Because high background signaling was also present, these results were inconclusive.

In order to determine if the 65 kDa band was the glycosylated form of FMO1, de-glycosylation experiments were conducted using microsomes prepared from duodenal tissue (DT1) and microsomes from jejunal mucosa (JM1, JM2, JM3). The western blot experiments indicated the possibility of the presence of *N*-glycosylation in FMO1. Duodenal microsomes indicated susceptibility to de-glycosylation because the 65 kDa signal in the duodenum sample that had been present in previous experiments was absent with the presence of endo H. The jejunum 65 kDa non-specific binding in previous experiments was reduced to a faint band. Further experiments were variable in jejunum samples. The strongest evidence for *N*-glycosylation detachment due to a verifiable signal at the FMO molecular weight of 58 kDa and an obvious absence of the non-specific binding at 65 kDa was in the supernatant samples, whereas the pellet signal for FMO at 58

kDa was indiscernable for verification. It appears the FMO1 protein was present in the supernatant after the de-glycosylation with endo H (data not shown).

3.4.3. Caco-2 cell microsomes

Figure 23 indicates the presence of FMO1. Western blots using the nitrocellulose and PVDF membranes were conducted. Band intensity was determined with alkaline-phosphatase chemiluminescence autoradiography followed by densitometry analyses. Each sample exposure contained 300 μg of protein. The presence of FMO1 was detected from the Caco-2 cells microsomes, but there was a high background signal and non-specific binding which were inconclusive. With the PVDF membrane, the background was reduced, but the apparent non-specific binding was still prevalent except with the 2 to 5% powdered milk blocking. With a 2% powdered milk blocking, the background was reduced and an immunoreactive FMO1 band at 58 kDa from the Caco-2 microsomal samples was present. Microsomal preparations of pass 27, 29, and 31 of two separate western blot experiments totaling five samples immunoquantitatively produced an average of 14.98 ± 9.94 pmol FMO1/mg microsomal protein. The results ranged from 2.2 to 25.1 pmol FMO1/mg protein, with the strongest signal from pass 29 shown in Figure 23. However, there were bands of non-specific binding. Both membranes PVDF and nitrocellulose indicated a FMO1 signal from the Caco-2 microsomes.

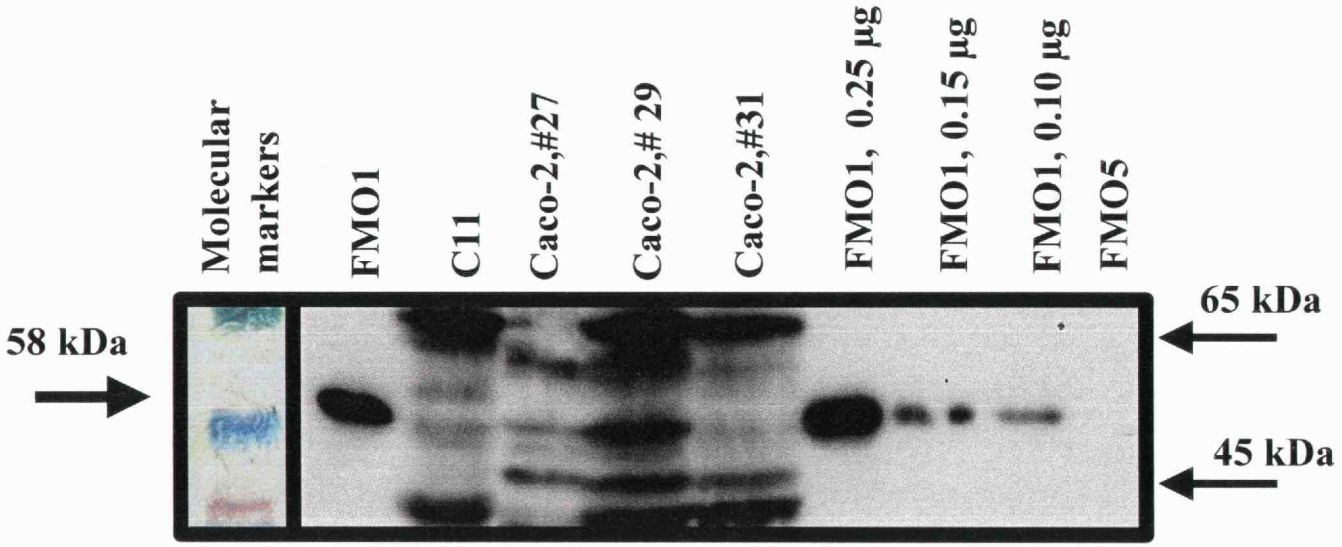

Figure 23: FMO1 western blot detection in Caco-2 cells on a PVDF membrane. FMO1 (0.50 µg-positive control); colon donor #11, JC11, (150 µg - positive control); Caco-2 passage 27, 29, and 31 (300 µg); standard curve of FMO1, 0.25, 0.15, 0.10 µg; FMO5 (0.50 µg – negative control).

3.4.4. FMO3/FMO5 in human donor microsomes

Figures 24 a and b shows that FMO3 and FMO5, with a nitrocellulose membrane and IgG-alkaline-phosphatase detection, are not present in the human microsomal intestinal samples J1, J2, J3, J4, J5, J6. Figure 26a utilized FMO3 and FMO5 for positive and negative controls, respectively, and Figure 26b utilized FMO5 and FMO1 as the positive and negative controls, respectively in human jejunum donor sample microsomes J1, J2, J3, J4, J5, and J6. Microsomal protein samples were loaded with 150 μg per lane as with previous western blot analyses of FMO1. Also Caco-2 cell passage 27, and 29 microsomes indicated a negative detection of FMO3 and FMO5 protein (data not shown).

a)

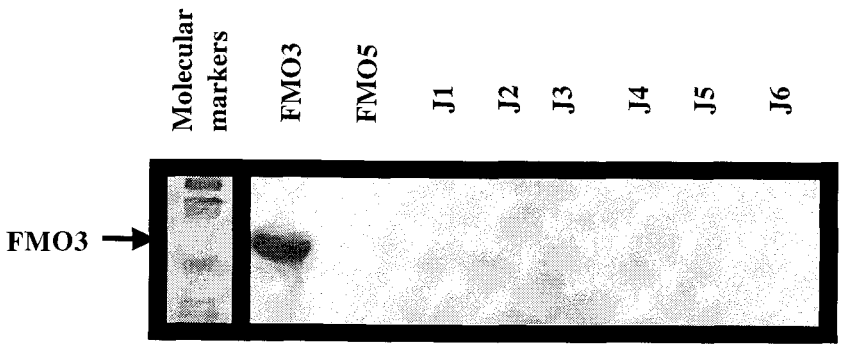

b)

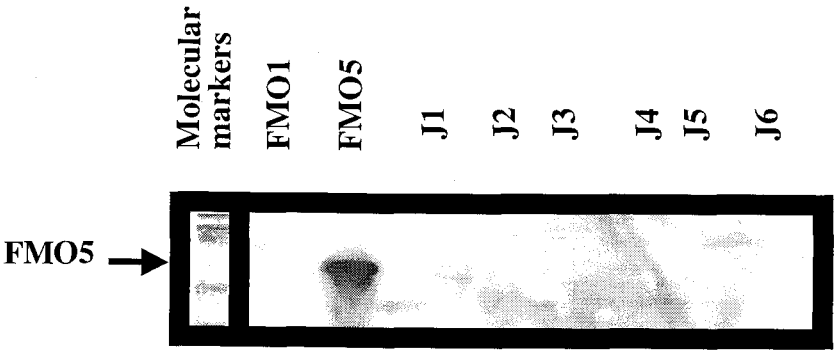

Figure 24: FMO3 and FMO5 western blot detection in human donor jejunal microsomes. Samples are J1, J2, J3, J4, J5, and J6, utilizing 150 µg per lane. **a)** FMO3 detection. FMO3, 0.5 µg and FMO5, 0.5 µg are the positive and negative controls, respectively. Indicated in each microsomal sample is the absence of FMO3. **b)** FMO5 detection. FMO5, 0.5 µg and FMO1, 0.5 µg as the positive control and negative controls, respectively. Indicated in each microsomal sample is the absence of FMO5.

3.5. DISCUSSION

Phase I metabolism of oral drugs may result in reduced bioavailability, diminished efficacy or toxicity. Elucidation of specific enzymes/isoforms involved in metabolic reactions and determination of xenobiotic inter- and intra-metabolism variability is essential for prediction of bioavailability and therapeutics (Hodgson, *et al.* 1995). Alteration in the relative amounts of FMO compared to CYP could result in serious consequences for toxicological or therapeutic properties (Williams, *et al.* 2001).

This study investigated the presence of the FMO1, FMO3, and FMO5 isoforms within the human intestinal tract and in the Caco-2 (HTB-37) cell line using microsomal preparations. Microsomal preparations were selected for all experimental analyses due to their stability for repetitive analysis. Hall *et al.*, in 1999 found that mucosa microsomal preparations were reliable in detection of the intestinal CYP3A. FMO1 was present in all of the donor samples and Caco-2 (HTB-37) cell line (Figures 18, 19, and 20), but FMO3 and FMO5 were not detected in any of the samples.

The expression of FMO1 was highly variable in the human jejunum at 54.2 ± 20.7 pmol FMO1/mg protein. This is comparable to the adult kidney which has been detected at a concentration of 47 ± 9 pmol/mg protein (Yeung, *et al.* 2000) and comparable to the adult liver for FMO3 detected at a concentration of 60 ± 43 pmol/mg protein (Overby, *et al.* 1997). This type of variability is seen with intestinal CYP3A4. For example, CYP3A4 protein expression with human

intestinal microsomes was variable between regions with a median and range of 31 (< 2 - 91), 23 (< 2 - 98), and 17 (< 2 - 60) pmol/mg protein, detected in duodenum, jejunum and ileum, respectively (Thummel, *et al.* 1997). Also, an eleven-fold range was detected in 20 human duodenal punch biopsies of CYP3A4 protein (Lown, *et al.* 1994) and total detectable content of CYP3A found within the small intestine has been estimated at 70 nmol, the majority found in the jejunum (Hall, *et al.* 1999).

Statistical analysis was conducted regarding comparable differences in donors. The data depicted in Figure 21a indicates that age was a significant factor ($p < 0.05$, $n = 12$, Figure 21b) that can be attributed to the inter-individual variability. With increasing age, a reduction in the amount of detectable FMO1 protein occurred. Whether this observation is an indication of FMO1 activity remains to be determined. FMO activity is not markedly dependent upon age or gender in adults (Cashman 1996), however decreased levels of a major oxidative enzyme could produce less activity, lead to toxicity due to a decline in first-pass metabolism and an increase in systemic concentrations. An improved understanding of the metabolic alterations associated with aging could be essential for the development of therapeutic interventions. Also, with a number of the donors being smokers, possibly a discernable alteration in FMO1 protein expression would be observed due to metabolism of nicotine by FMO1 and FMO3 (Cashman 2000). However, the statistical analysis did not indicate an alteration in

FMO1 expression due to smoking. No other discernable patterns such as gender, drug and alcohol consumption, or ethnicity were observed.

The 3 yr donor indicated an intermediate amount of FMO1 (44.8 pmol FMO1/mg protein), which could possibly be explained as due to developmental factors. For example, FMO1 and FMO3 mRNA in the liver is subject to developmental regulation which will effect protein expression (Gasser 1996). Also, it has been shown that there is an incremental decrease in FMO1 and increase in FMO3 that occurs from neonates, 1 – 11 yr followed by an increase to 18 yr (Hines and McCarver 2002). Possibly developmental regulation may have been attributable to the findings in the 3 yr donor, however the 12 yr displayed comparable adult readings.

Preliminary FMO analysis of carbohydrate attachment has indicated that FMO1 in pig contains complex oligosaccharides linked to high-mannose oligosaccharides. Sequences that have been derived from the pig FMO1 cDNA have predicted two putative sites of *N*-glycosylation. Glycosylation, found in pig FMO1 is specific and not random, therefore, suggested is a structural purpose for the *N*-glycosylation in pig FMO1 (Korsmeyer, *et al.* 1998). Due to ortholog identities of FMOs between species (81 – 89%, Hines, *et al.* 1994), and with a strong signal at approximately 65 kDa, microsomal samples were treated with endo H to determine whether an *N*-linked high-mannose oligosaccharides attachment was present in human FMO1. Endo H will hydrolyze and digest an *N*-linked glycoprotein attachment. Indicated was the presence of a sugar attachment

that could be removed. Duodenal microsomes indicated the presence of a glycan moiety, but jejunal microsomal results were variable. In the jejunum microsomes, the 65 kDa signal was decreased with endo H treatment, however the band did not completely disappear as in the duodenal microsomes. This suggests there is a glycosylation present in the jejunum microsomal FMO1, but with repeated experiments with the jejunum the signal varied as to visual intensity. It has been speculated that even if a carbohydrate attachment is present, the *N*-glycosylation of FMO1 would not grossly alter the enzyme function (Korsmeyer, *et al.* 1998).

Cellular models have become an instrument for increasing our knowledge of pharmaceutical potentials for an effective and rapid approach for delivery of new therapeutics to the patient (Bailey, *et al.* 1996). The Caco-2 (HTB-37) cell line is one of the model systems utilized for support in drug discovery early in the process of pharmaceutical development. Determination of the presence of a phase I enzymes such as FMO would be advantageous for an understanding of metabolite formation. The chemiluminescence results for the nitrocellulose and the PVDF membranes indicated the presence of FMO1 in the Caco-2 cells (Figure 23). The PVDF membrane reduced background and revealed an FMO1 band in cell passage 29. The detection of FMO would add increased credibility to future studies conducted with the Caco-2 cell line.

With discovery of substrates being metabolized by either or both CYP or FMO are increasing (Williams, *et al.* 2001), detection and quantification of specific intestinal FMO isoforms and their substrate specificity and catalytic

activity would be useful in future predictions of oral drug efficacy. This study provided information regarding FMO isoforms and the presence of FMO1 in the intestinal tract and the Caco-2 (HTB-37) cell line. With activity determinations, predictable responses of drugs regarding bioavailability and therapeutics as well as toxicological effects could be assessed.

CHAPTER 4: CONCLUSION

In summary, the studies conducted were to investigate a phase I oxidative enzyme, FMO. The first study was to determine whether FMO could be responsible for toxicity effects with the administration of an oral azole antifungal, KT utilizing both *in vivo* and *in vitro* methodology for comparative analysis. The second study analysis was to determine the presence of FMO isoforms in the small intestine and Caco-2 cells.

In the first study observed with KT administration, a covalent binding occurred that was correlated with increased serum levels of a hepatic cytosolic enzyme (alanine aminotransaminase) and a reduction of a hepatic oxidative scavenger (glutathione). These occurrences supported a relationship between metabolism, toxicity, and covalent binding. The parent compound was found to be suspect for a covalent binding effect, and a bioactivation of the parent compound was also indicated. The metabolic pathway implicated was FMO-mediation due to a reduction in covalent binding with heat inactivation analysis. FMO is heat labile. Drug induced toxicities are often caused by covalently binding to cellular macromolecules leading to enzyme inactivation, altered functions of structural proteins or transcription, disruption of intracellular calcium homeostasis, loss of cellular membrane integrity due to lipid peroxidation or apoptosis (Pohl, *et al.* 1996).

The second study used human donor intestinal microsomes to determine the quantitative presence of FMO isoforms that could be available for altered pharmacokinetics and pharmacodynamics of a compound. Indicated in these findings was the presence of FMO1 in the human duodenum, jejunum, ileum, and colon. Also, detection analyses were conducted using the Caco-2 cell line at passages 27, 29, and 31. However, FMO3 and FMO5 were not detected in any of the samples used for FMO1 detection. Caco-2 cells are utilized for determinations of intestinal drug metabolism with phase I oxidation (Carriere, *et al.* 2001). This study is the first to report FMO1 present in the colorectal cells and with the elucidation of FMO expression in the Caco-2 cell line, newly acquired soft-nucleophilic compounds containing sulfur, nitrogen, phosphorus or selenium could be tested for metabolite formation that would aid in predictable determinations of metabolism and toxicological effects.

Both studies revealed insightful information regarding FMOs. With oral administration of FMO substrates, the presence of FMO could alter predicted bioavailability and therapeutics or result in toxicity effects. Understanding of an enzymatic system, its location, prevalence, and inherent affinity for a particular compound family are all useful tools for aiding in a predictable outcome of future xenobiotics. These findings implicated FMO may play a significant role in drug metabolism and in the future may be considered a formidable enzyme.

REFERENCES

Adali O., Carver G. C. and Philpot R. M., The effect of arginine-428 mutation on modulation of activity of human liver flavin monooxygenase 3 (FMO3) by imipramine and chlorpromazine. *Exp Toxic Pathol* **51:** 271-276, 1999.

Al-Waiz M., Mitchell S. C., Idle J.R.and Smith R.L., The metabolism of ^{14}C-labelled trimethylamine and its *N*-oxide in man. *Xenobiotica* **17**(5)**:** 551-558, 1987.

Atta-Asafo-Adjei E., Lawton M. P.and Philpot R. M., Cloning, sequencing, distribution, and expression in *Escherichia coli* of flavin-containing monooxygenase. *J. Biol Chem* **268:** 9681-9689, 1993.

Bailey C.A., Bryla P.and Malick A.W., The use of the intestinal epithelial cell culture model, Caco-2 in pharmaceutical development. *Adv Drug Deliv Rev* **22:** 85-103, 1996.

Baxter J.G., Brass C., Schentag J.J.and Slaughter R. L., Pharmacokinetics of ketoconazole administered intravenously to dogs and orally as tablet and solution to humans and dogs. *J Pharm Sci* **75**(5)**:** 443-447, 1986.

Bercoff E., Bernau J., Degott C., Kalis B., Lemaire A., Tilly H., Ruef B.and Benhamou J.P., Ketoconazole-induced fulminant hepatitis. *Gut* **26:** 636-638, 1985.

Bok R.A. and Small E.J., The treatment of advanced prostate cancer with ketoconazole: safety issues. *Drug Saf* **20**(5)**:** 451-8, 1999.

Bonkovsky H.L., Hauri H., Marti U., Gasser R.and Meyer U. A., Cytochrome P450 of small intestinal epithelial cells. *Gastroenterology* **88:** 458-67, 1985.

Brusko C.S. and Marten J.T., Ketoconazole hepatotoxicity in a patient treated for environmental illness and systemic candidiasis. *Ann Pharm* **25:** 1321-1325, 1991.

Buckholz C. J. and Rodriguez R. J., Covalent binding of ketoconazole in rat hepatic tissue. In: *Society of Toxicology, Philadelphia, Penn.,2000.*

Caldwell J. and Marsh M. V., Metabolism of drugs by the gastrointestinal tract. In: *Butterworths International Medical Review. Clinical Pharmacology and Therapeutics.*, Vol. 1, pp. 29-42. Butterworth Scientific, 1982.

Campbell N. A., Animal Nutrition. In: *Biology*, pp. 802-806. The Benjamin/Cummings Publishing Company, 1993.

Carriere V., Chambaz J.and Rousset M., Intestinal responses to xenobiotics. *Toxicol inVitro* **15:** 373-378, 2001.

Cashman J. R., Human flavin-containing monooxygenase: Substrate specificity and role in drug metabolism. *Curr Drug Metab* **1:** 181-191, 2000.

Cashman J. R., Human flavin-containing monooxygenase (form 3): polymorphisms and variations in chemical metabolism. *Pharmacogenomics* **3**(3)**:** 325-339, 2002.

Cashman J. R., T. Perotti B. Y., Berkman C. E.and Lin J., Pharmacokinetics and molecular detoxication. *Environ Health Perspect* **104**(Supplement 1)**:** 23-40, 1996.

Cashman J. R., Xiong Y., Lin J., Verhage H., van Poppel G., van Bladeren P.J., Larsen-Su S.and Williams D.E., *In Vitro* and *In Vivo* inhibition of human flavin-containing monooxygenase form 3 (FMO3) in the presence of dietary indoles. *Biochem Pharmacol* **58:** 1047-1055, 1999.

Cashman J.R., Structural and catalytic properties of the mammalian flavin-containing monooxygenase. *Chem Res Toxicol* **8:** 166-181, 1995.

Cashman J.R., Drug discovery and drug metabolism. *Drug Discov Today* **1**(5)**:** 209-216, 1996.

Cashman J.R., Xiong Y.N., Xu L.and Janowsky A., *N*-oxygenation of amphetamine and methamphetamine by the human flavin-containing monooxygenase (Form 3): Role in bioactivation and detoxication. *J. Pharmacol Exp Ther* **288**(3)**:** 1251-1260, 1999.

Cashman J.R., Bi Y., Lin J., Youil R., Knight M., Forrest S.and Treacy E., Human flavin-containing monooxygenase form 3: cDNA expression of the enzymes containing amino acid substitutions observed in individuals with trimethylaminuria. *Chem Res Toxicol* **10**(8)**:** 837-841, 1997.

Cashman J.R. and Zhang J., Interindividual differences of human flavin-containing monooxygenase 3: Genetic polymorphisms and functional variation. *Drug Metab Disp* **30**(10)**:** 1043-1052, 2002.

Chien R., Yang L., Lin P.and Liaw Y., Hepatic injury during ketoconazole therapy in patients with onychomycosis: A controlled cohort study. *Hepatology* **25:** 103-107, 1997.

Chung W., Park C., Roh H.and Cha Y., Induction of flavin-containing monooxygenase (FMO1) by a polycyclic aromatic hydrocarbon, 3-methylcholanthrene, in rat liver. *Mol Cells* **7**(6)**:** 738-741, 1997.

Chung W., Park C., Roh H., Lee W.and Cha Y., Oxidation of ranitidine by isozymes of flavin-containing monooxygenase and cytochrome P450. *Jpn J. Pharmacol* **84:** 213-220, 2000.

Cribb A. E., Miller M., Leeder S., Hill J.and Spielberg S. P., Reactions of the nitroso and hydroxylamine metabolites of sulfamethoxazole with reduced glutathione. *Drug Metab Disp* **19**(5)**:** 900-906, 1991.

Cross H.S., Huber C. and Peterlik M., Antiproliferative effect of 1,25-dihydroxyvitamin D3 and its analogs on human colon adenocarcinoma cells (Caco-2): influence of extracellular calcium. *Biochem Biophys Res Commun* **179:** 57-62, 1991.

Daneshmend T.K., Warnock D.W., Ene M.D., Johnson E.M., Parker G., Richardson M.D.and Roberts C.J.C., Multiple dose pharmacokinetics of ketoconazole and their effects on antipyrine kinetics in man. *Antimicrob Agents Chemother* **12:** 185-188, 1983.

Daneshmend T.K., Warnock, D.W., Warnock, D.W., Ene, M.D., Johnson, E.M., Potten, M.R., Richardson, M.D., and Williamson, P.J., Influence of food on

the pharmacokinetics of ketoconazole. *Antimicrob Agents Chemother* **25**(1)**:** 1-3, 1984.

Daneshmend TK and Warnock DW, Clinical pharmacokinetics of ketoconazole. *Clin Pharmacokinet* **14:** 13-14, 1988.

Decker C. J.and Doerge D. R., Rat hepatic microsomal metabolism of ethylenethiourea. Contributions of the flavin-containing monooxygenase and cytochrome P-450 isozymes. *Chem Res Toxicol* **4:** 482-489, 1991.

Decoster R., Wouters W.and Bruynseels J., P450-dependent enzymes as targets for prostate cancer therapy. *J. Steroid Biochem Mol Biol* **56**(1-6 Spec No)**:** 133-143, 1996.

Doherty M.M. and Charman W.N., The mucosa of the small intestine:how clinically relevant as an organ of drug metabolism? *Clin Pharmacokinet* **41**(4)**:** 235-253, 2002.

Dolphin C., Shephard E. A., Povey S., Palmer C. N. A., Ziegler D. M., Ayesh R., Smith R. L.and Phillips I. R., Cloning, primary sequence, and chromosomal mapping of a human flavin-containing monooxygenase (FMO1). *J. Biol Chem* **266:** 12379-12385, 1991.

Dolphin C., Beckett D. J., Janmohamed, A., Cullingford, T. E., Smith, R.L., Shephard, E.A., and Phillips, J.R., The flavin-containing monooxygenase 2 gene (FMO2) of humans, but not of other primates, encodes a truncated, nonfunctional protein. *J. Biol Chem* **273:** 30599-30607, 1998.

Dolphin C., Cullingford, T.E., Shephard E.A., Smith, R.L., and Phillips, I.R., Differential developmental and tissue-specific regulation of expression of the genes encoding three members of the flavin-containing monooxygenase family of man, FMO1, FMO3, and FMO4. *Eur J. Biochem* **235:** 683-689, 1996.

Dolphin C., Shephard, E. A., Povey, S., Smith, R. L., and Phillips, I. R., Cloning, primary sequence and chromosomal localization of human FMO2, a new member of the flavin-containing monooxygenase family. *Biochem J.* **287:** 261-267, 1992.

Duarte P.A., Chow C.C. , Simmons F.and Ruskin J., Fatal hepatitis associated with ketoconazole therapy. *Arch Intern Med* **144:** 1069-1070, 1984.

Fang J., Metabolism of clozapine by rat brain: the role of flavin-containing monooxygenase (FMO and cytochrome P450 enzymes). *Eur J. Drug Metab Pharmacokinet* **25**(2)**:** 109-14, 2000.

Forrest S. M., Knight M., Akerman B. R., Cashman J.R.and Treacy E. P., A novel deletion in the flavin-containing monooxygenase gene (FMO3) in a Greek patient with trimethylaminuria. *Pharmacogenetics* **11:** 169-174, 2001.

Fromm M. F., Differential induction of prehepatic and hepatic metabolism of verapamil by rifampin. *Hepatology* **24:** 796-801, 1996.

Fuhr U., Klittich K.and Staib A. H., Inhibitory effect of grapefruit juice and its bitter principal, naringenin, on CYP1A2 dependent metabolism of caffeine in man. *Br J. Clin Pharmac* **35:** 431-436, 1993.

Gao P., Thornton-Manning J. R.and Pegram R. A., Protective effects of glutathione on bromodichloromethane *in vivo* toxicity and *in vitro* macromolecular binding in Fischer 344 rats. *J. Toxicol and Environ Health* **49**(2)**:** 145-59, 1996.

Gascoigne E.W., Barton G.J., Michaels M., Meuldermans W.and Heykants J., The kinetics of ketoconazole in animals and man. *Clin Res Rev* **1:** 177-187, 1981.

Gasser R., The flavin-containing monooxygenase system. *Exp Toxic Pathol* **48:** 467-470, 1996.

Gilman A. G., Goodman M.D., (Hon) D. Scand Hardman J. G., *Goodman and Gilman's The pharmacological basis of therapeutics*. McGraw-Hill, 1996.

Guyton A. C., General principles of gastrointestinal function-mortality, nervous control, and blood circulation (Chapter 62). In: *Textbook of Medical Physiology*, pp. 698-708, 1991.

Hall S., Thummel K.E., Watkins P.B., Lown K.S., Benet L.Z., Paine M.F., Mayo R.R., Turgeon K., Bailey D.G., Fontana R.J.and Wrighton S.A., Molecular and physical mechanisms of first-pass extraction. *Drug Metab Disp* **27**(2)**:** 161-166, 1999.

Halpert J. R., Domanski T. L., Adali O., Biagini C. P., Cosme J., Dierks E. A., Johnson E. F., Jones J. P., De Montellano P. O., Philpot R. M., Sibbesen O., Wyatt W. K.and Zheng Z., ANTHONY Y. H. LU COMMEMORATIVE ISSUE. Structure-function of cytochromes P450

and flavin-containing monooxygenases. Implications for drug metabolism. *Drug Metab Dispos* **26**(12)**:** 1223-1231, 1998.

Heel R.C., Brogden R.N., Carmine A., Morley P.A., Speight T.M.and Avery G.S., Ketoconazole: A review of its therapeutic efficacy in superficial and systemic fungal infections. *Drugs* **23:** 1-36, 1982.

Heykants J., Van Peer A., Van de Velde V., Van Rooy P., Meuldermans W., Lavrijsen K., Woestenborghs R., Van Cutsem J.and Cauwenbergh G., The clinical pharmacokinetics of itraconazole: an overview. *Mycoses* **32**(Supplement 1)**:** 67-87, 1989.

Hines R.N.and McCarver D.G., The ontogeny of human drug-metabolizing enzymes: Phase I oxidative enzymes. *J. Pharmacol Exp Ther* **300**(2)**:** 355-360, 2002.

Hines R.N., Cashman J. R., Philpot R. M., Williams D. E.and Ziegler D. M., The mammalian flavin-containing monooxygenases: Molecular characterization and regulation of expression. *Toxicol Appl Pharmacol* **125:** 1-6, 1994.

Hines R.N., Hopp K. A., Franco J., Saeian K.and Begun F. P., Alternative processing of the human FMO6 gene renders transcripts incapable of encoding a functional flavin-containing monooxygenase. *Mol Pharmacol* **62**(2)**:** 320-325, 2002.

Hodgson E., Rose R. L., Ryu D. Y., Falls G., Blake B.L.and Levi P.E., Pesticide-metabolizing enzymes. *Toxicol Lett* **82/83:** 73-81, 1995.

Hogberg J. and Kristoferson A., Glutathione turnover in isolateed hepatocytes. *J. Pharmacol Toxicol* **42:** 271-74, 1977a.

Hogberg J. and Kristoferson A., A correlation between glutathione levels and cellular damage in isolated hepatocytes. *Eur J. Biochem* **74:** 77-82, 1977b.

Holtbecker N. , Fromm M. F., Kroemer H. K., Ohnhms E. F.and Heidemann H., The nifedipine-rifampin interaction: Evidence for induction of gut wall metabolism. *Drug Metab Dispos* **24:** 1121-1123, 1996.

IIT Research Institute, Chemoprevention - prostate cancer. *Life Sciences Newsletter* **Fall**(2 - 4)**:** 3 - 4, 1999.

Ilett K. F., Tee L. B. G., Reeves P.T.and Minchin R. F., Metabolism of drugs and other xenobiotics in the gut lumen and wall. *Pharmac Ther* **46:** 66-93, 1990.

Ilett K. F. and Davies D.S., *In vivo* studies of gut wall metabolism. In: *Butterworths International Medical Reviews. Clinical Pharmacology and Therapeutics.*, pp. 43-65. Butterworth Scientific, 1982.

Itagaki K., Carver G.T.and Philpot R.M., Expression and characterization of a modified flavin-containing monooxygenase 4 from humans. *J. Biol Chem* **271**(33)**:** 20102-20107, 1996.

Iyer K. R.and Sinz, Characterization of phase I and phase II hepatic drug metabolism activities in a panel of human liver preparations. *Chem -biol Interact* **118:** 151-169, 1999.

Janssen P., Product monograph: Nizoral®, ketoconazole. 1995.

Karlsson J., S.M. Juo., Ziemniak J. and Artursson P., Transport of celiprolol across human intestinal epithelial (Caco-2) cells: mediation of secretion by multiple transporters including p-glycoprotein. *Br J. Pharmacol* **110:** 1009-1016, 1993.

Katchamart S., Stresser D.M., Dehal S.S., Kupfer D.and Williams D.E., Concurrent flavin-containing monooxygenase down-regulation and cytochrome P450 induction by dietary indoles in rat: implications for drug-drug interaction. *Drug Metab Dispos* **28**(8)**:** 930-6, 2000.

Kedderis G.L.and Rickert D.E., Loss of rat liver microsomal cytochrome P-450 during methimazole metabolism. Role of flavin-containing monooxygenase. *Drug Metab Disp* **13**(1)**:** 58-61, 1985.

Klaassen C. D., *Casarett and Doull's Toxicology; The Basic Science of Poisons.* McGraw-Hill, 1996.

Knight T.E., Shikuma C.Y.and Knight J., Ketoconazole-induced fulminant hepatitis necessitating liver transplantation. *J. Am Acad Dermatol* **25:** 398-400, 1991.

Korsmeyer K.K., Shengheng G., Yang Z., Falick A.M., Ziegler D.M.and Cashman J.R., *N*-glycosylation of pig flavin-containing monooxygenase form I: Determination of the site of protein modification by mass spectrometry. *Chem Res Toxicol* **11:** 1145-1153, 1998.

Koukouritaki S. B., Simpson P., Yeung C. K., Rettie A. E.and Hines R. N., Human hepatic flavin-containing monooxygenases 1 (FMO1) and 3 (FMO3) developmental expression. *Pediatr Res* **51**(2)**:** 236-243, 2002.

Krieter P. A., Ziegler D. M., Hill K. E.and Burk R. P., Increased biliary GSSG efflux from rat livers perfused with thiocarbamide substrates for the flavin-containing monooxygenases. *Mol Pharmacol* **26:** 122-127, 1984.

Krishna D. B.and Klotz U., Extrahepatic metabolism of drugs in humans. *Clin Pharmacokinet* **26:** 144-160, 1994.

Krueger S. K., Martin S. R., Yueh M., Pereira C.B.and Williams D. E., Identification of active flavin-containing monooxygenase isoform 2 in human lung and characterization of expressed protein. *Drug Metab Disp* **30**(1)**:** 34-41, 2002.

Krueger S. K., Williams D. E., Yueh M., Martin S. R., Hines R. N., Raucy J.L., Dolphin C. T., Shephard E. A.and Phillips I. R., Genetic polymorphisms of flavin-containing monooxygenase (FMO). *Drug Metab Rev* **34**(3)**:** 523-532, 2002.

Lacroix D., Sonnier M., Moncion A., Cheron G.and Cresteil T., Expression of CYP3A in the human liver. Evidence that the shift between CYP3A7 and CYP3A4 occurs immediately after birth. *Eur J. Biochem* **247:** 625-634, 1997.

Lampen A., Bader A., Bestmann T., Winkler M., Witte L.and Borlak J.T., Catalytic activities, protein- and mRNA-expression of cytochrome P450 isoenzymes in intestinal cell lines. *Xenobiotica* **28**(5)**:** 429-41, 1998.

Lang D. H., Yeung C. K., Peter R. M., Ibarra C., Gasser R., Itagaki K., Philpot R. M.and Rettie A. E., Isoform specificity of trimethylamine *N*-oxygenation by human flavin-containing monooxygenase (FMO) and P450 enzymes. *Biochem Pharmacol* **56:** 1005-1012, 1998.

Larsen-Su S. and Williams D. E., Dietary indole-3-carbinol inhibits FMO activity and the expression of flavin-containing monooxygenase form 1 in rat liver and intestine. *Drug Metab Disp* **24**(9)**:** 927-931, 1996.

LeCouter D. G. and McLean A. J., The aging liver drug clearance and an oxygen diffusion barrier hypothesis. *Clin Pharmacokinet* **34**(5)**:** 359-373, 1998.

Lewis J.H., Zimmerman H.J., Benson G.D.and Ishak K.G., Hepatic injury associated with ketoconazole therapy. Analysis cases. *Gastroenterology* **86**(3)**:** 503-513, 1984.

Lewis R.A., *Lewis' Dictionary of Toxicology*. CRC Press LLC, 1998.

Lin J.H., Chiba M.and Baillie T.A., Is the role of the small intestine in first-pass metabolism overemphasized? *Am Soc Pharmac Exp Ther* **51**(2)**:** 135-157, 1999.

Lomri N., Gu Q.and Cashman J. R., Molecular cloning of the flavin-containing monooxygenase (form II) cDNA from adult human liver. *Proc Natl Acad Sci USA* **89:** 1685-1689, 1992.

Lown K. S., Kolars J.C., Thummel K. E., Barnett J.L., Kunze K. L., Wrighton S.A.and Watkins P.B., Interpatient heterogeneity in expression of CYP3A4 and CYP3A5 in small bowel. Lack of prediction by the erythromycin breath test. *Drug Metab Disp* **22**(6)**:** 947-55, 1994.

Lown K. S., Bailey D. G., Fontana R. J., Janardan S.K., Adair C.H., Fortlage L.A., Brown M.B., Wensheng G.and Watkins P.B., Grapefruit juice increases felodipine oral availability in humans by decreasing intestinal CYP3A protein expression. *J. Clin Invest* **99**(10)**:** 2545-2553, 1997.

Lu X., Cheng L.and Fleisher D., Cimitidine sulfoxidation in small intestinal microsomes. *Drug Metab Dispos* **26**(9)**:** 940-942, 1998.

MacNair A.L., Gascoigne E., Heap J., Schueman V.and Symoens J., Hepatitis injury associated with ketoconazole therapy. *Br Med J.* **283:** 1058-1059, 1981.

Madara J. L. and Trier J. S., The functional morphology of the mucosa of the small intestine. In: *Physiology of the Gastrointestinal Tract*, pp. 1577-1622. Raven Press, New York, 1994.

Marieb E. N., The Digestive System. In: *Human Anatomy and Physiology*, pp. 892. Benjamin Cummings, 2001.

Maskalyk J., Grapefruit juice: potential drug interactions. *Can Med Assoc J.* **167**(3)**:** 279-280, 2002.

McNicholas C.M., Turnberg L.A.and Brow C.D., Sequential isolations of structural intact villus tip and crypt units form rat duodenum. *J. Biol Chem* **239:** 2370-2378, 1990.

Miniscalco A., Lundahl J., Regardh C.G., Edgar B.and Eriksson U.G., Inhibition of dihydropyridine metabolism in rat and human liver microsomes by flavonoids found in grapefruit juice. *J. Pharmacol Exp Ther* **261**(3)**:** 1195-1199, 1992.

Mitchell S.C.and Smith R.L., Trimethylaminuria: The fish malodor syndrome. *Drug Metab Dispos* **29**(4 part 2)**:** 517-521, 2001.

Oda Y. and Kharasch E.D., Metabolism of methadone and levo-α–acetylmethadol (LAAM) by human intestinal cytochrome P450 3A4 (CYP3A4): Potential contribution of intestinal metabolism to presystemic clearance and bioactivation. *J. Pharmacol Exp Ther* **298**(3)**:** 1021-1032, 2001.

Overby L.H., Carver G.C.and Philpot R.M., Quantitation and kinetic properties of hepatic microsomal and recombinant flavin-containing monooxygenases 3 and 5 from humans. *Chem -biol Interact* **106:** 29-45, 1997.

Owens R.B., Smith H.S., Nelson-Rees W.A.and Springer E.L., Brief communication: Epithelial cell cultures from normal and cancerous human tissues. *J. Natl Cancer Inst* **56**(4)**:** 843-849, 1976.

Paine M. F., Shen D. D., Kunze K. L., Perkins J. D., Marsh C. L., McVicar J. P., Barr D. M., Gillies B. S.and Thummel K. E., First-pass metabolism of midazolam by the human intestine. *Clin Pharmacol Ther* **60:** 14-24, 1996.

Park B.K. and Pirmohamed M., Toxicogenetics in drug development. *Toxicol Lett* **120:** 281-291, 2001.

Park C., Kang J., Chung W., Yi H., Pie J., Park D., Hines R. N., McCarver D. G.and Cha Y., Ethnic differences in allelic frequency of two flavin-containing monooxygenase 3 (FMO3) polymorphisms: linkage and effects on *in vivo* and *in vitro* FMO activities. *Pharmacogenetics* **12:** 77-80, 2002.

PDR, Physician's Desk Reference. 1999.

Perreault N. and Beaulieu J.F., Primary cultures of fully differentiated and pure human intestinal epithelial cells. *Exp Cell Res* **245**(1)**:** 34-42, 1998.

Peters W.H.and Roelofs H.M., Biochemical characterization of resistance to nitrosantrone and adriamycin in Caco-2 human colon adenocarcinoma cells: a possible role for glutathione *S*-transferases. *Cancer Res* **52:** 1886-90, 1992.

Phillips I. R., Dolphin C.T., Clair P., Hadley M. R., Hutt A.J., McCombie R. R., Smith R. L.and Shepherd E. A., The molecular biology of the flavin-containing monooxygenases of man. *Chem -biol Interact* **96:** 17-32, 1995.

Pirmohamed M., D. Williams, Madden S., Templeton E.and Park B.K., Metabolism and bioactivation of clozapine by human liver *in vitro. J. Pharmacol Exp Ther* **272**(3)**:** 984-90, 1995.

Pohl L. R., Pumford N. R.and L. Martin J., Mechanisms, chemical structures and drug metabolism. *Eur J. Biochem* **57**(suppl)**:** 98-104, 1996.

Pond S. M. and Tozer T.N., First-Pass Elimination Basic Concepts and Clinical Consequences. *Clin Pharmacokinet* **9:** 1-25, 1984.

Poulson L. L., Hyslop R. M.and Ziegler D. M., *S*-oxygenation of *N*-substituted thioureas catalyzed by the pig liver microsomal FAD-containing monooxygenase. *Arch Biochem Biophys* **198:** 78-88, 1979.

Renwick A. G., First-pass metabolism within the lumen of the gastrointestinal tract. In: *Presystemic drug elimination*, pp. 3-28. Butterworth Scientific, 1982.

Renwick A. G. and George C. F., Metabolism of xenobiotics in the gastrointestinal tract. In: *Intermediary xenobiotic metabolism in animals: Methodology, mechanisms, and significance*, pp. 13-40. Taylor and Francis, 1989.

Rettie A.E. and Fisher M.B., Transformation Enzymes: Oxidative; Non-P450. In: *Handbook of Drug Metabolism* (Ed. Woolf-Fed), pp. 131-151. Marcel-Dekker, NY, 1999.

Rodriguez R. J.and Acosta Jr., D., Metabolism of ketoconazole and deacetylated ketoconazole by rat hepatic microsomes and flavin-containing monooxygenases. *Drug Metab Disp* **25**(6)**:** 772-77, 1997.

Rodriguez R. J., Proteau P. J., Marquez B., Hetherington C. L., Buckholz C. J.and O'Connell K. L., Flavin-containing monooxygenase-mediated metabolism of *N*-deacetylketoconazole by rat hepatic microsomes. *Drug Metab Dispos* **27:** 880-886, 1999.

Rowland M. and Tozer T. N., Absorption. In: *Clinical Pharmacokinetics Concepts and Applications* (Ed. Balado D), pp. 119-136. Williams and Wilkins, 1995.

Simon D.L., Comment: ketoconazole hepatotoxicity. *Ann Pharmacother* **26**(4)**:** 564-565, 1992.

Stormer E., Roots I.and Brockmoller J., Benzydamine *N*-oxidation as an index reaction reflecting FMO activity in human liver microsomes and impact of FMO3 polymorphisms on enzyme activity. *Br J. Clin Pharmac* **50:** 553-561, 2000.

Stricker B.H. Ch., Blok A.P.R., Bronkhorst F.B., Van Parys G.E.and Desmet V.J., Ketoconazole-associated hepatic injury. A clinicopathological study of 55 cases. *J. Hepatol* **3:** 399-406, 1986.

Sugar A.M., Alsip S.G., Galgiani J.N., Graybill J.R., Dismukes W.E., Cloud G.A., Craven P.C.and Stevens D.A., Pharmacology and toxicity of high-dose ketoconazole. *Antimicrob Agents Chemother* **31**(12)**:** 1874-1878, 1987.

Sugimoto K., Ohmori M., Tsuruoka S., Nishiki K., Kawaguchi A., Harada K., Arakawa M., Sakamoto K., Masada M., Miyamori I.and Fujimura A., Different effects of St. John's Wort on the pharmacokinetics of simvastatin and pravastatin. *Clin Pharmacol Ther* **70:** 518-24, 2001.

Tam Y. K., Individual variation in first-pass metabolism. *Clin Pharmacokinet* **25**(4)**:** 300-328, 1993.

Thomson A.B.R., Relationship between physiology and clinical disorders of the small intestine. In: *Principles and practice of gastroenterology and hepatology*, pp. 281-289. Appleton and Lange, 1994.

Thummel K.E., Kunze K.L.and Shen D.D., Enzyme-catalyzed processes of first-pass hepatic and intestinal drug extraction. *Adv Drug Deliv Rev* **27:** 99-127, 1997.

Thummel K.E., Favreau L.V., Mole J.E. and Schenkman J.B., Further characterization of RLM2 and comparison with a related form of cytochrome P-450, RLM2b. *Arch Biochem Biophys* **266**(2)**:** 319-333, 1988.

Treacy E.P., Akerman B.R., Chow L.M.L., Youil R., Bibeau C., Lin J., Bruce A.G., Knight M., Danks D. M., Cashman J.R.and Forrest S.M., Mutations of the flavin-containing monooxygenase gene (FMO3) cause trimethylaminuria, a defect in detoxication. *Hum Mol Gen* **7**(5)**:** 839-845, 1998.

Tugnait M., M. Hawes E., McKay G., Rettie A.E., Haining R.L.and Midha K. K., *N*-oxygenation of clozapine by flavin-containing monooxygenases. *Drug Metab Dispos* **25**(4)**:** 524-527, 1997.

Van Parys G., Eenepoel C., Van Damme B.and Desmet V.J., Ketoconazole-induced hepatitis: a case with a definite cause-effect relationship. *Liver* **7:** 27-30, 1987.

Venkatakrishnan K, von Moltke L.L.and Greenblatt D.J., Effects of the antifungal agents on oxidative drug metabolism. *Drug Interact* **28**(2)**:** 111-180, 2000.

Villaverde C., Alvarez A., Redondo P., Voces J., Del Estal J.L.and Prieto JG., Small intestinal sulphoxidation of albendazole. *Xenobiotica* **25**(5)**:** 433-41, 1995.

Walter-Sack I. and Klotz U., Influence of diet and nutritional status on drug metabolism. *Drug Interact* **31**(1)**:** 47-64, 1996.

Weisbrodt N.W., Motility of the small intestine (Chapter 20). In: *Physiology of the Gastrointestinal Tract*, Vol. 1, pp. 631-663. Raven Press, New York, 1987.

Whetstine J.R., Yueh M. F., Hopp K.A., McCarver D.G., Williams D.E., Park C.S., Kang J.H., Cha Y.N., Dolphine C.T., Shephard E.A., Phillips I.R.and Hines R.N., Ethnic differences in human flavin-containing monooxygenase 2 (FMO2) polymorphisms: Detection of expressed protein in African-Americans. *Toxicol Appl Pharmacol* **168:** 216-224, 2000.

Whitehouse L.W., Menzies A., Dawson B., Zamecnik J.and Sy W., Deacetylated ketoconazole: a major ketoconazole metabolite isolated from mouse liver. *J. Pharm Biomed Anal* **8**(7)**:** 603-606, 1990.

Williams D. E., Katchamar S., Larsen-Su S., Stresser D.M., Dehal S.S.and Kupfer D., Concurrent flavin-containing monooxygenase down regulation and cytochrome P450 induction by dietary indoles in the rat: implication for drug-drug interactions. *Adv Exp Med Biol* **500:** 635-8, 2001.

Williams M. F., Dukes G. E., Heizer W., Han Y.H., Hermann D.J., Lampkin T.and Hak L.J., Influence of gastrointestinal site of drug delivery on the absorption characteristics of ranitidine. *Pharm Res* **9**(9)**:** 1190-94, 1992.

Winter M. E., Bioavailability (F). In: *Basic Clinical Pharmacokinetics* (Ed. Mary Anne Koda-Kimble PD), pp. 316. Applied Therapeutics, Inc., 1994.

Wyatt M.K., Overby L.H., Lawton M.P.and Philpot R.M., Identification of amino acid residues associated with modulation of flavin-containing monooxygenase (FMO) activity by imipramine: structure/function studies with FMO1 from pig and rabbit. *Biochemistry* **37**(17)**:** 5930-8, 1998.

Yang H.L., Lee Q.P., Rettie A.E.and Juchau M.R., Functional cytochrome P4503A isoforms in human embryonic tissues: Expression during organogenesis. *Mol Pharmacol* **46:** 922-928, 1994.

Yeung C. K., Lang D. H., Thummel K. E.and Rettie A. E., Immunoquantitation of FMO1 in human liver, kidney, and intestine. *Drug Metab Dispos* **28**(9)**:** 1107-1111, 2000.

Zhang Q. , Dunbar D., Ostrowska A., Zeisloft S., Yang J.and Kaminsky L., Characterization of human small intestinal cytochromes P-450. *Drug Metab Dispos* **27**(1)**:** 804-809, 1999.

Ziegler D. M., Metabolic oxygenation of organic nitrogen and sulfur compounds. *Drug Metab Drug Tox***:** 33-53, 1984.

Ziegler D.M., Microsomal flavin-containing monooxygenase: oxygenation of nucleophilic nitrogen and sulfur compounds. *Enzymatic Basis of Detoxication* **1:** 201-227, 1980.

Ziegler D.M., Microsomal flavin-containing monooxygenase: Oxygenation of nucleophilic nitrogen and sulfur compounds. In: *Enzymatic Basis of Detoxication*, Vol. 1, pp. 201-227. Academic Press, Inc., 1980.

Ziegler D.M., Flavin-containing monooxygenases: Catalytic mechanism and substrate specificities. *Drug Metab Rev* **19**(1)**:** 1-32, 1988.

Ziegler D.M., Bioactivation of xenobiotics by flavin-containing monooxygenases. In: *Biological Reactive Intermediates IV*, pp. 41-50. Plenum Press, 1990.

Zou Q., Bennion B.J., Daggett V.and K.P. Murphy, The molecular mechanism of stabilization of proteins by TMAO and its ability to counteract the effects of urea. *J. Am Chem Soc* **124**(7)**:** 1192-1202, 2000.

APPENDICES

PROTOCOL A

Covalent binding protocol for *in vivo* analysis in Sprague Dawley rats

Objective: The procedure for an analysis of a hepatic covalent binding effect resulting from the acute administration of ketoconazole (KT) *in vivo* to Sprague Dawley rats.

Equipment:

- Metabolic cages
- Needles 30 ½ G (Becton Dickson 305125)
- 3cc syringe (Becton Dickson 5585)
- Scintillation vials (7 mL) (Fisher 03-337-1)
- vortexer (Fisher 12-812)
- scale (Mettler PN323)
- centrifuge (Eppendorf 5415C)
- oven (Beckman, Model TJ-6, VWR Scientific Inc. 1340)
- disposable glass vials – (13X100 mm, Fisher-Scientific 14-961-26)
- eppendorf® tubes - polypropylene (Fisher 2.0 mL, 05-408-255)
- plastic pipet tips 1 mL, 200 µL (Fisherbrand Redi-tip 21-197-8E)
- glass homogenizer and pestle (10 mL)

Reagents

- homogenization buffer, pH to 7.5 with 1 M sodium bicarbonate ($NaHCO_3$) (Fisher S233-3)
  - ✓ 100 mM trizma or trizma hydrochloride (Sigma T-7-149)
  - ✓ 1 mM ethylenediaminetetraacetic acid (EDTA) (Sigma E-5134)
  - ✓ 250 mM sucrose (Sigma S-7-903)
- 0.6 M and 0.9 M trichloroacetic acid (TCA) (Sigma T-639, Fisher A322-100)
- 80% methanol (MEOH) (HPLC grade Fisher A457-4)
- 1 N sodium hydroxide (NAOH) (Malinckrodt 7708un1823)
- glacial acetic acid (Fisher Scientific A35 500)
- scintillation fluid (ICN Cyto Scint™ 882453)
- 70% ethanol (ETOH) (Oregon State University Chem Store 6061-00)
- Coomassie® Plus Protein Assay (Pierce 23236)

Instructions for injecting animals and harvesting liver

1. Prepare doses of 40 and 90 mg/kg and bring dose to room temperature.
2. Inject rat with interperitoneal (i.p.) injection of ^{3}H-KT (1.5μCi/mg).
3. Place rat in metabolic cage for allotted time point and obtain urine samples.
4. Sacrifice rat in a CO_2 chamber.
5. Use ETOH to sterilize stomach, make incision from lower part of stomach to upper part of sternum creating a circular opening.
6. Remove liver, cut a small section (~1 gm) from liver, and remove heart and kidneys.
7. Place liver, small section of liver, heart and kidneys in separately labeled containers.
8. Indicate: date, body part, dose used, and time point on container.
9. Snap-freeze in dry ice, store at –20 ° C for later analysis.
10. Collect urine and feces from cage and urine collector.
11. Clean cage, take wipe test of cage and work area to check for radioactive contamination.

Instructions for homogenization of liver tissue

1. All work should be conducted on ice at 4 ° C at all times.
2. Blot liver with Kim Wipe to remove excess blood for accurate weight analysis of liver section.

3. Weigh 1gm and deposit into glass homogenizer, with small amount of homogenization buffer. Homogenize until all tissue is suspended. Vortex.
4. Transfer to disposable glass tubes and vortex.
5. Pipet in 2 mL of 0.9 M TCA into clean glass tube, add 1 mL aliquot of homogenate, vortex, reserve 50 μL for protein concentration analysis.
6. Place all homogenate tubes into pre-cooled (4 ° C) centrifuge for 10 minutes at 1000 *g* for pelleting of homogenate. Discard supernatant.
7. Pipet 0.6 M TCA onto pellet, vortex. Centrifuge 3 minutes and discard supernatant. (Repeat 2 times).
8. Pipet 80% MEOH onto pellet (3 mL), vortex, centrifuge, discard supernatant. This procedure should be done 3 times each time discarding the supernatant **except** a radioactivity reading should be conducted on the last supernatant to insure background levels only.
9. Pipet onto pellet 1 mL 1N NAOH, vortex, place in oven at 60 ° C until pellet is dissolved.
10. Pipet 300 μL into each vial containing 2.75 mL of scintillation fluid (1:9) with glacial acetic acid (FisherA507-500) (150 μL per 10 mL of scintillation fluid).
11. Determine radioactivity reading using scintillation counter and protein concentration by Coomassie® Plus Protein Assay (Pierce).

PROTOCOL B

Alanine aminotransaminase (ALT) assay:

Objective: To determine the release of the hepatic enzyme ALT indicating damage to the liver has occurred. In this assay, ALT catalyzes the conversion of alpha-ketoglutarate and alanine to glutamate and pyruvate.

Equipment

- Centrifuge (Eppendorf 5415C)
- Spectrophotometer (SpectraMax 190, Sunnyvale, CA)
- 96-well plates (Falcon 35-3072, polystyrene, Beckton/Dickson)
- Disposable test tubes (13X100 mm, Fisher-Scientific 14-961-26)

Reagents

- Sigma Diagnostic Kit (505-P)
    1. Prepared substrate (Sigma 505-1)
        - ✓ DL-asparate (0.2 mol/L)
        - ✓ α-ketoglutarate acids (1.8 nmol/L)
        - ✓ in phosphate buffer (pH 7.5) (Fisher P250-500)
        - ✓ store at 2 – 6 ° C
    2. Color reagents (Sigma 505-2)
        - ✓ 2,4-dintrophenylhydrazine (DNP) (20 mg/dL)
        - ✓ store at 2 – 6 ° C

3. Calibration solution for transaminase (Sigma 505-10)
    - ✓ sodium pyruvate (1.5 mmol/L) (pH 7.5)
    - ✓ chloroform as a preservative
    - ✓ Store at 2 – 6 ° C
4. Alanine - α –ketoglutarate substrate (Sigma 505-51)
    - ✓ DL – alanine (0.2 mol/L)
    - ✓ Ketoglutarate acide (1.8 mmol/L)
    - ✓ in phosphate buffer (pH 7.5)
    - ✓ chloroform as a preservative
    - ✓ store at 2 – 6 ° C

- 0.4 N sodium hydroxide (NaOH) (Malinckrodt 7708un1823).
- 0.9% sodium chloride (normal saline) (Sigma S3014) in double distilled water (dds) (Barnstead/Thermolyne D7411 Easypure UF).

Instructions

1. Collect blood samples at designated time points.
2. Place on ice immediately and allow for coagulation.
3. Centrifuge 8000 *g* at 4 ° C.
4. Collect serum and keep on ice.
5. Assay samples with kit.
6. Prepare calibration curve of ALT activity in units/mL from serum samples.

7. Pipet into test tube alanine alpha-ketoglutarate (0.25 mL) in water bath at 37 ° C.
8. Pipet in 5 μL of serum and 45 μL of normal saline.
9. Mix gently and place back into 37 ° C water bath for 30 minutes.
10. After 30 minutes, add 0.25 mL of Sigma color reagent (505-2), vortex (low speed).
11. Leave at room temperature (25 ° C) for 20 minutes.
12. Add 2.5 mL of 0.4 N NaOH, vortex.
13. Wait 5 minutes pipet 200 μL of sample mixture into 96-well plate and measure absorbance at 505 nm.

PROTOCOL C

***In vivo* glutathione (GSH) evaluation** (Roberts and Francetic, 1993)

Objective: To determine total glutathione levels in rat hepatic tissue at individual time points using low (40 mg/kg), high (90 mg/kg), and a control (saline only) interperitoneal (i.p.) injection. Time points of 0, 0.5, 1, 2, 4, 8, 12, and 24 hours were used. Set absorbance reading at 412 nm.

Equipment:

- Spectrophotometer (Spectromax 190, Sunnyvale, CA)
- Glass homogenizer and plunger (10 mL)
- 96-well polystyrene plates (Falcon 35-3072, Beckton/Dickson)
- centrifuge (Beckman J2-HS, Rotor JA-17)

Reagents

- 100 ml of 5% sulfosalicylic acid (SSA) (5 grams/100 mL)
- Sample buffer:
    - ✓ 100 mM potassium phosphate buffer (pH 7.5) (Fisher P250- 500)
    - ✓ 5 mM ethylenediaminetetraacetic acid (EDTA, pH 7.5) (Sigma E-5134)
- Prepare in double distilled water (dds) (Barnstead/Thermolyne D7411 Easypure UF).

- ✓ 5 units/mL (GSSG reductase) (Sigma G-3664)
- ✓ 4 mg/mL 5,5'Dithiobis(2'-nitrobenzoic acid) (DTNB) (10mM) (Sigma D-8130)
- ✓ 2 mg/mL NADPH (2.4 mM) (Sigma N-1630)

- 0.9% sodium chloride (normal saline) (Sigma S3014) in dds (Barnstead/Thermolyne D7411 Easypure UF).

Instructions

All work should be conducted on ice (4 ° C).

1. Turn on centrifuge 15 minutes before work to obtain a temperature of 4 ° C.
2. Remove liver and cut piece from liver, minimum of 50 mg. Blot and weigh both pieces.
3. Store liver in –80 ° C.
4. Homogenize the small liver piece with 5% SSA in homogenizer tube with plunger until tissue is completely suspended.
5. Centrifuge at 3000 *g* for 10 minutes at 4 ° C.
6. Dilute supernatant 10-fold in sample buffer.
7. Aliquot 300 µL of supernatant and combine in a 1.5 mL cuvette with 450 µL of sample buffer, 100µL of GSSG reductase solution, and 50 µL DTNB solution.
8. Incubate for 1 minute.
9. Pipet into 100 µL into reading plate in duplicate.
10. Add 100 µL NADPH solution into each well with prior solution.
11. Monitor for two minutes measuring at 412 nm the change in absorbance per 30 seconds, start with time "0".

PROTOCOL D

Hepatic microsomes prepared from Sprague Dawley rats:

Objective: To prepare hepatic microsomes from Sprague Dawley rat livers for 'covalent' binding analysis *in vitro* to determine if 'covalent' binding effects would occur *in vitro* as well conduct a comparison with *in vivo* 'covalent' binding studies.

Animals

Sprague Dawley (SD) rats, 6 to 8 weeks (Simonsen Laboratories, Inc)

Equipment

- biohazard disposal container
- scale (Mettler PN323)
- centrifuge (4 ° C) (Beckman J2-HS, rotor JA-17)
- ultracentrifuge (4 ° C) (Beckman L8-70M, rotor J42.1 -1625)
- polypropylene centrifuge tubes (2 mL) (Fisher 05-408-255)
- homogenizer (ESGE Bio-homogenizer M133/1281-0)
- Pipet-aid® (Drummond Scientific Co., Broomall, PA)
- surgical tools: scissors, tweezers, etc.

Reagents

- Homogenization buffer (pH 7.5)

- ✓ 100 mM Trizma or Trizma hydrochloride (Sigma T-7-149)
- ✓ 1 mM ethylenediaminetetraacetic acid (EDTA) (Sigma E-5134)
- ✓ 250 mM sucrose (Sigma S-7-903)
- ✓ bring to volume with double distilled water (dds) (Mettler PN323)

- Resuspension buffer (pH 7.5)
  - ✓ 10 mM Trizma or Trizmahydrochloride (Sigma T-7-149)
  - ✓ 1 mM sodium ethylenediaminetetraacetic acid (EDTA)
  - ✓ (Sigma E-5134)
  - ✓ 20% glycerol (Fisher Biotech 56-81-5)
  - ✓ bring to volume with dds
- 70% ethanol (ETOH) (Oregon State University Chem Store 6061-00)
- Coomassie® Plus Protein Assay (Pierce 23236)

Instructions

1. Euthenize animal in CO_2 chamber.
2. Clean stomach area with 70% ETOH.
3. Remove liver and place in 30 mL of homogenization buffer on ice.
4. Weigh liver, place liver in 3 times the liver size of homogenization buffer in beaker and homogenize with blender until a solution forms.
5. Pipet solution through gauze into centrifuge tubes and cap on ice.
6. Centrifuge (4 ° C) at 8,500 rpm (10,000 *g*).
7. Remove white fat layer and pipet supernatant through gauze into clean centrifuge tubes obtain, dispose of pellet.

8. Weight each tube for balancing and ultracentrifuge for 90 minutes at 30,000 rpm (100,000 *g*) at 4 ° C.
9. Remove from ultracentrifuge and dispose of pellet.
10. Repeat steps 7 – 9, **except** keep pellet (microsomes) and discard supernatant.
11. Remove pellet, resuspend in resuspension buffer and homogenize.
12. Snap freeze in dry ice and store at –80 ° C.

PROTOCOL E

In vitro covalent binding analysis of Sprague Dawley (SD) and Fischer 344 hepatic microsomes

Objective: To utilize hepatic microsomes from SD rat livers for 'covalent' binding analysis of KT/metabolite(s) *in vitro* to determine if 'covalent' binding effects would occur *in vitro* as well conduct a comparison with *in vivo* 'covalent' binding studies. Also the hepatic microsomes of Fischer 344 rats treated with indole-3-carbinol (I-3-C) and without as the control for comparison with the *in vitro* findings of SD hepatic microsomes.

Equipment

- metabolic shaking incubator (Precision Dubnoff ES722)
- eppendorf® vials (2 mL volume) (Fisher 05-408-255)
- centrifuge (Eppendorf 5415C)

Reagents:

- microsomal preparation
- 100 μM potassium phosphate buffer (pH 7.4) (Fisher P250-500)
- 250 μM ketoconazole (KT): 1, 10, and 100 μM (A.S. Janssen Biotech N.V. R41400)
  - ✓ Dissolve in 1 N hydrochloric acid (HCL) (Sigma H-7020)
  - ✓ Filter with puradisc™ 25 (Whatman 6780-2502)

- KT: radiolabeled – 1 μCi ^{3}H/0.5 mL of test solution (American Radiolabeled, Inc. St. Louis, MS, ART794) (1 mCi/mL) (specific activity: 5 Ci/mmol)
- NADPH-generating system **Final concentrations**
  - ✓ glucose-6-phosphate (G-6-P) (Sigma G-7250) **1.25 mM**
  - ✓ glucose-6-phosphate dehydrogenase (1000 units/mL) **20 units/mL** (G-6-P DH) (Sigma G-5760)
  - ✓ $NADP^{+}$ (Sigma N-1630) **0.25 mM**
- 0.6 M and 0.9 M trichloroacetic acid (TCA) (Sigma T-639, Fisher A322-100)
- 80 % methanol (MEOH) (GC Resolv A457-4)
- 1 N sodium hydroxide (NAOH) (Malinckrodt 7708un1823)
- Scintillation fluid (ICN CytoScint™ 882453)

Instructions

Conduct experiments on ice (4 ° C) at all times.

Incubation solution - pipet into disposable glass vials (11X75 cm):

1. 1 M potassium phosphate buffer (pH 7.4) .
2. 1,10 or 100 μM KT (individual experiments).
3. 2 μCi/mL radiolabeled KT (^{3}H-KT).
4. 0.250 or 0.5 or 1 mg/mL microsomes (individual experiments).

5. NADPH-generating system: (1.25 mM G-6-P, 20 units/mL G-6-P DH, and 0.25 mM $NADP^+$).
6. Place in water bath with shaker at 37 ° C for individual time points.
7. Place on ice and pipet in 0.9 mL of 0.9 TCA, vortex.
8. Transfer to 2 mL eppendorf® vials, centrifuge 10 minutes at 14,000 rpm, discard supernatant.
9. Pipet in 1.2 mL 0.6 TCA, vortex, centrifuge at 14,000 rpm to 10 minutes, discard supernatant. Repeat this procedure a minimum of 4 times, **except** keep the supernatant from the last time. Pipet supernatant into another eppendorf® and take radioactive reading to determine if background levels have been reached (< 100 disintegrations per minute (dpm)), if still too high repeat procedure until background levels are obtained.
10. Into sample pellet pipet 0.5 mL 1.0 N NAOH, vortex.
11. Heat in over at 60 ° C for a minimum of 45 minutes or until dissolved.
12. Pipet 0.300 mL of sample into scintillation vials (0.7 mL) containing 2.75 mL scintillation fluid with added glacial acetic acid (3 mL/200 mL scintillation fluid).
13. Place in scintillation counter and take reading.

PROTOCOL F

Complete MEDIA for epithelial intestinal-CCL241 cell line

Objective: Preparation of media for nutritional supplement for growth of the intestinal epithelial cell line CCL241 for future analysis of the presence of the flavin-containing monooxygenase enzyme (FMO). When working with cell lines the area must be kept sterile and media must be filtered (acrocap-Pall4480). All cell work was conducted in water-jacketed incubators Nuaire Biological Safety Cabinets, Class II Type A/B3 (Model 1425-600).

Complete Media:

Dulbecco's Modified Eagle Medium (DMEM) (GibcoBRL 23700-024) powdered dissolved and to the incomplete solution add:

- ✓ Fetal Bovine Serum (20%) (Summit FP-200-05)
- ✓ Sodium pyruvate (1:100 final concentration) (Sigma S-2770)
- ✓ Antibiotic/antimycotic solution (1:100 final concentration) (Sigma A-9909): Solution contents in 100 mL: streptomycin (10 mg/mL), penicillin G (10,000 Units/mL), amphotericin B (25 μg/mL)
- ✓ MEM non-essential amino acids 10 mM (final concentration 1:100) (GibcoBRL1114050)
- ✓ Oxaloacetic acid (final concentration 1:100) (Sigma 07753)

- ✓ Insulin (final concentration 0.2 Units/mL) mix in double distilled water and added hydrochloride (HCL) (Sigma H7020) to complete the dissolving (Sigma I-500)

- Cell line CCL241 (American Type Culture Collection (ATCC))

PROTOCOL G

Epithelial colon-CRL1790 cell seeding and complete media

Objective: Preparation of plating and growth media for the epithelial colon-CRL1790 cell line for future analysis of the presence of the flavin-containing monooxygenase enzyme. The CRL 1790 cells are required to be plated before addition of growing media is added when starting cells as well as when splitting cells into new flasks. Pipet plating media into new flasks and incubate at least 2 hours before adding cells. When working with cell lines, the area must be kept sterile and media must be filtered (acrocap-Pall4480). All cell work was conducted in water-jacketed Nuaire Biological Safety Cabinets, Class II Type A/B3 (Model 1425-600).

Seeding (plating) media:

Dulbecco's Modified Eagle Medium (DMEM)/ F-12 (Ham) (GibcoBRL 12400-016) incomplete (without growing nutrients) media powder dissolved in double distilled water (dds) (Barnstead/thermolyne D7411 EasyPure UF). Final pH between 7.2 – 7.4. Per 100 mL add:

- ✓ Fibronectin - 0.598 mL of 0.167 mg/mL - human α-Chymotryptic 120K fragment (GibcoBRL 12159-018)
- ✓ Bovine serum albumin - 50 µL of 0.001 mg/mL (Sigma A-4503)

- ✓ Vitrogen (purified collagen) – 100 µL of 0.003 mg/mL (Cohesion Tech C100828)

- Pipet 14 mL into 75 cm^2 (Costar 0.2 µM vented cap, #3376) or 20 mL into 162 cm^2 flasks (Costar 0.2 µM vented cap 3151). See illustration, Figure 1a for cell growing chamber or flask.

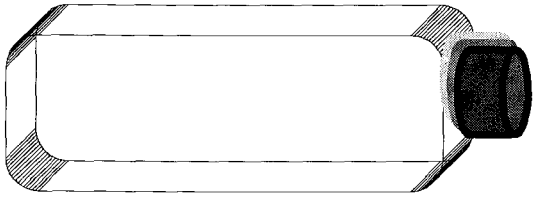

Cell growing flask

Figure 1a: Schematic portrayal of cell incubation flask. (25, 75, or 162 cm^2)

- Incubate for 24 hours. After the designated period of time aspirate plating media and add complete media.

Complete media:

Aspirate old media and add new complete media every 3 days for normal feeding after 24 hour seeding time period. Dissolve Dulbecco's F-12 (Ham) media powder in dds. Final pH should be between 7.2 – 7.4. **Per 500 mL:**

	Final
✓ Insulin (Sigma I-6634)	**0.02 mg/mL**
✓ Apo-transferrin (Sigma T-2036)	**0.128 µM**
✓ Epidermal growth factor (GibcoBRL53003-018) isolated from male mouse submaxillary glands	**0.001 µg/mL**
✓ Phosphorylethanolamine (Sigma P-0503) (10 mM)	**0.01 mM**
✓ Triiodothyronine (Sigma T-2877) (dissolved with NaOH)	**0.0001 nM**
✓ Ethanolamine (Sigma E-0135)	**0.01 mM**
✓ Bovine Albumin (Sigma A-4503)	**1 g**
✓ Hepes (Sigma H-3375)	**10 mM**
✓ Sodium pyruvate (Sigma S-2770)	**0.5 mM**
✓ Sodium selenite (Sigma S-5261)	**25 nM**
✓ Hydrocortisone (Sigma H-4881)	**50 nM**
✓ L-glutamic acid (Sigma G-5638)	**0.002 M**
✓ NaOH (Mallinckrodt 7708un1823) - pH to 7.2 – 7.4	
✓ Antibiotic/antimycotic solution (Sigma A-9909): (Solution contents in 100 mL: streptomycin (10 mg/mL), penicillin G (10,000 Units/mL), amphotericin B (25 µg/mL)	**1:100 (final)**

- Cell line CRL1790 (American Type Culture Collection (ATCC))

PROTOCOL H

Media for Caco-2 (HTB-37) cells

Objective: Preparation of media for growth of the Caco-2 (HTB-37) cell line for analysis of the presence of the flavin-containing monooxygenase enzyme.

MEDIA:

Dulbecco's Modified Eagle Medium (DMEM) (GibcoBRL 23700-024). Final pH 7.2 – 7.4. To DMEM add:

- ✓ Fetal Bovine Serum (FBS) (final concentration 10%) (Summit FP-200-05)
- ✓ Sodium pyruvate (final concentration 1:100) (Sigma S-2770)
- ✓ MEM Non-essential amino acids (final concentration 1:100) (GibcoBRL1114050)
- ✓ Antibiotic/antimycotic solution (final concentration 1:100) (Sigma A-9909): Solution contents in 100 mL: streptomycin (10 mg/mL), penicillin G (10,000 Units/mL), amphotericin B (25 μg/mL)

- HTB-37 (American Type Cell Culture (ATCC))

PROTOCOL I

Procedure for seeding, trypsinizing, or freezing cell lines

Objective: The following procedure is to start a cell line, continue growth after confluency for continued passage (replating), or for freezing for future use. Sterile conditions should be utilized therefore procedure should be conducted in a laminar hood or equivalent and wearing gloves for contamination-free as well as for protection.

A. Prepare complete growing media for individual cell lines (Protocol F, G, or H) Warm in water bath at 37 ° C prior to use: (Precision, ES722)

- Complete growing media for selected cell line
- Dulbecco's phosphate buffered saline (PBS) Ca^{++}, Mg^{++} free (GibcoBRL14090-144)
- 50 mL aliquot of trypsin-EDTA (GibcoBRL25200-072) thawed at room temperature

B. **Trypsinize and reseed:**

- Remove cells from incubator (Cascade Scientific 2700/2700E), aspirate cell culture medium, add PBS covering cells, shake to remove debris and aspirate, and repeat 3X.
- Add trypsin-EDTA covering cells. Wait for a few seconds and remove all but a couple of drops.

- Incubate at 37 ° C for 5 –10 minutes. Terminate trypsin with the addition of warm complete media (Protocol F, G, or H).
- Pipet into new flasks evenly increasing the number of flasks by 3 to 6, dependent upon the number of cells for distribution. Return to incubator and grow at 37 ° C with 5% CO_2.

C. **Freezing cells:**

- Follow above procedure to trypsinize cells for detachment and resuspend in growing media (Protocol F, G, or H)
- Pipet into equal volumes into 15 mL centrifuge tubes. Centrifuge at 300 – 400 rpm for 5 minutes. Aspirate supernatant carefully and resuspend in 2 – 3 mL of the following 100 mL volume of freezing media.
    a. 7.5 mL dimethyl sulfoxide (DMSO) (Sigma D-8779)
    b. 30.0 mL fetal bovine serum (FBS) (30%) (Summit FP-200-05)
    c. 62.5 mL Dulbecco's Modified Eagle Medium (DMEM) only without added growth factors (incomplete)
- Pipet $1.0x10^6$ cells determined by hemocytometry into individual 1 cryogenic vials (Nalgene® Company, 5000-0020), freeze for 1 hour at 20 ° C. Move to –80 ° C for 24 hours, then store in liquid nitrogen
- Dispose of all used disposable items in biohazard bags and autoclave for disposal. Clean all glassware with 10% bleach and soap.

PROTOCOL J

Microsomal preparation from cell culture

Objective: To prepare microsomes from cell lines for future analysis of the presence of the flavin-containing monooxygenase enzyme with western blotting procedure (Protocol L).

Equipment

- 500 mL beaker for biohazard waste
- Pipette-Aid® - 263 (Drummond Scientific Co., Broomall, PA)
- Homogenizer (ESGE Bio-homogenizer – M133/1281-0)
- Cell scraper (25 cm) (Fisher Scientific 08-773-2)
- Centrifuge (Beckman J2-HS, rotor JA-17)
- Ultracentrifuge (L8-70M, rotor J42-1)

Reagents

- Dulbecco's Phosphate Buffer Saline (PBS) Ca^{++}/Mg^{++} Free (GibcoBRL14090-144)
- Homogenization Buffer
  - ✓ **100 mM** trizma or trizmahydrochloride (Sigma T7-149)
  - ✓ **1 mM** sodium ethylenediaminetetraacetic acid (EDTA) (Sigma E-5134)
  - ✓ **250 mM** Sucrose (Sigma S-7-903)

- ✓ bring to volume with double distilled water (dds)

  (Barnstead/thermolyne D7411 Easypure UF)

Add protease inhibitors to homogenization buffer:

	Final
✓ **1 mL** of 10 mM phenylmethylsulfonyl fluoride (PMSF) (Sigma #P-7626)	**0.25 mM**
✓ **0.25 mL** protease inhibitor cocktail, (Sigma #P-8340)	**0.25/20mL**
✓ **0.5 mL** trypsin inhibitor (Sigma #T-6522)	**10 mg/20 mL**
✓ **0.5 mL** of 10 mM 4-amidinophenylmethanesulfonyl fluoride (APMSF) (Sigma #A-6664)	**0.25 mM**
✓ **0.5 mL** of 9.1 mM Pepstatin A (P-5318 Sigma)	**0.228 mM**

- Resuspension buffer solution (pH 7.5), qs dds
  - ✓ **10 mM** trizma or trizmahydrochloride
  - ✓ **1 mM** EDTA
  - ✓ **20%** glycerol (Fisher Biotech 56-81-5)
- Coomassie® Plus Protein Assay (Pierce 23236)

Instructions

1. Prepare mixture of protease inhibitors by adding 20 mL ice cold of homogenization buffer, 1 mL PMSF, 0.25 mL protease inhibitor cocktail, 0.5 mL trypsin inhibitor, 0.5 mL APMSF, and 0.5 mL pepstatin A with dimethyl sulfoxide (DMSO) (Sigma D-8779) into a 50 mL centrifuge tube made the day of microsomal preparation.
2. Take one flask and discard medium, wash flask 3X with 37 ° C PBS. Repeat with the second flask.
3. Add 2 mL of the protease mixture to each flask. Add 2 mL of ice-cold homogenizing buffer, dislodge cells, and place both flasks on ice tilted so that cells rest in back of flask bathed in homogenizing buffer. Let flasks sit on ice for 5 to 10 minutes. (This part of the procedure can be done with as many flasks as you can handle at one time).
4. Wash the sides of the flask using a pipette to ensure all cells are suspended in solution. Transfer this solution to the second flask
5. Repeat this procedure with the remaining flasks.

   If necessary, 2 mL of the protease mixture can be used to wash the original flask. This solution can be transferred in a stepwise fashion to subsequent flasks to ensure that a majority of the cells are suspended in the final flask.
7. All tubes and working materials for making microsomes should be kept cold. Keep everything on ice.

8. The cell suspension in the final flask should be divided equally into two 50 mL centrifuge tubes on ice. Observe by microscope a small portion of the cell suspension to see if the cell walls have been lysed, by using the trypan blue exclusion test (Sigma T-8154). If not, a small homogenizer tube and plunger should be used to homogenize the cells. Observe after homogenization to make sure the cells are lysed.
9. Centrifuge set at 4 ° C at 4,000 rpm (2.2K*g) for 5 minutes to pellet down. This is a suspension.

Microsomal preparation:

1. Second low-spin centrifuge step. Run the supernatant at 4 ° C at 8,000 rpm (9K*g) for 5-10 minutes to pellet again. Keep supernatant.
2. The final spin was conducted using an ultracentrifuge. Temp: 4 ° C; Time: 90 minutes; Speed: 30,000 rpm (100,000 g).
3. When the cells have been pelleted, discard the cytosol (supernatant), add a minute volume of resuspension buffer (~0.5 mL) to create a suspension in one tube, transfer this suspension to as many tubes used to create a suspension of all of the pelleted microsomes, until a final suspension occupies the last tube. The final preparation should be transferred to cryogenic vials (Nalgene® Company, 5000-0020). Determine protein concentration.
4. Flash-freeze and store at –80 ° C.

PROTOCOL K

Microsomal preparation from donor tissue of human duodenum/jejunum
(Lu et al., 1998)

Objective: To prepare microsomes from donor tissue for analysis of the presence of the flavin-containing monooxygenase enzyme for determinations by western blot analysis. Human samples are considered biohazard waste. Double glove for entire process of microsomal preparation. All cell work should be conducted in Nuaire Biological Safety Cabinets, Class II Type A/B3 (Model 1425-600).

Equipment:

- ice, cloth material with ice and place glass tray on top
- small thick glass pieces for scraping
- homogenizer (ESGE Bio-homogenizer – M133/1281-0) (Biospec Products, Inc.)
- sonicator dismembrator (Fisher Scientific – model 100)
- surgical tools: Long tweezers, scissors
- biohazard waste container
- centrifuge (Beckman J2-HS, rotor JA17)
- ultracentrifuge (Beckman L8-70M, rotor J42.1).
- cryogenic vials (Nalgene® Company, 5000-020)

Reagents:

Homogenization buffer (bring to volume with double distilled water (dds))

- ✓ 100 mM potassium phosphate, pH 7.4 (Fisher P250-500)
- ✓ 1 mM sodium ethylenediaminetetraacetic acid (EDTA) (Sigma E-5134)
- ✓ 150 mM potassium chloride (Sigma P-9541)
- ✓ 0.1 mM dithiothreitol (Fisher Biotech BP172-5)
- ✓ 250 mM sucrose (Sigma S-2378)

Add these inhibitors the day of process to homogenization buffer:
(Gobinet-Georges, 2000; Kelly and Struthers, 2001)

	Final
✓ pepstatin A (Sigma P-5318)	**0.228 mM**
✓ trypsin inhibitor (Sigma T-6522)	**10 mg/20 mL**
✓ 4-amidinophenylmethanesulfonyl fluoride (APMSF) (Sigma A-6664)	**0.25 mM**
✓ phenylmethylsulfonyl fluoride (PMSF) (Sigma P-7626)	**0.25 mM**
✓ protease inhibitor cocktail (Sigma P-8340)	**0.25 mL/20 mL**
✓ aprotinin (Fisher BP250310) (activity: 10,980 kallikrein inhibitory units (KIU/mL)	**4000 KIU/total vol**

(100 mL of total volume of homogenization buffer will accommodate 25 g of raw tissue plus 5.6 g of already prepared mucosal tissue).

Other reagents: **Final**

- tetrasodium pyrophosphate pH 7.4 (Sigma P-8010) **100 mM**
- Coomassie® Plus Protein Assay (Pierce 23236)

Instructions:

1. Remove the upper villus layer of the mucosa with edge of a glass slide or razor blade.
2. Weigh before suspending in homogenizaton buffer.
3. Suspend the mucosal cells in cold homogenization buffer.
4. Pellet mucosal cells – centrifuge at 5,000 rpm (3,440 *g*) for 6 minutes at 4 ° C.
5. Wash with 100 mM potassium phosphate homogenization buffer.
6. Homogenize in a 4-fold (by pellet weight) volume of homogenization buffer using hand homogenizer 10 strokes, if unable to homogenize, use automatic homogenizer then sonicate for 10 sec at #3 setting with sonic dismembrator.
7. Pellet homogenate at 9,500 rpm (12K**g*) for 30 minutes at 4 °C.
8. Filter S9 supernatant through two to four layers of cheesecloth.
9. Pellet supernatant at 30,000 rpm (100K**g*) in ultracentrifuge for 70 minutes, at 4 ° C.
10. Wash in minimal buffer volume containing:
    a. 100 mM tetrasodium pyrophosphate, pH 7.4

b. 1 mM sodium EDTA in homogenizer to remove hemoglobin

11. Pellet at 30,000 rpm (100K*g) for 15 minutes at 4 ° C.

12. Resuspend microsomes in 100 mM potassium phosphate buffer (pH 7.4) containing: 250 mM sucrose and 1 mM EDTA.

13. Transfer to cryogenic vials, snap-freeze, store at – 80 ° C.

14. Determine protein concentrations.

PROTOCOL L

Western blot analysis

Objective: To determine the presence of FMO protein presence within: the Caco-2 (HTB-37) cell model; jejunum and duodenum microsomal preparations from human donors; the epithelial cell lines of colon (CRL1790) and intestine (CCL241).

A) Preparation of Separating Gels:

Reagent Stock Solutions:

Buffer 1: To prepare 500 mL, pH 8.8,

90.85 g Tris Base (Fisher BP 152-5)

0.4% sodium dodecyl sulfate (SDS) (Fisher Biotech BP166-500)

Buffer 2: To prepare 100 mL, pH 6.8.

6 g Tris HCl (Sigma T-5941)

0.4% SDS

2 mg bromo blue dye (Fisher Biotech 11-39-9)

Running Buffer: To prepare 2 Liters

6 g Tris Base

28.8 g glycine (Zaxis 910-9000457)

0.1% SDS

2X Sample Buffer: To prepare 10 mL,

3 g of urea (Zaxis 910-9000760)

500 mg SDS

600 mg dithiothreitol (DTT) (FisherBiotech BP172-5)

50 mM Tris base (pH 8.0) (Fisher BP152-5)

1 mg bromophenol blue (1 mg/10 mL) (Fischer Biotech 115-39-9)

4X Sample Buffer: To prepare 10 /mL,

6 g of urea

1 g SDS

1.2 g DTT

100 mM Tris base (pH 8.0)

1 mg bromophenol blue (1 mg/10 mL)

Transblot Buffer: To prepare 4 liters,

12 g (final – 25 mM) Tris base

59.6 g (final -192 mM) glycine

800 ml (final - 20%) MeOH (HPLC grade, Fisher A457-4)

Immunoblot Buffer: To prepare 2 liters,

4.84 g 20 mM Tris base, pH 7.2

58.44g 500 mM NaCl (Fisher S-3014)

50% Glycerol: To prepare 20 mL,

10 mL glycerol (Fisher Biotech 56-81-5)

10 mL double distilled water (dds) (Barnstead/thermoloyne D711 EasyPure UF)

30% Acrylamide/0.8% bisacrylamide (BioRad 161-0158)

Store at 4 ° C for up to 6 months.

TEMED (BioRad 161-0800)

10% Ammonium persulfate (APS) (Zaxis 910-9110057) - 100 mg/mL:

(good for one week).

0.1% SDS - 0.1%SDS 100 mL

2% Sodium Azide (Fisher Biotech BP9221-500): 2.0% Na-Azide 45 mL,

1.0% BSA (Sigma A-9909): 10 mg/mL

Chemiluminescence detection (BioRad immunostar 170-5012 and Amersham Pharmacia Biotech ECL RPN2106)

Molecular weights (MW) (BioRad 161-0324)

FMO1, FMO3, FMO5 of human cDNA purified in a baculovirus system (Gentest, A241, A243, A245, respectively)

For a SDS-PAGE separation gel, the following ingredients are needed for 2 small gels:

	15.0%	**12.5%**	**10%**	**7.5%**	**6.0%**
Buffer 1	6.0 mL	6.0 mL	**6.0 mL**	6.0 mL	6.0 mL
Water	4.2 mL	6.2 mL	**8.2 mL**	10.2 mL	11.4 mL
30% Acrylamide	12 mL	10 mL	**8.0 mL**	6.0 mL	4.8 mL
50% Glycerol	1.6 mL	1.6 mL	**1.6 mL**	1.6 mL	1.6 mL
TEMED	8 µL	8 µL	**8 µL**	8 µL	8 µL
APS	90 µL	90 µL	**90 µL**	90 µL	90 µL

Note: When TEMED and APS are added to mixture, the gel will start to solidify. Pour mixture into gel casting system 10 X 10 cm (Fisher Scientific, FB-GC10-1) and gently layer 0.1% SDS on top to flatten interface. Set for 2 hours.

Procedures for the preparation of the SDS-PAGE gel:

1. Wipe glass plates with ethanol, (Kim Wipes).
2. Arrange plastic spacers between metal and glass plate. Put the set inside a plastic bag.
3. Put the plates (inside the bag) on the stand in the proper place.
4. Align with white spacer card. Card should fit loose, secure mold and remove card.
5. Mark the level of gel that we will pour gel up to this level. In this case, 4.5 cm from the bottom of the plate will be marked. The MW of FMOs is about 50-65 Dalton (Da); thus, FMOs will be in the middle of a 10% separating gel.
6. Prepare APS 10%, vortex, label, and store at 4 ° C.
7. Mix components. Pour the gel between the plates up to the level marked. Pipette 1 mL of 0.1% SDS on top of the separating gel to flatten the interface of the gel. This gel needs to set for 2 hours or it can be kept in refrigerator for 1 week at 4 ° C. If the gel is to be stored away for later use, tape down the plastic bag until ready to use.

B) Components and procedures for stacking (loading) gels preparation.

For Stacking Gels, the following ingredients are needed for 2 small gels:

Buffer 2	3.75 mL
Water	9.75 mL
30% Acrylamide	1.50 mL
TEMED	8 µL
APS	0.150 mL

Procedures for the preparation of stacking (loading) gels

1. After the resolving gel has solidified, pour off the 0.1% SDS .
2. Mix components for stacking gels.
3. Pipette the stacking gel mixture on top of the separating gel and insert combs into the gels. Thick style (12 mm) – 10 loading spaces. (Fisher FB EC129B)
4. Solidifies in approximately 30 min.

Prepare microsomal samples.

1. Prepare samples including molecular weights (MW) and purified proteins by adding 15 µl of 4X loading buffer, desired protein concentration, and re-suspension buffer for a total volume of 60 µL.
2. Vortex, place samples on boiler (~100 ° C) for 2 –3 minutes, re-ice, and vortex.

3. Set-up and run SDS-PAGE gels. For 2 gels. Fill inner chamber with running buffer to the level above the inner glass plates and check for leaks. Fill catch basin half way with running buffer.

Procedures for loading and running samples

1. After the running time, separate the gel plates and discard the stacking gel.
2. Nick the upper right corner of one of the gels, if running two to identify later.
3. Soak the gel in transblot buffer for 20 min.
4. Assemble the gel sandwich into transfer apparatus (CBS Scientific Company, Inc., EBU-202, Del Mar, CA) with a nitrocellulose (BioRad 162-0115) or polyvinyliden difluoride (PVDF) (Immobilon™-P, IPVH000010) membrane and chromotography paper (Whatman 3mm, 3030690), pre wet in transblot buffer in the following order from top to bottom:

**********White side support**********
Foam pad
1 sheet of Whatman paper (CN#303-690)
Membrane
GEL
1 sheet of Whatman paper
Foam pad
**********Black side support**********

Load the gel sandwich in the transblot cell with the black support facing the negative plate (black) and the red support facing the positive plate (red) and add ice to opaque white container for mini-gels and run transblot 100 volts for 1 hour.

C) **Blocking and washing for enchanced chemiluminescence detection for nitrocellulose or PVDF membranes.**

1. Remove the membrane and gel from transblot sandwich and cut the upper right edge of membrane even with the gel for marker.
2. Lift off the gel and check that pre-stained MW standards (BioRad #161-0324) have transferred to nitrocellulose.

Procedure for blocking, incubation, and washing for NITROCELLULOSE

1. Air-dry the nitrocellulose briefly.
2. Block the nitrocellulose with immunoblot buffer (IB) + 3% BSA for 30 min at room temperature on rotating shaker (Labline Rotator, Model 1314) at room temperature (RT) (setting # 4).
3. Pour off blocking buffer and add ~20 mL of diluted primary antibody (Gentest A241). Dilute primary antibody to desired concentration in IB + 1% BSA 1:500 – 1:1000 dilution of polyclonal sera. Incubate nitrocellulose membrane with primary antibody overnight on rotating shaker at RT (setting #4).
4. Wash the membrane with 2 changes of IB + 0.05% Tween-20 (TW20-IB) (Fisher BP337-100) and 1 change of IB without Tween-20 for 20 minutes each wash on rotating shaker at RT (setting #4).
5. Incubate with secondary antibody at desired concentration of (BioRad #170-6518) goat anti-rabbit IgG (H +L)-alkaline phosphatases (Ap) conjugate in IB + 1% BSA for 1 hour on rotating shaker at RT (setting #4).

6. After incubation time, remove the secondary antibody and save for later use by adding 0.2% Na-azide at 4 ° C.
7. Wash nitrocellulose for a total of 5 washes. Wash with 4 changes of immunoblot buffer + 0.05% TW20-IB solution at 20 minutes each wash. Wash once with IB for 20 minutes on rotating shaker at RT (setting #4).

Procedure for blocking, incubation, and washing for PVDF membrane

1. Rinse PVDF membrane in IB briefly (15 seconds)
2. Rinse membrane in MEOH (Fisher A457-4) briefly (15 seconds)
3. Place on chromotography paper – air dry 20 minute or more
4. Place in plastic bag sealed stored at 4 °C until exposure.
5. Primary incubation – submerge PVDF membrane in MEOH (15 seconds)
6. Submerge into IB (15 seconds)
7. Block in IB with 2% or to desired concentration of powdered milk (Safeway nonfat dry milk) for 30 minutes at room temperature on rotating shaker at room temperature (setting #4).
8. Pour off blocking buffer in the sink and add ~20 mL of diluted primary antibody to membrane. (Dilute primary antibody to desire concentration in IB + 0.5% powdered milk generally 1:500 – 1:1000 dilution of polyclonal sera).
9. Incubate PVDF with primary antibody 4 hours on rotating shaker at RT (setting #4).

10. Wash the membrane with **2** changes of immunoblot buffer + 0.05% TW20-IB and 1 change of IB without Tween-20 for 10 minutes each wash on rotating shaker at room temperature (setting #4).
11. Incubate with secondary antibody (Gentest 458241) of goat anti-rabbit IgG (H +L)-horseradish peroxidase (Hrp) conjugate in IB + 0.5% powdered milk for 1 hour on rotating shaker at RT (setting #4).
12. Wash membrane for a total of 3 washes. Wash with **2** changes of IB buffer + 0.05% TW20-IB solution for 10 minutes each wash. Lastly, wash once with IB for 10 minutes on rotating shaker at room temperature (setting #4).

D) Development of membrane.

Items needed for film developing:

- Film (Kodak Sigma F-1274)
- Exposure cassette (Sigma E-8510)
- Developer and fixer (Fisher Scientific 05-728104)
- Acetic Acid, glacial (Fisher Scientific A35 500)
- Chemiluminescence

Instructions for development by chemiluminescence

1. Briefly, blot-dry the membrane and place the membrane on a piece of Saran plastic wrap (enough to fold over and cover the membrane).
2. Prepare the Bio-Rad Immune-Star Substrate Pack (170-5012) immunoblot

substrate by adding 2 mL Immun-Star substrate (170-5018) + Immuno Star enhancer 100 μL (170-5019) for AP or prepare Amersham Pharmacia Biotech ECL reagent for Hrp mixing a 1:1 ratio (RPN2106). Vortex.

3. Pour enhancer substrate mixture onto the membrane.
4. Pour excess solution off onto a paper towel and wrap membrane with plastic.
5. Place wrapped membrane into the exposure cassette.
6. Develop film in dark room. (Exposure times variable)

The following figure, Figure 25 is a depiction of the minigel electrophoresis apparatus.

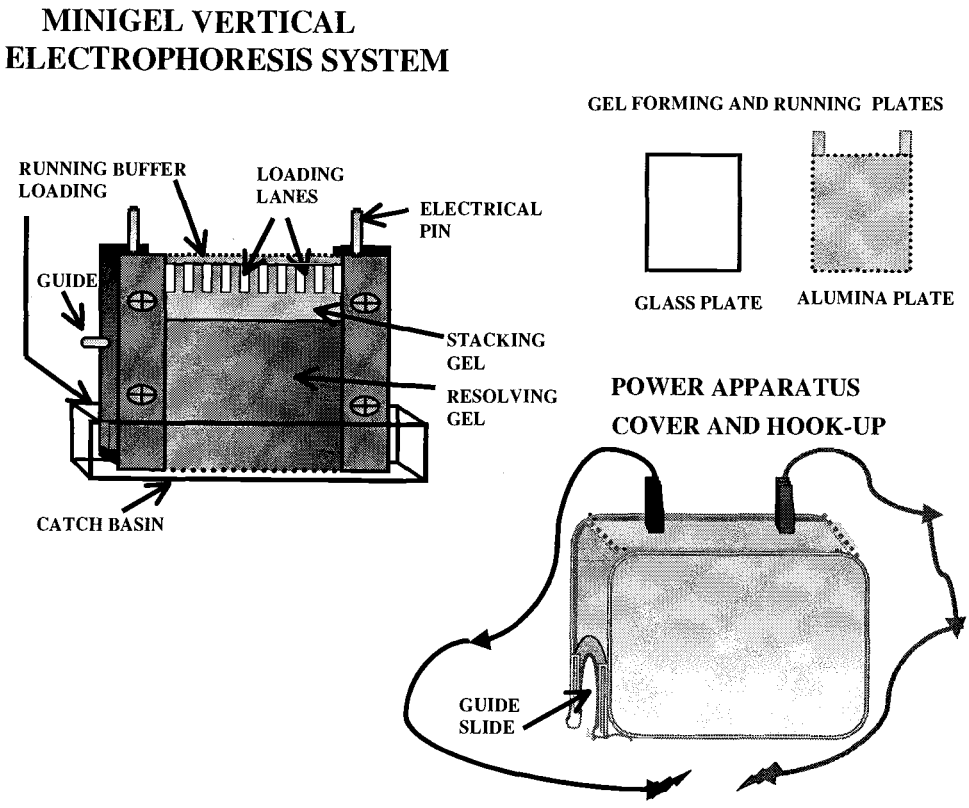

Figure 1b: Schematic drawing of the minigel electrophoresis apparatus.

PROTOCOL M

Immunoprecipitation and Western Blotting

Objective: Immunoprecipitation was utilized to form an antibody-antigen complex for determination of the presence of the flavin-containing monooxygenase enzyme. Immunoprecipitation in conjunction with western blotting takes three days to complete the analysis.

Samples - Microsomal preparations from cell culture

Equipment

- Rotary platform (in house apparatus)
- Centrifuge (Eppendorf 5415C)

Reagents

FMO1, FMO3, FMO5 from human cDNA purified in a baculovirus system (Gentest A241, A243, A245).

Homogenization buffer (pH 7.4):

- ✓ 100 mM trizma (Sigma T-7-149)
- ✓ 250 mM sucrose (Sigma S-7-903)
- ✓ 1 mM ethylenediaminetetraacetic acid (EDTA) (Sigma E-5134)

Add to 100 mL of homogenization buffer:

- ✓ 2.5% Triton X-100 (2.5 mL) (Sigma X-100)
- ✓ 50 uL (0.2%) Protease Inhibitor Cocktail (Sigma #P-8340)

Day 1

1. Obtain microsomal samples from –80 ° C freezer. Be sure to keep samples on ice. Determine protein concentration for each sample.
2. Dilute samples (300 μg) with 0.5 mL 2.5% Triton dilution/homogenization buffer.
3. Tumble mixture using a rotary platform for 1 hour at 4 ° C.
4. Incubate supernatant with a 1:500 dilution of primary antibody overnight at 4 ° C using tumbler (2 μL of stock FMO-1 or FMO-3 or FMO-5 primary antibody).

Day 2

1. For the last hour, add 50 μL of the 50% slurry (75 mg PAS/0.6 mL homogenization buffer) of Protein A Sepharose (PAS) to each sample and incubate at 4 ° C.

   NOTE- Before incubation with samples: The stabilizers are sugars (dextran and lactose), therefore the homogenization buffer can be used to dissolve and remove the sugars and leave the PAS in tact. Use equal amounts of homogenizing buffer and PAS, vortex briefly, and centrifuge at 14,000 rpm for 15 seconds to pull down beads. Remove supernatant. Repeat this procedure 3 times. Soak and swell the PAS with homogenization buffer for a minimum of half-hour at room temperature in eppendorf® tube.

2. Centrifuge samples (table-top centrifuge) at 14,000 rpm for 30 seconds to 8 minutes, or until a pellet is obtained. (Freeze the centrifuge rotor for 15 minutes prior to loading to keep samples cool). Pipette off supernatant.
3. Wash each sample pellet 4 times with an equal volume (~ 1mL) of 2.5% triton Dilution/ homogenization buffer. It is difficult to see the pellet for, therefore centrifuge samples briefly following each wash to be sure the pellet is forced to the bottom to avoid pipetting off the pellet along with the supernatant.
4. Wash 2 times with homogenization buffer without detergent. Pipette off supernatant following each wash and save.
5. Follow western protocol for sample preparation, resolve, and expose to primary antibody overnight (Protocol L), **except** for sample preparation boil 2 - 3 minutes, centrifuge to create pellet and load supernatant.